Dynamical Torsional Analysis of Schweizer 300C Helicopter Rotor Systems

تحليل الإلتواء الديناميكي لأنظمة الحركة في المروحية العمودية (Schweizer 300C)

by

HAITHAM KHAMIS MOHAMMED AL-SAEEDI

Dissertation submitted in fulfilment
of the requirements for the degree of
MSc SYSTEMS ENGINEERING
at
The British University in Dubai

January 2019

DECLARATION

I warrant that the content of this research is the direct result of my own work and that any use made in it of published or unpublished copyright material falls within the limits permitted by international copyright conventions.

I understand that a copy of my research will be deposited in the University Library for permanent retention.

I hereby agree that the material mentioned above for which I am author and copyright holder may be copied and distributed by The British University in Dubai for the purposes of research, private study or education and that The British University in Dubai may recover from purchasers the costs incurred in such copying and distribution, where appropriate.

I understand that The British University in Dubai may make a digital copy available in the institutional repository.

I understand that I may apply to the University to retain the right to withhold or to restrict access to my thesis for a period which shall not normally exceed four calendar years from the congregation at which the degree is conferred, the length of the period to be specified in the application, together with the precise reasons for making that application.

_____

Signature of the student

COPYRIGHT AND INFORMATION TO USERS

Abstract

The study in this research focuses on building simulation model the motion systems of Schweizer 300C helicopter and Emphasises is put on examine the most suitable simulation techniques used to deal with the most accurate and closest to reality dynamical torsional response of the motion systems which will lead to the best analysis.

In The first part of this research, an introductory to the history of helicopters and their dynamic fundamentles and the development and expansion of the Modeling methods from the beginning to the current forms adopted for wide variety engineering system applications.

The problem identified examines the chances and possibilities of simulating the motion systems (tail and main rotors) of Schweizer 300C helicopter .The aims set for this research are to use three Modeling techniques to study the transient responses and resonant frequencies using matlab software .

In this research three different techniques were adopted and compared for the simulation of the movement system of this heilcopter to identify the best and most accurate representation of dynamic torsional analysis of motion systems.

The Modeling techniques used in this research are the Lumped Parameter Modeling-LPM, Finite Element Method-FEM and the Distributed-Lumped Parameter (Hybrid) model-DLPM.

Finally, Modeling techniques and results obtained from each technique are compared and it can be concluded that Distributed-Lumped Parameter technique (DLPMT) is the most accurate and closest to the reality for this and such applications.

خلاصة البحث

تتركز الدراسة في هذا البحث حول تصميم نموذج محاكاة لأنظمة الحركة في المروحية العمودية Schweizer 300C ويتم التركيز على إختبار طرق المحاكاة الأكثر ملائمة للتعامل مع الإلتواء الديناميكي لأنظمة الحركة الأدق والأقرب للواقع الذي سيؤدي إلى تحليل أدق للأنظمة المتحركة في هذه المروحية العمودية.

في الجزء الأول من هذا البحث ، مقدمة لتاريخ المروحيات وهياكلها الديناميكية وتطوير وتوسيع طرق النمذجة من البداية إلى الأشكال الحالية المعتمدة لتطبيقات الأنظمة الهندسية المتنوعة.

وتبين المشكلة التي تم تحديدها فرص وإمكانيات نمذجة أنظمة الحركة (الذيل والدوارة الرئيسية) للمروحية العمودية (طراز Schweizer 300C). وتتمثل الأهداف المحددة لهذا البحث في إستخدام ثلاث تقنيات لوضع النماذج لدراسة الإستجابات العابرة وترددات الرنين بإستخدام برنامج Matlab.

في هذا البحث تم إعتماد ومقارنة ثلاث طرق مختلفة لمحاكاة أنظمة الحركة في هذه المروحية العمودية للتعرف على أفضل وأدق تمثيل للتحليل الإلتوائي الديناميكي لأنظمة الحركة.

تقنيات النمذجة المستخدمة في هذا البحث هي النمذجة الموزعة والنمذجة المتقطعة والنمذجة الهجين، (الموزع-المتقطع).

أخيرا ، تتم مقارنة تقنيات المحاكاة والنتائج التي تم الحصول عليها من كل طريقة ، وتم التوصل إلى أن تقنية المحاكاة الهجين (التمثيل المقطعي والموزع) هو الأدق والأقرب للواقع لهذا التطبيق، والتطبيقات المشابهة.

Dedication

To my wife, for believing in me

To my father, mother, brothers and sisters

To my kids Noor & Al-Mulhem

I dedicate my work to you

Acknowledgments

I am sincerely grateful to my supervisor, Dr. Alaa Abdul-Ameer, for his great assistance and the patience shown throughout this research. It has been a great honor to learn of the theory outlined herein from the mouth of the theorist himself, and to be one of his students. I would like also to show my gratitude and appreciation to the late Prof. Robert Whalley, for his support and guidance throughout my period in BUID.

Table of Contents

Chapter III: System Mathematical Modeling

Chapter IV: Simulation Results and Discussions

List of Notations

$\boldsymbol{A}\ (i\omega)$	Impedance matrix, $(m \times m)$
c_{m1}	Viscous damping at the drive end of main shaft
c_{m2}	Viscous damping at the load end of main shaft
C_m	Compliance of main shaft
c_{t1}	Viscous damping at the drive end of tail shaft
c_{t2}	Viscous damping at the load end of tail shaft
C_t	Compliance of tail shaft
d_{m1}	Diameter of gear box at the drive end of main shaft
d_{m2}	Diameter of gear box at the load end of main shaft
d_{sm}	Diameter of main shaft
d_{st}	Diameter of tail shaft
d_{t1}	Diameter of gear box at the drive end of tail shaft
d_{t2}	Diameter of gear box at the load end of tail shaft
G	Shear modulus
$\boldsymbol{I_m}$	Identity matrix, $(m \times m)$
J_{m1}	Polar moment of inertia of drive end gear box in main shaft
J_{m2}	Polar moment of inertia of load end gear box in main shaft
J_{sm}	Polar moment of inertia of main shaft
J_{st}	Polar moment of inertia of tail shaft
J_{t1}	Polar moment of inertia of drive end gear box in tail shaft
J_{t2}	Polar moment of inertia of load end gear box in tail shaft

$\boldsymbol{J}, \boldsymbol{K}, \boldsymbol{C}$	Inertia, stiffness and damping arrays $(m \times m)$
K_m	Torsional stiffness on the main shaft
K_t	Torsional stiffness on the tail shaft
l_m	Length of tail shaft
l_t	Length of tail shaft
L_m	Polar moment of inertia of main shaft
L_t	Polar moment of inertia of tail shaft
m	Number of rotors
$\boldsymbol{P}\ (\omega), \boldsymbol{Q}\ (\omega)$	Admittance matrices, $1 \leq j \leq m$
T_{mi}	Input torque for the main shaft
T_{mo}	Output torque for the main shaft
T_{ti}	Input torque for the tail shaft
T_{to}	Output torque for the tail shaft
$\gamma_j(s)$	Lumped inertia and damping function, $1 \leq j \leq m$
Γ_m	Time delay of main shaft
Γ_t	Time delay of tail shaft
$\Lambda, \boldsymbol{\Gamma}\ (\omega)$	Impedance matrices, $(m \times m)$
ξ_m	Characteristic impedance of main shaft
ξ_t	Characteristic impedance of tail shaft
ρ	Density
$\varphi_j(t)$	Propagation delay, $1 \leq j \leq m$
ω	Resonant frequency

$\omega_j(t), \bar{\omega}_k(t)$ Angular velocity, $1 \leq j \leq m, 2 \leq k \leq 5$

List of Terminologies

2-D	Two dimensional
3-D	Three dimensional
ASEE	American Society for Engineering Education
BC	Boundary conditions
BUID	British University in Dubai
CAD	Computational aided design
DLPM	Distributed lumped parameter modeling
DLPMT	Distributed lumped parameter modeling technique
DOF	Degree of freedom
DSCT	Discrete space continuous time
ETG	Gear ratio between engine and tail
FAA	Federal Aviation Administration
FEM	Finite element method
HM	Hybrid method
ICE	internal combustion engines
LHS	Left hand side
LPM	Lumped parameter model
ODE	Ordinary differential equation
PDE	Partial differential equation
RAeS	Royal Aeronautical Society
RHS	Right hand side

rpm	Revolution per minute
SIMO	Single input- multiple output
STC	Supplemental Type Certificate
TF	Transfer function
TLM	Transmission line matrix
TMG	Gear ratio between tail and main shaft
WSEAS	World Scientific and Engineering Academy and Society

List of Figures

List of Tables

Chapter I

Introduction

1.1. Research Background

Rotating machines are extensively used in engineering applications. The demand for more powerful rotating machines has led to higher operating speeds resulting in the need for accurate prediction of the dynamic behavior of rotors. It is vital to precisely determine the dynamic characteristics of rotors in the design and development stages of turbo machines in order to avoid resonant conditions. Thus, much research has been carried out in the field of rotor dynamics (Jalali, Ghayour, Ziaei-Rad, & Shahriari, 2014).

It is vital to precisely determine the dynamic characteristics of rotors in the design and development stages of engines in order to avoid resonant conditions. Thus, much research has been carried out in the field of rotor dynamics (Jalali, Ghayour, Ziaei-Rad, & Shahriari, 2014).

The helicopter is an aircraft that uses rotating wings to provid lift, propulsion and contorl, The rotor blades rotate about a vertical axes, discribing a disc in a horizontal or nearly a horizontal plane.aerodynamic forces are generated by the relativemotion of a wing surface with respect to the air.the helicopter with its rotatry wings can genearate these force even when the velocity of the vichle itself is zero, in contrast to fixed wing aircraft, which require a translational velocity to sustain flight.the helicopter therefore has the capability of vertical

flight, including vertical take-off and landing.the effeicint accomplishment of vertical flight is the fundamental characteristic of the helcopter rotor (Johnson, 1980).

Helicopters are defined as those aircraft which derive both lift and propulsive force from a powered rotary wing and have the capability to hover and to fly rearward and side ward, as well as forward. Existing configurations used by the Army include a single lifting rotor with an antitorque rotor, and tandem lifting rotors. A compound helicopter is a helicopter which incorporates fixed-wing surfaces to partially unload the lifting rotor and/or additional thrust producing devices. Such devices supplement the thrust-producing capability of the lifting rotor(s) (U.S. Army materiel, 1974).

Table 1.1 Rotor Control Input for Various Configurations (Venkatesan, 2015)

Helicopter Configuration	Height	Longitudinal	Lateral	Directional	Torque Balance
	Vertical Force	Pitch moment	Roll Moment	Yaw Moment	
Single main rotor and tail rotor	Main rotor collective	Main rotor cyclic	Main rotor cyclic	Tail rotor collective	Tail rotor thrust
Coaxial*	Main rotor collective	Main rotor cyclic	Main rotor cyclic	Main rotor differential	Main rotor differential torque
Tandem*	Main rotor collective	Main rotor differential collective	Main rotor cyclic	Main rotor differential collective	Main rotor differential torque
Side by side*	Main rotor collective	Main rotor cyclic	Main rotor differential collective	Main rotor differential cyclic	Main rotor differential torque
*combined pitch differential control					

1.1.1. Helicopter Dynamics Modeling Principles

Helicopter dynamics Modeling was originally, based on mechanical systems and its fundamnetal components: mass (or inetria),springs (stiffness) and dampers. it can simply classified as a linear-one dimensional field problem.

The basis of this was the well-known relationship between input torque (T_i) and angular speed (ω) and torque travelling in the drive shafts.

The advantages gained when Modeling helcopter dynamics using torsional reponse models is being a simple method to assess the errors in most cases.

1.1.2. Helicopter Dynamics Modeling and Computational Tools

The complexity of Modeling and analyzing helicopter dynamics required highly sphostocated computational tools like computers and supporting software. However, such tools cannot be considered as assisting method from understanding and deriving the mathematical formulas and conceptual ideas of helicopter dynamics which from the core knowledge and specialization of the design engineers.

In general, these computational tools for helicopter dynamics are defined as computational algorithms which are able to analyze, simulate and solve the dynamics of any object depending on selecting the suitable boundary and initial conditions.

Such famous computational softwares for analyzing helicopter dynamics (torsional response) problems are but not limited to CFD simulation and matlab (simulink).

Before investigating some of these following methods, which are of research interest, it is important to state here that the drawbacks and differences in these methods are not an indicators of weakness.they are varying in applicability and suitability of usage according to the exercise to be studied and modeled.

Generally speaking; one technique is complementing the other one in other aspects instead of competing each other. This can be decided by the designer or researcher, and based on the chosen application the appropriate and suitable method will used.

1.2. Research Problem Statement

In this research, a high speed rotors with particular geometrical and also mechanical properties are modeled using lumeped parameter theory, finite element modeling and distributed-lumped (hybrid) modeling. The transient response and natural frequencies under zero initial boundary conditions are acquired and the results of the three models are compared. The Bode diagrams are drawn and natural frequencies are calculated numerically for all the models and copmpared to investigate the system dynamics.

Generally speaking, the research is focused on stuyding and investigating the torsional response of the motion systems (tail and main rotors) in helicopter considering three different modeling

techniques: lumped (pointwise) prameter, finite element (distributed) and lumped-distributed (hybrid).

1.3. Research Aims and Objectives

The major objective of this dissertation is to use the hybrid Modeling method which was developed in 1988 by prof R. Whalley to be used for Modeling a spatially dispensed system model while considering all parameters polar moment of inetria, compliance, impedance and propajation.

A comparison of the Lumped Parameter Modeling (LPM), Finite Element Method (FEM) and Distributed-Lumped Parameter Modeling-Hybrid (DLPM) will be given and the results achieved will be compared.

Mainly, the outcomes of this dissertation will cover the following objectives: -

a. Model mathematically the system which comprise of bearings, inertia discs and shafts using lumped parameter theory, Finite Element and hybrid (Distributed –Lumped) methods.
b. Building system simulation model and fulfillment the requirement of accuracy, integrity and computational effeceincy of the three modeling techniques used.
c. Simulate the modeled system using matlab software and validate the results for :-

b.1. The accuracy, integrity and computational efficiency for lumped parameter,finite element and hybrid Modeling techniques.

b.2. compare the system dynamical torsional responses achieved from the three techniques used.

b.3. check the system time domain responses assuming no internal frictional damping in the shafts.

b.4. comparison of the system dynamical resonant frequencies obtained from the three modleing techniques.

1.4. Research Dissertation Organization

Generally, chapter II will be literature review of the former work in the field of modeling and simulation of torsional response of rotor systems using three differenet Modeling method: lumped,finite element (five sections) and hybrid Modeling and how these methods were introduced and developed to be used in the present time applications. Hence,this will illustrate the different techniques used for Modeling the selected system, in terms of the three Modeling methods, on which this dissertation will focus.

Chapter III will explain the Modeling techniques and methodologies used for the choosen system.

A brief introductory to the Schweizer 300C and the description for the choosen hybrid system (distributed-lumped) will be itroduced.

After that, the mathematical derivation of formulas and analysis using the lumped parameter theory,Finite Element Method and hybrid Modeling will be demonstrated in details for comparison purposes. In each Modeling method, two mathematical models will be derived from

the systems,tail and main shafts and rotors. Chapter three will provide a theoretical background for the chapter IV.

Chapter IV presenting the utilixation of simulation using the selected software and discussions of the simulation results for the responses of the system model comparing them collectively. Comparison in details is presented regarding the differneces, advantages, disadvantaged and difficulties of each approach. Finally, the resonant frequency calculated and measured of each method will be compared to each other.

Chapter V concludes the dissertaion. it will discusses the main advantages gained by using the different approches and provide a summary of the outcomes achived and list the recommendations for development of the future work and conclusion from it.

Chapter II

Literature review

2.1. Introduction

The word “system” has become widely popular in the recent years. It is utilized in engineering, science, sociology, economics, and even in politics. Regardless of its popular employ, the exact and accurate meaning of the terminology is not fully understood always. A system can be defined as a set of elements that is acting together to implement a certain task. A little more philosophically, a system could be comprehend as a theoretically isolated portion of the universe that is of interest to the designer. Other portions of the universe that is interacting with the selected system include the neighboring systems or system environment (Kulakowski, Gardner, & Shearer, 2007).

The system is **static** if the output is dependent only on the instantneous input. Then system is **dynamic** when the output is a function of the histort of the input (Kelly, 2009).

System dynamics is dealing with the mathematical modeling and analysis of processes and devices for the aim of understanding their time dependent characteristics (Palm, 2010).

System dynamics affirms techniques for working with systems including various types of processes and elements for example, fluid-thermal procsses, electrohydraulic devices and electromechanical devices. Since the objective of system dynamics is the understanding

the time-dependent performance of the selected system comprising interconnected processes and devices as a whole, the modeling and analysis approaches applied in system dynamics should be properly chosen to detect how the interconnections between the elements of the system influence the overall behaviour (Palm, 2010).

Mathematical modeling is the process through which the dynamic response of a system is obtained. Mathematical modeling lead to the development of mathematical equations that describe the behaviour of the chosen system. The dynamic system behaviour is usually governed by a set of differential equations in which time is the independent variable. The dependent variables repersent the system outputs (Kelly, 2009).

Furthermore, it is substantial noteing that basically all engineering systems are nonlinear when studied over the all possible ranges of their input variables. Anyway, solving the mathematical models of nonlinear systems is generally more difficult and hence complicated than it is for the systems that can reasonably be deemed to be linear. (Kulakowski, Gardner, & Shearer, 2007).

2.2. Historical Background of Helicopters

Leonardo da Vinci, the distinct Italian scientist, mathematician, and artist, noticed that the birds can control the smoothness of their flight effectively by play with the side end of the wings. By 1483, with such idea in mind, da Vinci draw a flying tool depending on Archimedes screw. He represent his craft (wire-framed) as an “device made with

helix of flaxen linen in which one has locked the pores with force, and hence, is turned at a high speed, the mentioned helix is capable to make the screw in air and to ascent high". In his elaboration da Vinci hired Greek word (helix), meaning twist or spiral, using the terminilogy to the principles of flight. Similarly, others followed da Vinci's lead and implement the term for representing their flying instruments. Also, Da Vinci symbolize the fabric-covered frame in his flying device, the building technique used in later centuries by both helicopter and airplane inventors.

Approximately in 1754, Russian innovator Mikhail Lomonosov designed a tiny coaxial rotor reduplicated from the Chinese plaything but driven using wound-up springs. While releasing, his model flew for few seconds. After that in 1783 Launoy, a French naturalist, contributed by his mechanism, by usunig turkey feathers in order to build a coaxial edition of the Chinese toy. while their model hovered into the ambience it stirred massive interest through certain scholars .

Sir George Cayley, was very famous for his contribution regarding the fundamental principles of the flight during 1790s, had successfully constructed various models of vertical flight equipments by the end of eighteenth century. Coiled springs was used to power the rotors which was cut from tin sheets. later in 1804, he build a whirling-arm instrument that will be utilized to scientifically investigate the aerodynamic forces generated by the lifting surfaces. After that in 1843, Cayley presented a scientific paper explaining the theory of a

comparatively large vertically flighting aircraft that he nammed an “aerial carriage.” Cayley’s concept, generally speaking, stayed only estimation, since the existing steam engines at that time were too much heavy in order to power flight (McGowen, 2005).

Though inventors who operated their models using lightweight, miniature steam engines relished some exclusive success, the shortage of approbriate power plant choked further aeronautical enhance for decades. In the mid of 1800s, Horatio Phillips, reveal a vertical-flight device that is powered using a small boiler. the rotors was turned using the steam that is produced by the miniature engine and ejected out of the blade tips. Certainly impracticable at the full size, Phillips’s model was nonetheless important because it was recorded as the first model with an engine (not storing energy equimpments), powered flying helicopter . the name “helicopter” was first used by Frenchman Ponton d’Amecourt in the early 1860s after he flew successfully differenet small models that is steam-powered. The word “helicopter”, was originally derived from the Greek adjective elikoeioas, which means “winding” or “spiral” and also the noun pteron, which means “wing” or “feather” producing the modern terminilogy “helicopter.” (McGowen, 2005).

Many pathfinders of the vertical flight promoted original models, but, generally speaking, all of the early experimenters face the problem of shortage of two principles: a true realization and recognition of the inwardness of the aerodynamics and the enough power source. flight

records documents a huge number of unsuccessful rotary-wing devices. Most failures where because of either bad aerodynamics or the mechanical design used, or an inappropriate power-generating source; some of them just vibrated themselves into segments.

Few who speculated manufacturing a helicopter recognized the real complexities and difficulties of the vertical flight, and most of them failed to draw near their adventure in a proper scientific way. In the 1880s, U.S. well known inventor Thomas Edison experimented some models of small helicopter, testing various rotor arrangmets powered by a gun cotton engine (nitrocellulose). An early style of the internal combustion engines (ICE), Edison's gun cotton engines were exploded over a series of experiments; it was an ingredient for both dynamite and gunpowder. For his later experiments, Edison transfered to electric motor with less volatile. From his experiments he noticed that both high power source and high lift coefficient from the rotor system were needed to endure vertical flight (McGowen, 2005)

A considerable technological sudden huge progress came as a result of the beginning of using the internal combustion engines (ICE) at the end of the nineteenth century. Later by the 1920s,with the progression in metallurgy introduced lighter engines and also with higher power to weight ratios. Prviously, (ICE) were manufactured using cast iron, but some progress was achieved after the World War I where aluminum has became more extensively used in the aviation applications, enabling fabrication of full size helicopters comercialy with a samll weight to

power source. regrettably for manufacturers, increased power didn't resolve their obsacles and difficulties but only increae the complexity of the vertical flight.

2.3. Lumped Parameter Modeling(LPM) Technique

2.3.1. General Overview of LPM

As it is known, detailed numerical modeling is requiring large amounts of data, costly and time consuming. Lumped parameter Modeling will be good choice in some cases,as it can be a cost effective alternative. It requires a very little time since it has been developed to tackle simulation using lumped models as an inverse problem.

In general, the lumped parameter model or as it is sometimes called lumped element model or rarely lumped component model, is a simplification of a spatially distributed physical models into a topology contains discrete entities approximating the distributed system accodring to certain assumptions.

It is useful in a wide variety feilds such as electrical and electronics, systems, hydraulic systems, mechanical multibody systems,fluid systems, heat transfer, etc.

Mathematically speaking, using lumped parameter modeling will simplify the system and the state space of the system will be reduced to a finite dimension, and accordingly, partial differential equations (PDEs) will be reduced to ordinary differential equations (ODEs) since there will be a movement from infinite-dimensional (continous) model of the system to finite (descrete)

number of parameters. The main advantage here is that the ordinary differential equations (ODEs) can be solved semi-analytically.

There are many advantages for the LPM are the simplicity and also the fact that they can be easily deal without requiring the use of large computers.

2.3.2. Lumped Mechanical Systems

Mechanical systems is a unit consisting of mechanical components owing properties of damping, stiffness and mass. The damping, stiffness and mass of a structure are substantial parameters because they determine the dynamic behavior of the system. systems can be considered to be lumped parameter system if the elements can be separated by distinguishing the dampings, stiffnesses and masses, assuming them to be lumped in separate components. In this case, the position at a given time depends on a finite number of parameters (Lalanne, 2014).

Practically, and mostly for a real structure, these components are distributed uniformly, continuously or not, with the properties of damping, stiffness and mass, not being separate. The system is consisting of an unlimited (infinite) number of tiny elements. The behavior and performance of such a system with distributed parameters must be studied and investigated using complete differential equations with partial derivatives (Lalanne, 2014).

It is usually motivating to facilitate the selected system to be able to represent its movement via ordinary differential equations (ODE), by

dividing it into a discrete (discontinous) number of specific masses linked by elastic massless components and of energy dissipative components, so as to acquire the lumped parameter system (Lalanne, 2014).

The conversion of a physical structural system with (continous) distributed parameters into a model or system with centeralized parameters is in general a delicate process, with the selection of the points that having an significant impact on the outcomes of the computations carried out with the derived model (Lalanne, 2014).

2.4. Finite Element Method (FEM) Technique

2.4.1. General Overview of FEM

A numerical approach for sloving a differntial equation problem is to descetize this problem, which has infinitely many degrss of freedom, to produce a discrete problem, which has finitely many degrees of freedom and can be solved using a computer. Compared with the classical finite differnece method, the introduction of the finite element method is relatively recent (Chen, 2005).

Of course, in acknowledging the system dispersal the prospect of dynamical processes characterization dominated by partial differential equations (PDE) looms. In these exemplifications, analysis of the system is established on continuous formularization where an unlimited number of tiny segments are utilized, as a part of the system specification (Bartlett & Whalley, 1998).

The advantage of the finite element method over the finite differnce method are that general boundary conditions, comlex geometry, and variable material porperties can be relatively easily handeled. Also, the clear structure and versatility of the finite element method makes it possible to develop general purpose software for applications. Futhermore, it has a solid theoritical foundation that gives added reliability, and in many situations it is possible to obtain conctete error estimates in finite element solutions (Chen, 2005).

2.4.2. Historical Background of the FEM

Since the differential equations describing the displacement field of a structure are difficult (or impossible) to solve by analytical methods, the domain of the structural problem can be divided into alarge number of small subdomains, called finite elements (FE). The displacement field of each element is approximated by polynomials, which are interpolated with respect to prescribed points (nodes)located on the boundary (or within) the element. The polynomials are referred to as interpolation functions, where variational or weighted residual methods are applied to determine the unknown nodal values (Pavlou, 2015).

Though the term of fininte element method (FEM) was introduced for the first time by Clough in 1960,the concept and idea dates back sundry centuries. As an example, past mathematicians calculate the circle circumference through approximating it by the perimeter of the polygon . According to presenet-day notation, every side of the polygon can be called a “finite element.” (Rao, 2011).

To derive the differential equations of the surface of minimal area confined by a specific closed curve, Schellback in 1851 disceretized the selected surface into various triangles and employed the finite difference term to calculate the descrtized area (Rao, 2011).

In the present finite element method (FEM), differential equations are resolved by displacing it by a group of algebaic equations. Since the early 1900s, the torsional behaviour of structural frameworks, comprised of various bars arranged in a uniform style, has been deal with as an isotrpoic elastic body (Rao, 2011).

Basisc ideas of the fininte element method originated from advances in aircraft structural analysis. In 1941, Hrenikoff preseneted a solution of elasticity problems using the "frame work method." (Tirupathi & Ashok, 2012).

In a 1943 paper, the mathematcian Courant described a piecwise polynomial solution for the torsion problem. His work wwas not noticed by engineers and the procedure was impractical at the time due to the lack of digital computers (Cook, 1995).

Courant introduced a technique of calculating the hollow shaft torsional rigidity through division of cross section area into many triangles and utilizing the linear variation of the stress function (φ) over every triangle in terms of the values of φ at net points (known as nodes in terminilogy of the current finite element) (Rao, 2011).

According to some, the previous work was considerd as the origin of the current finite element method (FEM). during the mid-1950s,

engineers and designers in the industries of aircrafts have worked on improving similar techniques for the prognosis of stress generated in the aircraft wings (Rao, 2011).

In 1956, Turner introduced a technique for Modeling the wing skin by three node triangles. Nearly, at the same period, Kelsey and Argyris published variuos papres that outlines matrix procedures, including some ideas of the finite element, that is dealing with the solution of structural analysis problems. In this regard, this study was considred as one of the important contributions in the finite element method development (Rao, 2011).

For the first time in 1960, the terminilogy ‘Finite Element Method’ was used by Clough (1960) in his paper on plane elasticity. In 1960s, a large number of papers appeared ralated to the applications and devlopments of the fininte element method.Engineers use FEM for stress analysis,fluid flow poblems and heat transfer (Desai, Eldho, & Shah, 2011).

A flat, rectangular-plate bending-element stifness matrix was devloped in 1961 by Melosh. Following this, the devlopment of stiffness matrix for the curved-shell bending element for axisymmetric pressure vessels and shells in 1963 by Storme and Grafton (Logan, 2012).

Extension of the (FEM) to problems with three dimensions with the devlopment of a tetrahedral stiffness matrix was achieved in 1961 by Martin, in 1962 by Gallagher, and in 1963 by Melosh. Further three-

dimensional comnponents were considered in 1964 by Argyris. Finally, the special case of axisymetric solids was cosidered in 1965 by Wilson, Rashid and Clough, (Logan, 2012).

In 1965 Arsher considered dynamic analysis in the devlopment of the consistent-mass matrix, which is applicable to analysis of distributed-mass system such as bars and beams in structural analysis (Logan, 2012).

A number of internasional conferences related to FEM were organized and the method got established. The first book on FEM was published by Zienkiewiz and Cheung in 1967 (Desai, Eldho, & Shah, 2011).

In 1976, Belytschko considred problems related to with large-dispalcement nonlinear dynamic behaviour, and improved numerical methods for solving the generated set of equations (Logan, 2012).

By the late 1980s the software was availabe on micocomputers, complete with color graphics and pre- and postprocessors (Cook, 1995).

By the mid mid-1990s roughly 40,000 papers and books about the FE method and its applications has been published (Cook, 1995).

With the advent of digital computers and finding the suitability of FEM in fast computing for many engineering problems, the method become very popular among scientists, engineers and mathmiticians. By now, a large number of research papers, proceedings of internasional conferences and short-term courses and books habe been

published on the subject of FEM. Many software packages are also availabe to deal with various types of enginerring problems. As a result,FEM is the most acceptable and well established numerical method in engineering sciences (Desai, Eldho, & Shah, 2011).

Today, the developments in maimframe computers and availability of powerful microcomputers have brought this method within the reach of students ans engineers working in samll industries (Tirupathi & Ashok, 2012).

2.4.3. Applications of the FEM

An nother method to dynamics analysis is possible by finite element method (FEM). This technique implicitly enhances the assumption that the studied model is build from comparatively compact, pointwise, multiple, interconnected damping, mass-inertia and stiffness, components in which the lumped parameter theory can be used (Whalley, Ebrahimi, & Jamil, The torsional response of rotor systems, 2005).

Moreover, providing the overall model of the modeled system these divided finite elements or sections can be connected either in series or in parallel arrangment.

Using finite element method (FEM) approach, some simple, rational functions models are derived, which could be handeled and analysed with ease either by utilizing popular numerical methods or any available commercial softwares.

There are inescapable drawbacks and weaknesses with finite element method. For example, one of them is that there is no guidelines specifying the number of elements or sections that need to be considered to get the best design. It has been noticed that as the number of the used sections or segments increases, the mathematical Modeling complexity will also increases requiring long computation time and higher random access memory required for the data storage. Even though, there is no guarantee of the accuracy of the obtained results.

One example of earliest applications using finite element method-FEM, was in 1976 by Nelson who utilized this technique in analyzing the dynamical phenomena in mechanical systems consisting og rotors and bearings. the contribution concluded by a methematical model containing big number of eigenvalues, and that was a result of increasing the number of segments used. And that was not the only difficulty with this approach, but also it become more complicated to perform the mathematical calculations (Aleyaasin & Ebrahimi, 2000).

In 1988, Watton and Tadmori declared that the instability of finite element method-FEM can be observed if the time step size was not selected appropriately.

Furthermore, increasing node numbers may not lead to changes while comparing the achieved results. On contrary, for such cases,it will be highly advisable to select less number of nodes (Watton & Tadmori, 1988).

Bioengineering is a comparatively new area of application and using of the (FEM). This area is still facing some difficulties such as geometric nonlinearties. nonlinear materials, and other complexities yet being revealed (Logan, 2012).

The above statement regardnig this method will be examined and proven in datails and compared with lumped and hybrid Modeling by the author in this dissertation.

2.5. Distributed-Lumped Parameter Modeling (Hybrid) Technique-DLPM

2.5.1. Historical Background of the (DLPM) Technique

Recalling contribution of Nelson's (1976) in investigating ing the dynamic response of a rotor and bearing systems utilizing finite element method-FEM, this was the major reason for evloving other methods in order to help in the reduction of the the substantial numbers of eigenvalues generated by FEM.

One of these methods is the distributed-limped (Hybrid) modeling. Below is the historical background and the application of this technique.

By definition, any scheme or system containg discrete time, expressed using difference equations, and continuous subsystem expressed via differential equations, is a hybrid system.

Nodays, there are so many can be categorized as hybrid systems because of containing both continuous and discrete time subsystems and usually, categorized according to the equations used in the derivation of the system mathematical model.

For example, lumped parameter systems are modeled using ordinary differential equations (ODE), whereas distributed systems are modeled by partial differential equations (PDE).

Furthermore, distributed parameter system represent the situation, in which scalar field concerning the concentrated quantities are functions of both time and position (Dynamic Models Distributed parameter systems, Chapter 7).

It is important here to bring to light that, alteration the distributed parameter systems to lumped parameter approximations is necessary occasionally, specifically, while considering the resources available to solve the selected model (Close & Frederick, 1993).

2.5.2. Applications of the (DLPM) Technique

Below, there are some illustrations and examples of a hybrid systems consisting of lumped systems, distributed systems or a collection of distributed and lumped systems.

1- Before 1977, the dynamical simulations exists was restricted to the processing a unit described by lumped parameter models-LPM. After that, in 1977 Heydweiller, , Sincovec and Fan published a paper, which shows the whole procedures that can represent chemical processes of particular unit utilizing both the distributed and lumped parameter systems (Heydweiller, Sincovec, & Fan, 1977) .

   The mathematical of distributed parameter model (DPM) derived by Heydweiller, Sincovec and Fan was founded as partial

differential equations (PDEs). Subsequently, the PDEs are transformed to a set of ordinary differential equations (ODEs) which only depends on time. Moreover, the approximations of finite difference is utilized for the spatial variables discretization (Heydweiller, Sincovec, & Fan, 1977).

As it could be noticed here, according to the available computional resources and capabilities, the distributed systems was simplified to lumped one for the seek of ease and to be able to solve it and deal with it with the availabe resources at that time.

Initial boundary conditions (BC), describing unit inlet and outlet need to be specified during modeling to pair the combiniation of discretized formuas extracted from the LPM with the other combination of discretized formulas extracted from the distributed parameters model from another unit. Hence, this collection produced a huge number of time dependent ordinary differntial equations (ODEs), which needed to be resolved. In such regard, gear-type integrator has been utilized in order to resolve these combination of generated ordinary differential equations (ODEs).

2- Again in (1977), J. W. Bandler applied the a new Modeling technique called transmission line matrix-TLM in analyzing the lumped networks in time domain. The technique showed its capability to end up with the exact solution of the model. Though, regarding the error appearing during Modeling the componenets of

the selected network, this was recovered by adding more elements (Bandler, 1977).

3- One year later, in 1978, Ray executed a survey regarding the modern implementations and usage of distributed parameter systems theory. The survey indicates some areas of the empolyments for example, chemical reactors, heat transfer, mechanical systems, open-loop stability problems , control and monitoring, sociological and physiological systems, and finally, process control for example, polymer processing implementaiton, nuclear reactor control, control of plasma and for a wide variety of the process control usages.

   Actually, number of above described applications required nearly lumped parameter system models at first. Then, the LPM theory was utilized on the final built model. Actually, this technique was effective with the declared experimental results limitation (Ray, 1978).

4- After ten yaers, in 1988, Prof.Whalley published a paper titled as "*The response of distributed lumped parameter systems*", to help in overcome one of major flaws of FEM, the lengthy computation time consumed without enhancing the reliance in the results acquired, and to consider the wave propagation principle. He inspected Modeling a system which consists dynamical distributed parameter elements followed by the lumped componenets connected togther in series.

The conclusion accomplished from this realization, indicates that mapping the input signal to the output signal can be carried throgh a rational functions belongs to the concerning the frequency domain and time domain as long as lumped parameter componenets are described in both frequency and time domains by similar rational functions to the distributed elements.

cosequently, while selecting Prof.Whalley's HM method, utilizing long driving shafts can be provided using the distributed parameter modeling method as it is shown in the following format:-

$$\begin{bmatrix} Input_1(s) \\ Input_2(s) \end{bmatrix} = \begin{bmatrix} \xi w(s) & -\xi(w^2(s)-1)^{\frac{1}{2}} \\ \xi(w^2(s)-1)^{\frac{1}{2}} & -\xi w(s) \end{bmatrix} \begin{bmatrix} Output_1(s) \\ Output_2(s) \end{bmatrix}$$

here, the system impedance or matrix relates the outputof the system to the input.

moreover, as it could be observesd from the previous model, that the system transfer function (TF) is inherently multidimensional matrix, this indded denotes that the system is not only one lumped parameter element and also one distributed parameter element, even though it is rational.

Compared with torque and angular speed as the inputs and outputs in such rotor systems,then for any other type of systems, for example, thermal, hydraulic, mechanical, etc, the concerned inputs and outputs can be replaced easily in the distributed model mentioned above.

5- Two years later, in (1990), R. Whalley suggested a (HM) method employing distributed parameter technique in modeling long transmission lines. it was then utilized by Bartlett, Whalley, and Rizvi to inspect the dynamical response of a hollow and relatively long shafts of marine transmission configuration, revealing that this method can be used with such investigations (Bartlett, Whalley, & Rizvi, Hybrid modelling of marine power transmission systems, 1988).

6- Subsequently in (1998) Bartlett and Whalley published a paper which investigate the model and analysis of inconstant geometry; exhaust gas hybrid systems. It is offering general Modeling method using the same modeling method (distributed-lumped) in modeling the long exhaust pipes with dual linked cross sections having different lengths utilizing lumped both restrictions and impedances. This is how they were able to investigate the steady state and dynamic responses of the selected system (Bartlett & Whalley, 1998).

   It should be realized here that distributed-lumped method used in modeling the choosen pipeline accroding to the distributed nature where the LPM was not the suitable technique in modeling the long pipeline (Bartlett & Whalley, 1998).

7- In 2000, M. Ebrahimi and M. Aleyaasin, worked on modeling rotary system consisting of shaft-disc by using the method of series of linked, distributed and lumped components improved by R,

Whalley in 1988 (mentioned earlier in this section). In this system, the dics are modeled as lumperd parameter element while the shaft is modeled as distributed parameter element divided into number of equal length sections (Aleyaasin & Ebrahimi, 2000).

There are two parts of the modeling as exlplained earlier, lumped and distributed.

There were left and right endings in the distributed modeling part, and each ending consisting of four parameters. Specifically, these four parameters were displacement, vertical slopes, bending moments and shear forces. Similarly for the left and right endings of the lamped modleing part, each ending is consisting of the same parameters of the distributed part (Aleyaasin & Ebrahimi, 2000).

Moreover, the authors investigated the response in time domain of the selected system using the response from frequency domain results. To do that, the inverse Fourier transform was used since the noise is not included in the obtained results and outcomes of the simulations (Aleyaasin & Ebrahimi, 2000).

8- In 2009, Whalley and Abdul-Ameer published a paper titled '*The computation of torsional, dynamic stresses*' where they used this technique in formulating the system shown in figure 2.1 below.

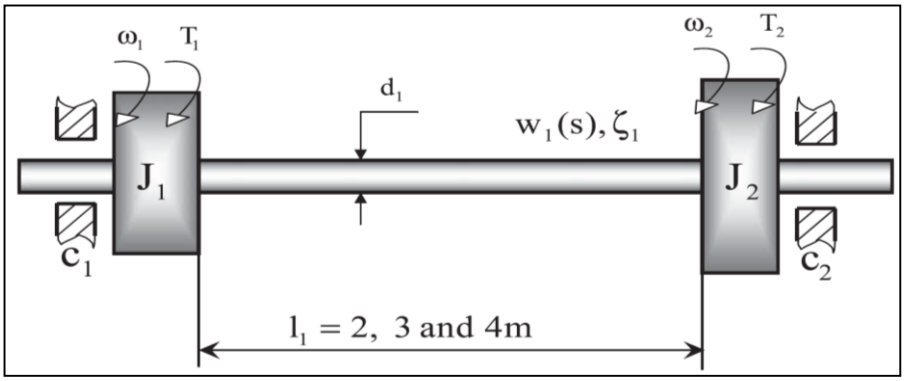

Figure 2.1 Two rotor lumped-distributed parameter system

(Whalley & Abdul-Ameer, 2009)

Here the bearings and rotors were considered as rigid, (point-wise) lumped parameter. The drive shaft will be treated as distributed parameter component because of its dimensions, since the stiffness and inertia are generally, continuous functions of shaft length.

9- In 2010, Whalley and Abdul-Ameer worked out a DLPMT of heating, ventilation and air conditioning system.

The studied system is shown below in figure 2.2 where the application of lumped parameter and distributed parameter in the elements is shown clearly

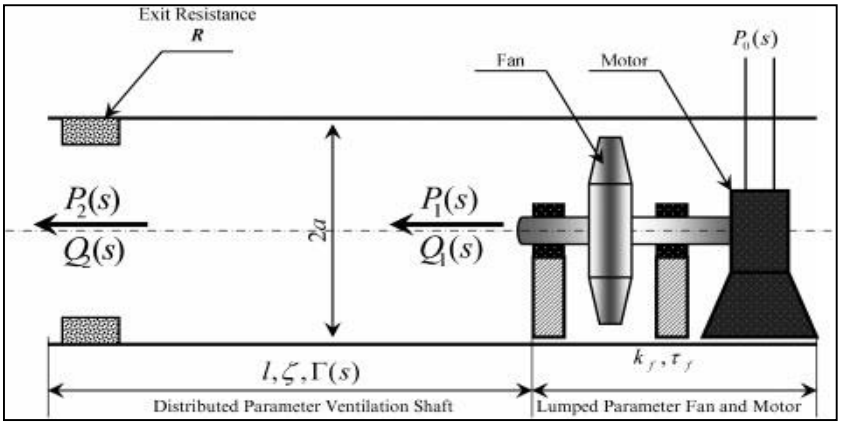

Figure 2.2 Distributed–lumped parameter model of ventilation shaft, fan, and motor

(Whalley & Abdul-Ameer, 2010)

The inlet and extraction fans were considered as point-wise components for the aim of easy modulation of changes in pressure at the outlet and inlet inside the ventilated area through varying the voltage in the motors of the fan. On the outlet side, the dimension of the ventilated volume was modeled using the distributed parameter technique. The useful part of this approach is that it is enabling varying the dynamics of airflow as a introductory to prepare automatic control investigations (Whalley & Abdul-Ameer, 2010).

Regarding the constructed model, as it was explained earlier in example 4, the input pressure changes is mapped to the two outputs of the system; airflow rates and volume input. Furthermore, the fan dynamics is modeled as point-wise (lumped) and it will be be expressed as simple exponential time delay (Whalley & Abdul-Ameer, 2010).

10- One year later, in (2011), Abdul-Ameer demonstrated that Whalley,R method (mapping the input into the output) can be used for hydraulic systems. This was approached using the new method improved for modeling and analysis of fluid pipeline utilizing the HM method suggested by Whalley,R (Abdul-Ameer, 2011).

Abdul-Ameer furthermore, expanded this method in order to get transient response expectations with more accuracy for the system model (fluid pipeline), whilst including the frequency dependent fluid friction (Abdul-Ameer, 2011).

11- In the same year, 2011, R.Whalley and Abdul-Ameer used the same technique, hybrid modeling (distributed-lumped parameter) to investigate some dynamical responses of the cyclic ventilation applications (Whalley & Abdul-Ameer, 2011).

In this research the system consisting of re-circulation, dual fan, and air conditioning, shown below in Figure 2.3, will be investigated. Temperature control units, chilled water and filtered air, are utilized for conditioning the recycled air which will be mixed at the inlet of the ventilation unit with atmospheric air. The return air can be defined as The air re-circulated from the ventilated volume whereas the exhaust air is the part of the return air which is expelled to the atmosphere.

The atmospheric air which is required to neutralize for the volume of the exhaust (expelled) air, indeed needs filtration, and adjustment of humidity and temperature prior to mixing it with the recycled air. This creates the ‘mixed air’ which is to be transferred to the ventilated volume providing herewith the acceptable specified air quality (Whalley & Abdul-Ameer, 2011).

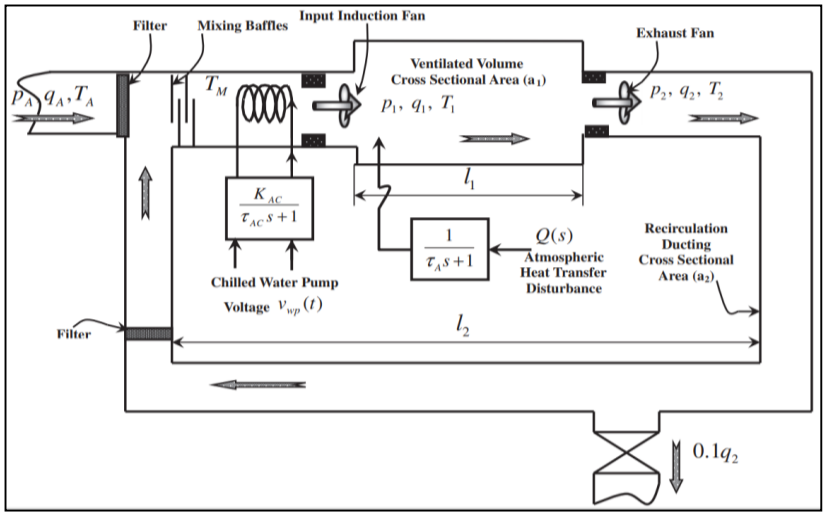

Figure 2.3 Airflow ventilation and air conditioning system

(Whalley & Abdul-Ameer, 2011)

12- Again in the same year, 2011, R. Whalley, Abdul-Ameer and M. Ebrahimi performed the HM of a machine tool (milling machine) axis drives. To compute the X,Y and Z axes responses and resonant frequencies for the selected milling machine, the distributed-lumped parameter Modeling method was used to extract the equations for the model. Figure 2.4 below is showing the X and Y traverse drives of the milling machine (Whalley, Abdul-Ameer, & Ebrahimi, 2011).

Furthermore, because of required accuracy of results, system's spatial dispersal was considered during the modeling it (Whalley, Abdul-Ameer, & Ebrahimi, 2011).

In this application, the lead screw was considered as a pair of distributed-lumped elements, while, the workpiece, motor drive, saddle, ball-nut, bearings and slides were considered as lumped parameter elements (Whalley, Abdul-Ameer, & Ebrahimi, 2011).

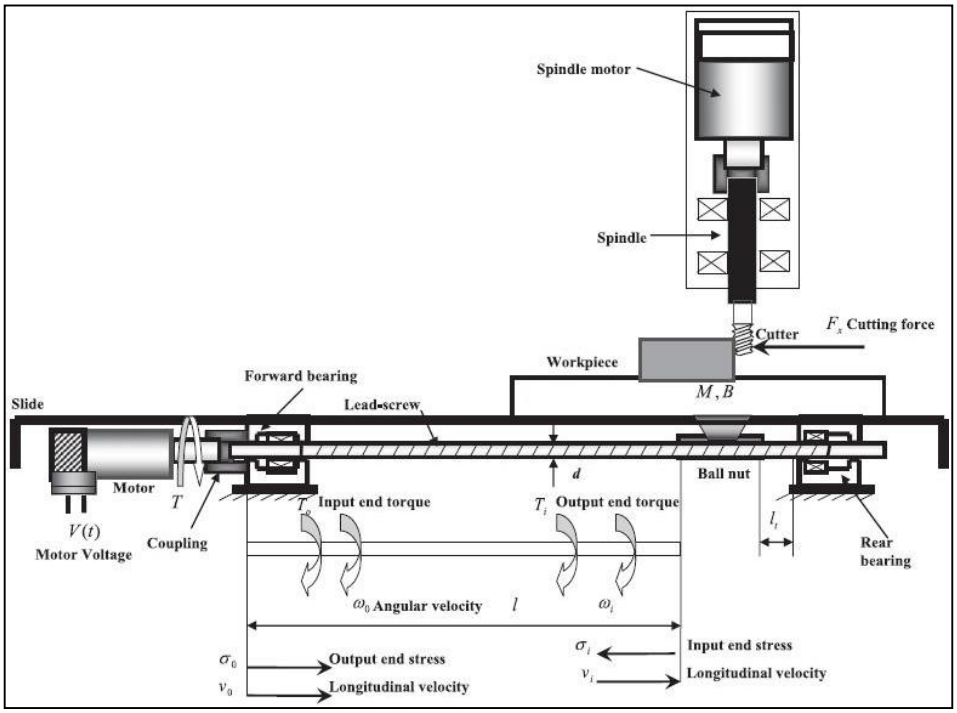

Figure 2.4 Milling machine X and Y traverse drive

(Whalley, Abdul-Ameer, & Ebrahimi, 2011)

To conclude all listed applications earlier, this research will concentrate on Distributed-Lumped Parameter Modeling Technique (DLPMT) which was developed by prof.Whalley as it was mentioned in application (4) in 1988 as the must suitable technique to model the hybrid systems related to long drive shafts whilst considering the five segments parameters. At the end, the results obtained will be compared with the lumped parameter and finite element methods and demonstrated later in details in chapters III and IV.

Chapter III

System Mathematical Modeling

3.1. Helicopter Dynamics Fundamentals

Rotating machines are widely used in various engineering applications, like marine propulsion systems, vichles, power stations, , helicopter engines, machine tools, household accessories. The trend for such systems design in the modern engineering is to lower weight and operate at super critical speeds. The accurate prediction of the rotor system dynamic performance is much important in designing any type of such machinery. During past years, There was many studies related to the area of rotor dynamic systems. In this regard, of the huge number of published works, the most comprehensive part of the literature on the rotor dynamics analysis are concerned with the determination of critical speeds, natural whirling frequencies, the frequency instability sills and regions (or bands), and finally the unbalance and the transient responses. Apart from the mentioned analyses above, some works also study balancing of rotors, estimation of the bearing dynamic parameters, the nonlinear response analysis and condition monitoring.

The helicopters have different aerodynamic characteristics according to their type; therefore different mathematical models can be developed to represent their flying dynamics, which is very complex (Salazar, 2010).

Control and Stability analysis is a quite complex process since it is dealing with both angular motions and linear of the helicopter studied with respect to all of the three axes required to specify the position of the helicopter in space. Stability can be defined as the trend of the helicopter to preserve or to deviate from an settled flight condition.

Control is the ability of the helicopter to be maneuvered or steered from one flight condition to another. The term “flying qualities” is used to designate those characteristics that are relevant to both of these aspects. Helicopter stability and control analyses are similar to those for other aircraft types but are complicated by the ability of the helicopter to hover as well as to fly in any direction without change of heading (U.S. Army materiel, 1974).

For the helicopter to be able to flight, the lift produced via main rotors should be more than the helicopter’s weight.

Once airborne, if the thrust produced by the main rotors of the helicopter is higher than the drag force the helicopter can move.

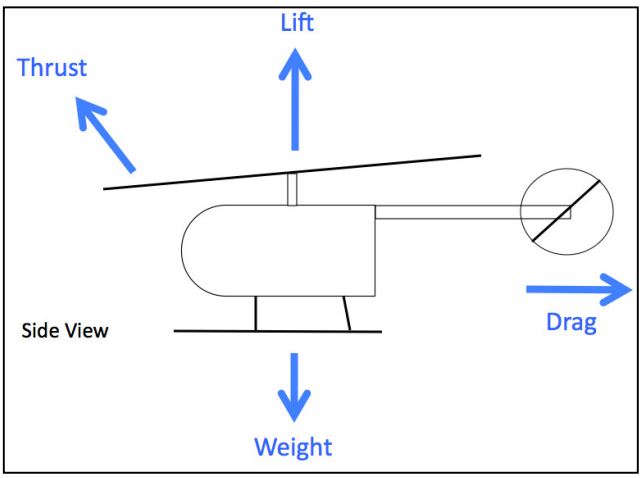

Figure 3.1 Forces acting on helicopter in flight

(121st ASEE Annual Conference & Exposition, 2014)

Helicopters require four essential systems to flight properly. Two of this systems (the engines & controls) can be found in other type of vehicles (for example cars, trains, boats, etc.), but the mission of helicopter requires special design regards and that is why the remaining two systems (tail or anti-torque and main rotor systems) are unique.

1- Engine: All helicopters need a "master mover". Internal combustion engines (ICE's) have been utilized in the early helicopter designs and still are used in wide variety smaller helicopters (for example Robinson helicopters). And differently, turbine jet engines (mostly uising two) are utilized with higher performance purposes, such as military needs and heavy lifting. Newly, as an attempts to reduce the emissions, passenger carrying helicopters powered with an electrical engines were tested successfully (European Rotorcraft Forum 2014, Conference Programme & Proceedings, 2014).

   Many helicopters use the turbo-shaft engine in order to drive both the main transmission and the rotor systems. The major difference between the turboshaft and the turbojet engine is that the most of the energy generated by the expanded gases is used to actuate the turbine rather than generating thrust throughout the expulsion of the exhaust gases.

   Helicopter engines can be classified into two main categoties:

a- Reciprocating engines, or as it is called sometimes piston engines, are mostly used in the smaller helicopters. Hence, training helicopters are almost using the reciprocating engines since they are inexpensive and comparatively easy to operate.

b- Turbine engines: they are relatively more powerful, robustness and they are applied in a different types of helicopters. They can generate an enormous power compared with their immensity but thay are ordinarily more costly and expensive to run and operate. Turbine engines that are hired in helicopters works in a different way from those implemented in airplane implementations. Generally speaking, In the most applications and uses, the outlets of exhaust are simply releases expanded gases and don't participate to the helicopter forward movement. It can be concluded that approximately 75% of the incoming air flow is used to cool down the engine.

2- Main rotor: The main rotor of the helicopter is the rotary wing that is providing the lift in order to make the helicopter able to fly. Using the power generated from the engine to rotate the rotor blades, lift will be produced. Flight can be accomplished the moment that the liftting force is greater

than the helicopter weight (European Rotorcraft Forum 2014, Conference Programme & Proceedings, 2014).

The main rotor comprises of a rotor blades, hub and mast. The mast is a simple hollow shaft extending upwards and in some models is supported by the transmission. Secon part the hub can be defined as the attachment point for the main rotor blades. The blades are attached to the hub using any number of available different methods.

The classification of the main rotor systems is according to the way in which the main rotor blades are installed and move relatively with the main rotor hub. At the end, main rotor systems are classified into three basic classifications: rigid, semirigid, or fully articulated where some modern rotor systems, for example the bearingless main rotor system, is using an engineered set of these types. The primary objective of main rotor transmission is the reduction of the engine output rpm to the best rotor rpm. Obeviously, the reduction is differs for various helicopters. For example, suppose that the rpm of a paticular helicopter engine is 2,380, so for rotor speed of 476 rpm would require a 5:1 reduction. Similarly, if 7:1 reduction is used, that would denote the rotor will turn at 300 rpm.

3- Anti torque (tail rotor) system: The helicopter realize flight via main rotor rotation. Since the helicopters are not

grounded during flight, a system is required to neutralize the torque generated via main rotor in order to avoid making the body spinning in the other direction. This system “anti-torque” is achieved using a minial propeller (rotor) that generates a moment required to neutralize or oppose the torque generated by the main rotor. The tail (anti-torque) rotor is run using the same engine for the main rotor. (European Rotorcraft Forum 2014, Conference Programme & Proceedings, 2014).

separate antitorque system is needed in helicopters with a single (not co-axial) main rotor system. This is mostly accomplished using a differenet pitch, tail rotors or antitorque rotors. Pilots change the thrust generated from antitorque system in order to preserve directional control when there is any changes in the main rotor torque, or it can be used to make the necessary heading changes during the flew. Most helicopters can actuate the shaft of the tail rotor (antitorque) from the transmission system to assure the rotation and control of the tail rotor in case if the engine somehow quits. mostly, antitorque negative thrust is required in auto-rotations in order to dominate transmission friction. The system of antitorque drive comprise of the antitorque drive shaft and the antitorque transmission fixed at the side end of the tail boom. The tail drive shaft might

comprise of a long shaft or a number of shorter shafts joined at the ends with couplings and This will allow the tail shaft to twist with the tail boom. Furthermore, The tail rotor transmission supply a right angle drive for the antitorque rotor and might include gearing to control the output angular speed to the best revelution per minute (rpm). In addition, tail rotors can also consist of an intermediate gearbox in order to turn the power up a vertical fin or pylon.

Since the amount of power given to the msin rotor is changeable, this changes the torque reaction on the fuselage, and the thrust of the tail rotor must be increased or decreased to neutralize the torque effect (Coyle, 2009).

In a typical light helicopter, the tail rotor can take between 5 and 15% of the total power installed (Coyle, 2009).

4- Controls: in helicopters there are many complex control systems. Because of the rotational dynamics of the system, numerous factors including the torque and particularly gyroscopic effects should be considered in the pilot/machine interface. In helicopter controls can be classified into five main types: collective pitch control, cyclic pitch control, engine throttle, and two anti-torque/rudder pedals. The pilot can control the all of the degrees-of-freedom of helicopter movement.

Though most of the modern helicopters are designed with computerized control system capabilities, mostly all helicopters nowadays in service are using direct mechanical connections (linkages) linking the pilot flight controls to the rotor blades (European Rotorcraft Forum 2014, Conference Programme & Proceedings, 2014).

3.2. Project Overall Description (Schweizer 300C)

In this research, Schweizer 300C (shown in figure 3.2) will be considered as case study to apply the selected modeling techniques.

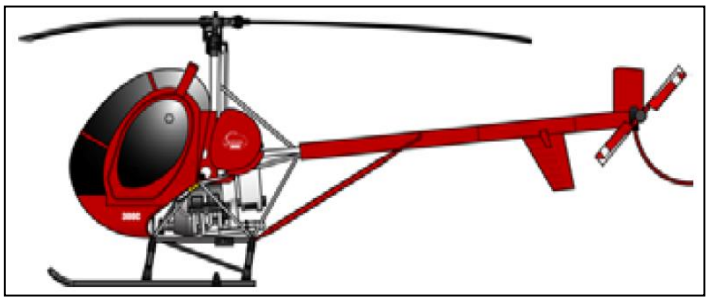

Figure 3.2 Schweizer 300C

(Schweizer 300C Helicopter Technical information/SZR-004, 2008)

The RSG 300 series (previously known as Sikorsky S300, then Hughes 300 and finally Schweizer 300) class of swift usefulness helicopters was initially manufactured by the Hughes Helicopters, as an upgrade of Hughes 269. Then produced by Schweizer Aircraft, its basic design was in manufacturing for about 50 years. Its single main rotor with three blades and piston powered (S-300) is primarily used for training and agriculture because of its cost-effective platform.

After that, in 1964, Hughes shows the slightly larger Model 269B with three seats which was called Hughes 300. Also in 1964, the Hughes 269 helicopter set a wear record of 101 hours.

In 1969, the Hughes 300 was improved and the replacement take place with Hughes 300C (or as it is called sometimes 269C), which received Federal Aviation Administration (FAA) certification in May 1970 after its first successful flew on 6 March 1969. The new model introduced a high powerful 190 hp (equal 140 kW) Lycoming HIO-360-D1A engine with increased diameter rotors, allowing a payload increase up to 45%, plus other overall performance enhancements. This model was the beginning that Schweizer began manufacturing under license of Hughes in 1983.

Later in 1986, Schweizer get all rights of the helicopter from the manufacturer McDonnell Douglas, which already had purchased Hughes Helicopters two years earlier in 1984. After Schweizer get the Federal Aviation Administration (FAA) Certificate, the helicopter -for short time- was called (Schweizer-Hughes 300C). Then it was simplified as Schweizer 300C. Over the years, the basic design kept unchanged, as Schweizer doing more than 250 minor elaborations.

After that, on August 26th, 2004 Schweizer was sold to Sikorsky Aircraft. The purchased Schweizer 300 models help filling a gap in Sikorsky helicopter line, which was well recognized for its heavy and medium usefulness and also cargo helicopters.

About five years later in February 2009, the Schweizer 300C was again rebranded as Sikorsky S-300C.

In the last year (2018) the model certificate of the Hughes 269 product line again sold by Sikorsky manufacturer to Schweizer RSG located in Fort Worth Texas. As a result, the new manufacturer, which affiliated with Rotorcraft Services Group, will back up the existing fleet and as per plans it will begin to produce new aircraft at the airport of Meacham located in Fort Worth, Texas.

Over the last 50 years, approximately 3,000 units of Schweizer 269/300 have been manufactured and flown with two different branch names Schweizer and Hughes including foreign-licensed building military and civil training aircraft. It was manufactured by redesigning the body of the model 300 and also by adding a turbine.

Finally, Schweizer S-333 is developed by extra improvements of the dynamical elements to get better performance of the turbine engine. In the few recent years the cabin was upgraded when a supplemental type certificate (STC) was widened to install the helicopters dual screen electronic flights display known as Garmin (G500H) as well as the Standby Attitude Indicator (Mid-Continent MD302).

At the end, it can be concluded that the model 269C is basically the same design and specifications as the basic configuration of the helicopter described in the 269s series excluding for equipment, furnishings, paint finish and also the later general design improvements.

3.2.1. Transmission System

The power train system consists of a belt drive tranmission, belt drive cluch control, main rotor gear drive assembly (main transmission), main rotor drive shaft, tail rotor drive shaft, tail rotor trannsmission and related miscellaneous components. Engine output is coupled through the belt drive transmission and associated pulleys to the tail rotor and the main transmission which drives the main rotor (Hughes Schweizer 269 helicopter maintenance instructions 2, 2014).

Awareness is being given to recovering the monitoring the helicopter rotor systems, for the following reasons:

a- additional safety development via the premature detection and revelation and of primary failures.

b- minify the maintenance load by reducing or basically changing high-frequency on aircraft rotor element checkings (European Rotorcraft Forum 2014, Conference Programme & Proceedings, 2014).

To achieve these objectives, rotor monitoring must go beyond the classical path and balance management according to measurement of airframe vibration and one way is more centeralized sensing on the rotor elements.

The primary purpose of a helicopter drive system is to transmit the power from engine(s) to the lifting rotor(s) and to the antitorque rotor, if one is provided. Power takeoff from the main drive is used to power the accessories. The basic transmission elements required to

accomplish these tasks depend upon the aircraft rotor configuration (single rotor, tandem rotors, coaxial rotors, etc.) and also upon the location and orientation of the engine(s) with respect to the rotor. In general, the largest reduction is taken in a main gearbox, whose output drives the main rotor (U.S. Army materiel, 1974).

Supplementary gearboxes may be used where necessary to change the direction of the drive and speed. Reductions can be accomplished in these as well. Special-purpose gearboxes may be included in the drive system; e.g., the tail gearbox that drives the antitorque rotor in a single-rotor machine, and the intermediate and combining gearboxes necessary to provide a synchronizing link between the main rotors of a multirotor machine (U.S. Army materiel, 1974).

Initial considerations that affect the design of the transmission drive system should consider the tasks to be assigned for the helicopter. They are usually used for:

a- Search and rescue.

b- Observation.

c- Transport.

d- Attack.

e- Heavy lift.

f- Any combination of the mentioned tasks.

Helicopter performance requirements which affect the final selected design process of a power train is including:

a- Payload.

b- system reliability.

c- hovering capability.

d- power requirements of various mission segments.

e- operational environment.

f- noise level.

g- mission altitude.

After taknig in considration these mission requirements can be converted into some certain design requirements and specifications such as design life of every transmission components, power of the engine and speed versus the rotor reveutions per minute, and the reliability of each individual component.

The design process of the transmission system also is governed by the selected configuration of the helicopter.

The loads that must be withstanded by the transmission system elements are a function of both power to be transmitted and speed (T~hp/rpm). Hence, the required engine power from the engine can be calculated according to the maximum performance needs of the mission. Similarly, The input revelutions per minute (RPM) is based on the output speed from the engine while speed of the rotor is usually specified by the tip angular speed of the blades.

Thus, the overall transmission ratio can be obtained readily if rotor diameters are known. Splitting this ratio among the various transmission elements to obtain the minimum-weight design can be accomplished by preliminary design layout iterations. In general,

however, it is better to take the largest reduction in the final stage. Trade-off studies should be made to evaluate different arrangements to determine minimum weight design. These studies should include housing design and should be sufficiently extensive to provide data for plotting a graph of weight versus gear ratio distribution (U.S. Army materiel, 1974).

Main tramsmission input shaft speed is 2162 rpm and main transmission output speed to rotor is 483 rpm belt tranmission output speed through the tail rotor driveshaft to the tail rotor transmission is 2162 rpm.tail rotot tranmission output to the tail rotor is 3178 rpm (Hughes Schweizer 269 helicopter maintenance instructions 2, 2014).

3.2.2. Mechanical Rotational Systems

As specified earlier in Chapter II, there are three basic componenets are existing in modeling basic mechanical systems: springs, dampers and masses. Though each of these components is a system with all the features (inputs, state variables, parameters, and outputs), using the expression “system” usually means a collection of interacting componenets. Rotational componenets (rotats about one axis) are briefly explained to handle the rotary mechanical systems. (Kulakowski, Gardner, & Shearer, 2007).

In this part, lumped parameter systems will be considered, in which every specific element will be identified based on its characteristics and can be recognized from other components (in distinction from distributed systems) (Lalanne, 2014).

Three basic passive components can be realized, each one has its own function in the linear mechanical systems which coincide to the coefficients of the expressions of the three kinds of forces which are objecting the movement. These passive components are frequently utilized in the structures modeling to symbolize a physical systems in simple terms (Lalanne, 2014).

The three elements to be defined below are mass (Inertia), stiffness and damping.

3.2.2.1. Rotational Inertias (Gears and Blades)

In helicopters, gearboxes are crucial elements. They are in general, compact and employ trains which comprise of various types of gears (spur, bevel, planetary and helical). There are many challenges and questions regarding the gearbox design, for example: why specific type of gears were choosen and how to select the ratios in order to reduce the space needed. Other challenge is to detect the suitable ratios for the substantial reductions of speed in the drive train, after that, design and implement the gearbox in such a way to accomplish it.

High-performance gears are case hardened and ground with a surface finish of 20 rms or better. Gearing usually is designed for unlimited life with 0.999 reliability or better at the maximum power (other than instantaneous transients) transmitted by that mesh. Primary drive gears should be made from consumable electrode vacuum melt (CEVM) processed steel, which is less susceptible to fatigue failure than is air-processed steel (U.S. Army materiel, 1974).

One of the primary causes of premature gear failures can be traced to high load concentrations induced by flexible mounting, especially when the housings are made of lightweight, low-modulus materials such as magnesium or aluminum. Experience indicates that, wherever possible, all heavily loaded gears should be straddle-mounted to minimize deflections and prevent end loading (U.S. Army materiel, 1974).

The gears to be used are didicated according to the type of engine(s) used to operate the helicopter, and the location in relationship to both the transmission and rotor.

In this research, an ideal inertias, illustrated schematically in the free-body diagram in Figure 3.3 rotates relatively to rotational non-accelerating reference frame, which is commonly considered as the ground (earth).

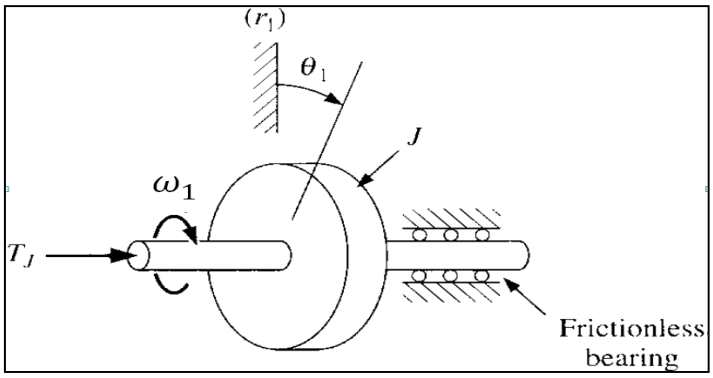

Figure 3.3 Free-body diagram of an ideal rotational inertia

The componental equation for the inertia (J), according to Newton's second law ($F = ma$) applied with rotational motion, can be expressed as following

$$T_J = J\alpha_1$$

$$T_J = J\frac{d\omega_1}{dt}$$

where ω_1 is the angular speed of the (mass) inertia measured relatively to the selected reference (ground or earth) and T_J is the total external torques (or as it can be twisting moments) uilized on the inertia.

Because $\omega_1 = \frac{d\theta_1}{dt}$, the variation of θ_1 can be related to T_J as

$$T_J = J\frac{d^2\theta_1}{dt^2}$$

From the above equation, it can be noticed that, the response of the inertia according to the utilized torque T_J is analogous and similar to the acquired response of the mass subjected to some applied force F. Furthermore, it takes some time for the angular displacement, angular velocity,and kinetic energy, to be accumulated after the implementation of the torque, and hence it will not be factual to try to force a sudden changes in angular speed ω_1 on the rotational inertia.

3.2.2.2. Rotational Stiffness (Shafts)

Deflection and stiffness are relevant to nearly every part in design of helicopter. These concepts are related to helicopters via numerous examples, inclusive the blades of main rotor where stiffness is one of the most distinct. Since they are spinning during normal running, the blades should be designed in order to reduce the axial deflection because of the tension generated from centrifugal loading also to reduce bending due to the blades weight because of static loading. According to that, blades of helicopter may be modeled as a fixed-free cantilever

beam (European Rotorcraft Forum 2014, Conference Programme & Proceedings, 2014).

Since shafts are a focal part of the helicopter and they are flight critical elements, failure may give rise to control wastage and induce a crash. Many shafts are used in the drive train of a helicopter to transfer the power from the engine to the main rotor and then from the tail rotor gearbox to the tail (anti-torque) rotor. The tail rotor is usually a long distance from the main rotor and must operated at angular speeds of 4,000 - 8,000 rpm, leading to various design challenges (European Rotorcraft Forum 2014, Conference Programme & Proceedings, 2014).

There are many challenges to transmit torque over long distances at high speeds. The natural frequencies of main and tail helicopter shafts, and investigations of the design considerations will affect the shafts geometry choices. There are an alternative helicopter designs that can fulfill the anti-torque role without using tail rotors.

Transmission shafting usually is hollow with as high a diameter-to-thickness ratio as is practicable for minimum weight. These shafts are subjected to torsional loads, bending loads, axial tension or compression, or to a combination of all of these. Because the shaft is rotating with respect to the bending loads, this loading is of a vibratory nature. Due to this combination of steady and vibratory loads, an interaction equation must be used to calculate a margin of safety. Such an equation based upon the maximum shear theory of failure can be

used when all three types of stresses are present (U.S. Army materiel, 1974).

Gear shafting usually is designed for unlimited life at a power level and reliability commensurate with the geartooth design. Engine drive and tail rotor drive shafting carry torsional loads primarily, although some bending may be induced by semiflexible couplings spaced dong such shafts to accommodate misalignment (U.S. Army materiel, 1974).

Based on the that, the rotating shaft can be modeled and treated as a perfect spring in case if the torque (moment) needed for accelerating the rotational inertia of the shaft can be assumed negligible when compared with the transmitted torque. Occasionally, the transmitted torques by the shafts are small when compared with the torques required to accelerate the inertia of the given shaft and in this case it should be treated and modeled as a normal inertia; and even sometimes a real shaft can be modeled as a combination of inertias and springs.

Figure 3.4 below shows the an ideal shaft when transmitting torque T_K when both ends of it are displaced rotationally according to the local references r_1 and r_2.

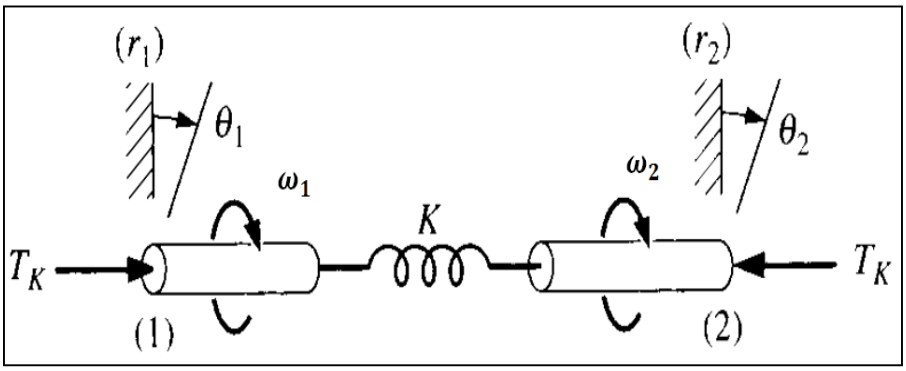

Figure 3.4 Free-body diagram of an ideal (shaft) spring

The componental equation for the rotational spring, according to Hook's law ($F = kd$) applied with rotational motion, can be expressed as following

$$T_K = K(\theta_1 - \theta_2)$$

where θ_1 and θ_2 are the angular displacements of the shaft ends compared with their local references r_1 and r_2 , so, in derivative form, the above equation can be writtin as

$$\frac{dT_K}{dt} = K(\omega_1 - \omega_2)$$

where ω_1 and ω_2 in the above equation are the angular velocities of the both ends of the shaft. As it can be seen from figure (3.4) In this case, the utilized sign for motion will be clockwise positive when the shaft was viewed from the left hand side (LHS), and the sign for torque will be clockwise positive when applied from the left hand side (LHS).

The comments regarding the output response from a translational springs to the step input change in the velocity difference between the shaft ends apply simialrly well to that of a rotational springs to the step input change in the angular velocity difference between the rotasional shaft ends.therefore, it will be unconscionable to try to force a step input change of the torque in the rotational springs since that would be an attempt to suddenly change the energy stored in the studied shaft and in a real case that does not include sources of an infinite power.

3.2.2.3. Rotational Viscous Dampers (Bearings)

Bearings are flight critical elements of helicopters. They are used to support considerable rotating components substantial to fulfill flight.

The most significant bearings are that used for the main rotor. They are typically consisting of large ball bearing assemblies that provide the connection between the stationary helicopter fuselage and the shaft of the rotating main blades (European Rotorcraft Forum 2014, Conference Programme & Proceedings, 2014).

The bearings for the power train are selected or designed for overhaul intervals of at least 3000 hr. All critical bearings are made from M-50 type steel made by the consumable electrode vacuum remelt process (AMS 6490),SAE 52100 steel consumable electrode vacuum melted (AMS 6440) to obtain maximum reliability. In high speed applications, bearing life is a function of the centrifugal fbrce imposed upon the bearing rotating elements as well as of the radial and thrust load. Where a stack of Bearings is required to support a gear shaft, distribution among the individual bearings must be considered. The selection of high speed bearings often involves a complex computer solution that considers the effects of load and speed as well as of minute changes of internal bearing geometry, i.e., contact angle and radial-axial clearances (U.S. Army materiel, 1974).

Usually, Bearings are build with separate races (inner and outer), although sometimes as an economical option,shaft may be used in such way as inner or outer race. Advisability of using such criteria would depend upon so many factors for example: the complexity, size, and total costs of the involved components. At this time, in advanced design applications, integral races are used extensively.

In the selection of bearings for helicopter transmissions, the principal trade-offs are combinations of standardization, initial cost, noise, resistance to shock, frequency and ease of repair or replacement, degree of complication in shaft and housing design, and resistance to contamination. In some instances, it may be necessary to employ special-purpose bearings for reliable high-speed operation and for thrust reversals. Special attention to such trade-offs and requirements is necessary during the preliminary design phase because system weight, cost, reliability, and maintainability are affected significantly by decisions involving transmission bearings and supports (U.S. Army materiel, 1974).

Same as friction in the translational systems between the moving elements gives translational dampings, friction between the rotating elements in a rotational systems is the source of the rotational damping. When the surfaces are lubricated perfectly, the friction in this case is generated from the shearing of the thin film of the used viscous fluid, leading to constant damping coefficient B, as shown below in Figure 3.5, which utilizes a diagram of the cross section with the transmitted torque.

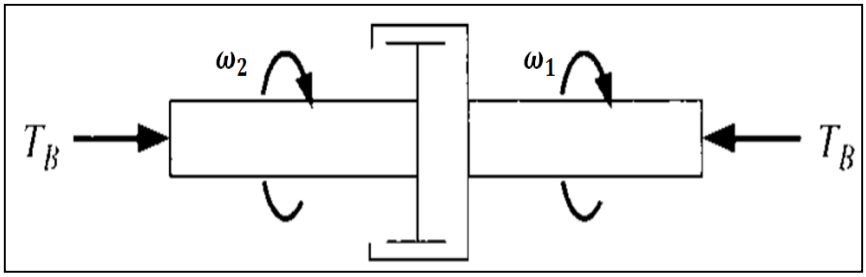

Figure 3.5 Free-body diagrams of an ideal rotational damper

The componental equation for an idea rotational damper can be presented as

$$T_B = B(\omega_1 - \omega_2)$$

Where B is the damping coefficient and T_B is the transmitted torque by the selected damper.

Since it dissipates energy, the rotational dampers are specified as a D-type element.

3.3. System Mathematical Modeling Methodology

The well recognized method used to deal with engineering problems is via formulating the model mathematically, which could be transformed to the discrete (separated) time domain in order to estimate the system response performance, taking in consideration the different aspects with the set of required objectives (Hui & Christopoulos, 1991).

As declared earlier, Lumped parameter method- LPM, Finite element method - FEM and the Hybrid Modeling method - HM are proposed to be used in this study, to investigate and examine the performance and response of the system introduced earlier in section (3.2) with the objectives and outcomes in Chapter I, section (1.3).

Actully, the system shown in section (3.2) can be categorized as a hybrid system, since it includes lumped and distributed components. The distributed component represents the stiffness throughout the entir length of the main and tail shafts. On the other hand, the lumped components represent the viscous damping of the bearings and the

inertia of the gearboxes and blades at each side of the main and tail shafts.

The modeling technique of the hybrid systems will be based on the modeling methodology of long, slim shafts developed by Whalley, Ebrahimi and Jamil in 2005. Finalley, the outcomes of this method will be compared with the lumped parameter and finite element methods.

According to that, the mathematical derivation of the elements is divided mainly into two parts. Lumped is the first part, representing the bearings, gearboxes and blades and it is modeled using ordinary differential equations (ODE). Distributed will be the second part, to represent the main and tail shafts and it is modeled using partial differential equations (PDE).

It need to be observed here that the distributed parameter systems will not have a limited number of points where the state variables can be defined. Conversely, the lumped parameter system can be represented by a limited number of state variables (Close & Frederick, 1993).

In short, the bearings, gearboxes and blades of the referred hybrid system will deal with them and modeled as lumped parameters. This is common for all LPM, FEM and HM methods. With respect to the main and tail shafts, these will deal with them and modeled as lumped parameters while using both the LPM and FEM and will deal with them as distributed while using HM.

Finally, it is important to note that, the main and tail long, slim shafts will be modeled assuming that no torque at the load end.

Figures 3.6, 3.7 and 3.8 showing the detailed dimensions of the slected helicopter model.

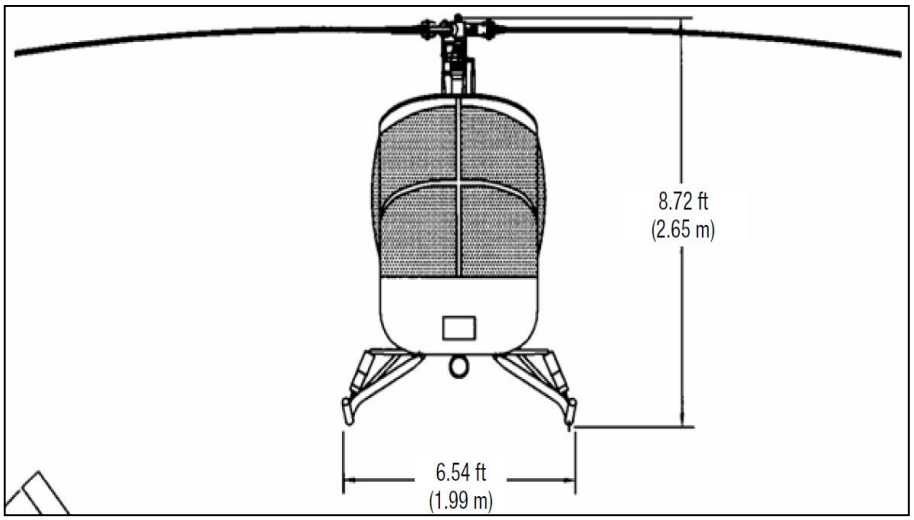

Figure 3.6 Aircraft dimensions (1)

(Hughes Schweizer 269 helicopter maintenance instructions 2, 2014)

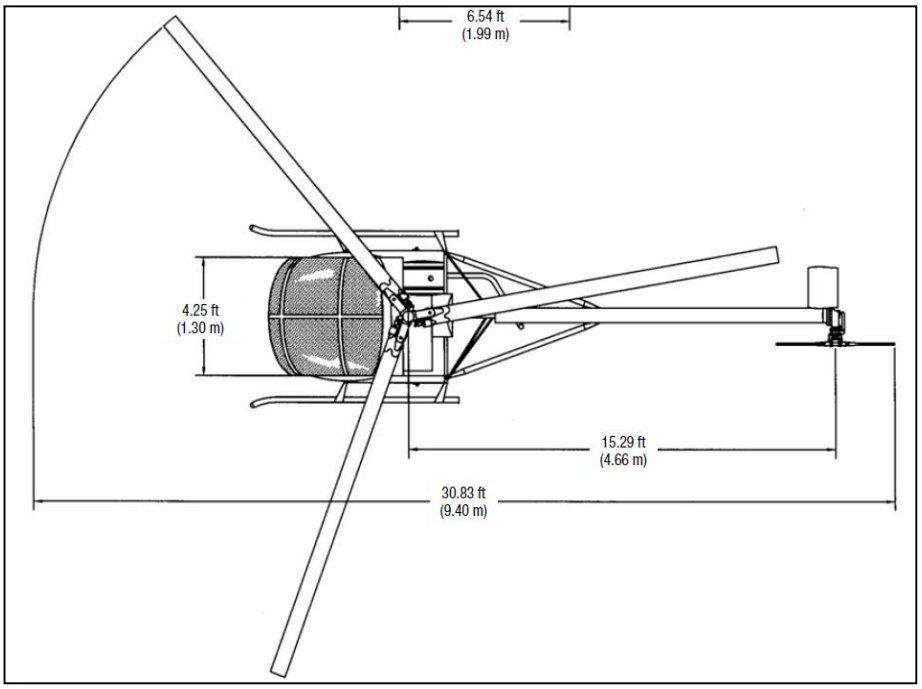

Figure 3.7 Aircraft dimensions (2)

(Hughes Schweizer 269 helicopter maintenance instructions 2, 2014)

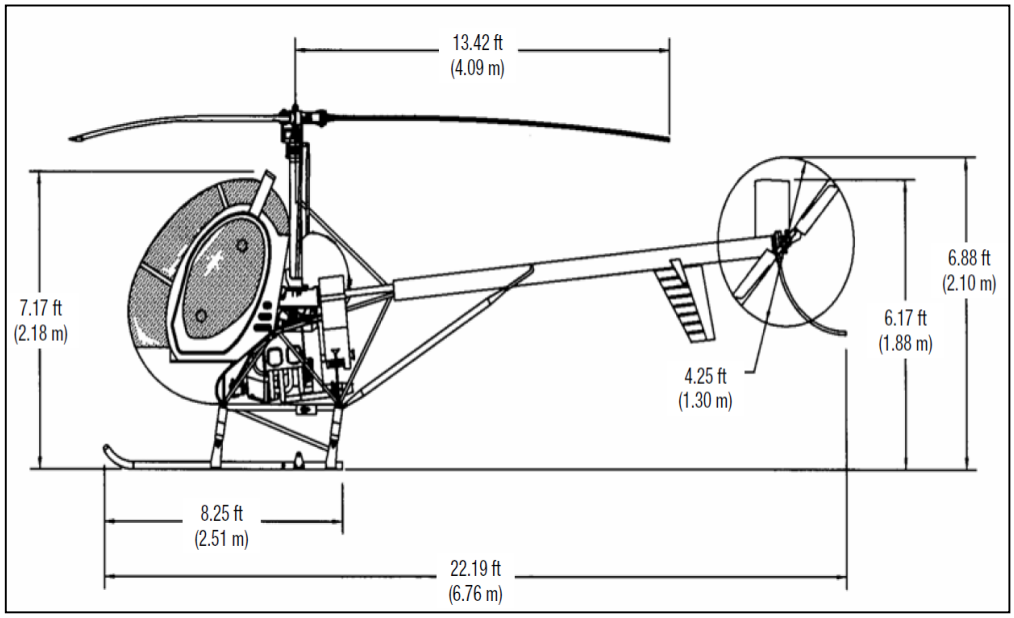

Figure 3.8 Aircraft dimensions (3)

(Hughes Schweizer 269 helicopter maintenance instructions 2, 2014)

3.3.1. Lumped Parameter Modeling Technique

In this part the selected system (tail and main rotors ans shafts) will be modeled as lumped parameter model, with two rotors and long, slim shaft as it is shown below in figure 3.9

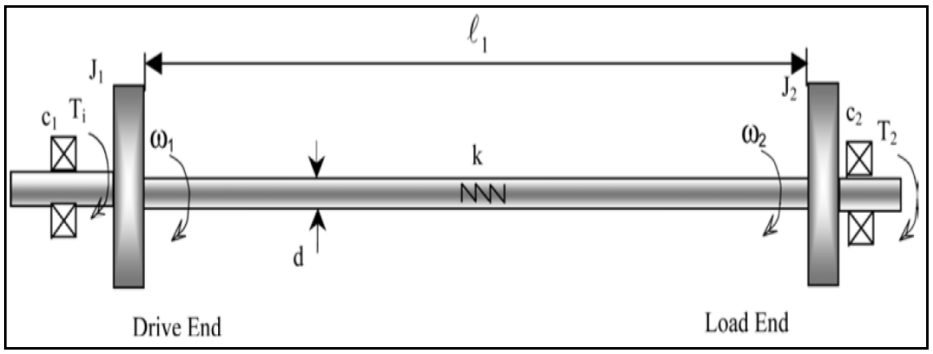

Figure 3.9 Lumped parameter model

(Whalley, Ebrahimi, & Jamil, 2005)

The governing equations for this system can be derived as following

$$T_i(t) = J_1\alpha_1(t) + c_1\omega_1(t) + k\left(\theta_1(t) - \theta_2(t)\right) \quad (3.1)$$

In terms of $\theta_1, \theta_2, \dot{\theta}_1, \ddot{\theta}_1$

$$T_i(t) = J_1\ddot{\theta}_1(t) + c_1\dot{\theta}_1(t) + k\big(\theta_1(t) - \theta_2(t)\big) \tag{3.2}$$

Using $D = \frac{d}{dt}$

$$T_i(t) = J_1D^2\theta_1(t) + c_1D\theta_1(t) + k\big(\theta_1(t) - \theta_2(t)\big) \tag{3.3}$$

Similarly for $T_2(t)$

$$T_2(t) = J_2\alpha_2(t) + c_2\omega_2(t) + k\big(\theta_2(t) - \theta_1(t)\big) \tag{3.4}$$

Uning $k\big(\theta_2(t) - \theta_1(t)\big) = -k\big(\theta_1(t) - \theta_2(t)\big)$ and express the above equation in terms of $\theta_1, \theta_2, \dot{\theta}_2, \ddot{\theta}_2$

$$T_2(t) = J_2\ddot{\theta}_2(t) + c_2\dot{\theta}_2(t) - k\big(\theta_1(t) - \theta_2(t)\big) \tag{3.5}$$

Using $D = \frac{d}{dt}$

$$T_2(t) = J_2D^2\theta_2(t) + c_2D\theta_2(t) - k\big(\theta_1(t) - \theta_2(t)\big) \tag{3.6}$$

Using the following assumptions:

a- Zero initial conditions

b- $T_2(t) = 0$ (load end)

Following laplace transform and inversion, equations (3.3) and (3.6)

$$\begin{bmatrix}\omega_1(s)\\ \omega_2(s)\end{bmatrix} = \frac{\begin{bmatrix}J_2s^2 + c_2s + k & k\\ k & J_1s^2 + c_1s + k\end{bmatrix}}{\Delta(s)}\begin{bmatrix}T_i(s)\\ 0\end{bmatrix} \tag{3.7}$$

Note that in equation (3.7) the denominator is

$$\Delta(s) = J_1J_2s^3 + (J_1c_2 + J_2c_1)s^2 + (J_1k + J_2k + c_1c_2)s + (c_1 + c_2)k$$

Now if the input torque is considered as sinusoidal wave $T_i(s) = \sin(\omega t)$

Then for $t >> 0$

$$\begin{bmatrix}\omega_1(s)\\ \omega_2(s)\end{bmatrix} = \begin{bmatrix}J_2s^2 + c_2s + k\\ k\end{bmatrix}_{s=i\omega} T_i(s)/\Delta(s) \tag{3.8}$$

The resonance frequency is acquired when the output to input ratio amplitude reaches its maximum value, and in this case the phase at the load end is $\varphi_2 = -\pi/2$. Since

$$\Delta(i\omega) = k(c_1 + c_2) - (J_1c_2 + J_2c_1)\,\omega^2 + \{(J_1 + J_2)k + c_1c_2 - J_1J_2\omega^2\}i\omega \tag{3.9}$$

Then from equation (3.8) at resonance

$$\varphi_2(\omega) = -\tan\frac{(J_1 + J_2)k + c_1c_2 - J_1J_2\omega^2)\omega}{k(c_1 + c_2) - (J_1c_2 + J_2c_1)\,\omega^2} = -\frac{\pi}{2} \tag{3.10}$$

And from the above equation, the resonant frequency is given by

$$\omega^2 = \frac{k(c_1 + c_2)}{J_1c_2 + J_2c_1} \tag{3.11}$$

3.3.2. Finite Element Modeling Technique

While dealing with continuous engineering systems, the equations representing the response are dominated by partial differential equations (PDE), as mentioned in chapter II. The accurate solution of PDE considring all of the boundary conditions (B.C) is reachable for only comparatively simple systems (for example a uniform shaft). Numerical procedures and methods need to be utilized to solve the PDE and from that predict the response of the the selected system (Juang & Phan, 2001).

The finite element method (FEM) is a very usual method used in solving engineering complex problems. It is a method of solving PDE that symbolize physical systems through discretizing the systems in space dimensions.generaally, the discretizations are done locally through small parts of simple and arbitrary shapes (finite elements). In structural engineering for example, the structure is usually demonstrated as a collection of discrete (separate) trusses and beams components. The discretization method changes the PDE to matrix formulas or equations linking the inputs at particular points in the components to the outputs at the same points. In order to deal with equations through large areas, matrix equations of the smaller regions or subregions can be summed togther node by node to achieve the universal matrix equations (Juang & Phan, 2001).

FEM are usually patronized in order to be able to upgrade the accuracy of predicted results, from the LPM. This technique produces numerous eigenvalues, eigenvectors, and consequently mode shapes and decay rates with the increase of the parameters dimensions (stiffness, damping and mass) matrices (Whalley, Ebrahimi, & Jamil, The torsional response of rotor systems, 2005).

When using Finite Element Method (FEM) in modeling a long helicopter tail and main shafts,the modeling principle is dividing the shafts into n number of segments (sections) of the same length and each new sement will have its own features and can be considered as a

lumped. Here each shaft (tail and main) will be divided into five sections.

The lumped parameter elements are always expressed with using ordinary differential equations(ODEs), which will be evolved from the system shown eariler in this section with respect to the whole system by calulating the inertias and dampings.

Detailed ordinary differential equations (ODEs) and parital differntial equations (PDEs) and derivations using Finite element methods-FEM are outlined below.

Now, for example, If the considered shaft is splitted into five equal segments in which all segmens having the same properties, then this system can be modeled, as shown in fig 3.10

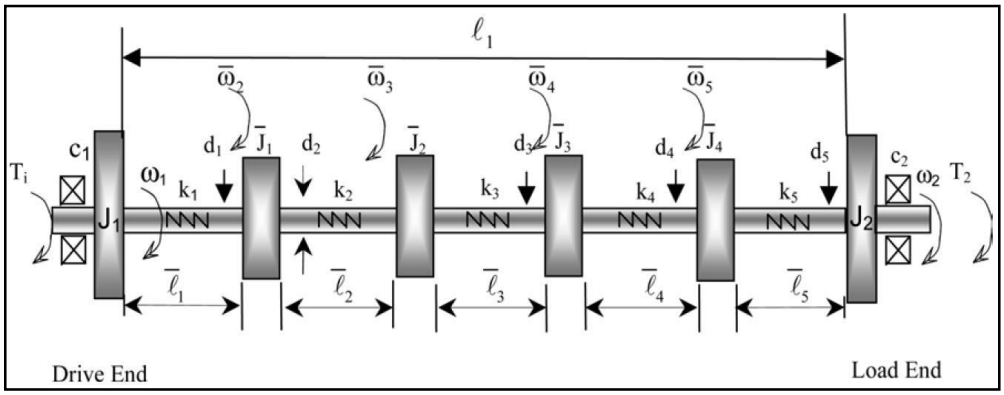

Figure 3.10 Finite element model

(Whalley, Ebrahimi, & Jamil, 2005)

The equations for the above system are

$$T_i(t) = J_1 D^2\theta_1\,(t) + c_1 D\theta_1\,(t) + k_1(\theta_1\,(t) - \bar{\theta}_2(t)) \tag{3.12}$$

$$0 = \bar{J}_1 D^2\bar{\theta}_2(t) + k_2(\bar{\theta}_2(t) - \bar{\theta}_3(t)) - k_1(\theta_1\,(t) - \bar{\theta}_2(t)) \tag{3.13}$$

$$0 = \bar{J}_2 D^2 \bar{\theta}_3(t) + k_3(\bar{\theta}_3(t) - \bar{\theta}_4(t)) - k_2(\bar{\theta}_2(t) - \bar{\theta}_3(t)) \quad (1.14)$$

$$0 = \bar{J}_3 D^2 \bar{\theta}_4(t) + k_4(\bar{\theta}_4(t) - \bar{\theta}_3(t)) - k_3(\bar{\theta}_3(t) - \bar{\theta}_2(t)) \quad (3.15)$$

$$0 = \bar{J}_4 D^2 \bar{\theta}_5(t) + k_5\left(\bar{\theta}_5(t) - \bar{\theta}_4(t)\right) - k_4\left(\bar{\theta}_4(t) - \bar{\theta}_3(t)\right) \quad (3.16)$$

$$0 = J_2 D^2 \theta_2(t) + c_2 D\theta_2(t) - k_5\left(\bar{\theta}_5(t) - \theta_2(t)\right) \quad (3.17)$$

Where

$$D\bar{\theta}_j(t) = \bar{\omega}_j(t)\ ,\ 2 \le j \le 5$$

And

$$D\theta_k(t) = \omega_k(t)\ ,\ 1 \le k \le 2.$$

Same as lumped parameter, using zero initial conditions and following Laplace transformation for the six equations (3.12) to (3.17)

$$[T_i(s), 0,0,0,0,0]^T = [Js^2 + Cs + K] \times [\theta_1(s), \bar{\theta}_2(s), \bar{\theta}_3(s), \bar{\theta}_4(s), \bar{\theta}_5(s), \theta_2(s)]^T \quad (3.18)$$

Equation (3.18) can be writtin in details as following:

$$\boldsymbol{K} = \begin{bmatrix} k_1 & -k_1 & 0 & 0 & 0 & 0 \\ -k_1 & k_1 + k_2 & -k_2 & 0 & 0 & 0 \\ 0 & -k_2 & k_2 + k_3 & -k_3 & 0 & 0 \\ 0 & 0 & -k_3 & k_3 + k_4 & -k_4 & 0 \\ 0 & 0 & 0 & -k_4 & k_4 + k_5 & -k_5 \\ 0 & 0 & 0 & 0 & -k_5 & k_5 \end{bmatrix}$$

$$\boldsymbol{J} = Diag(J_1, \bar{J}_1, \bar{J}_2, \bar{J}_3, \bar{J}_4, J_2)$$

$$\boldsymbol{C} = Diag(c_1, 0,0,0,0, c_2)$$

Since all the sections of the selected shaft are parallel and have equal lengths and diameters, then most symbols can be expressed as one symbol as shown below

$$\bar{J}_1 = \bar{J}_2 = \bar{J}_3 = \bar{J}_4 = J$$

And

$$k_1 = k_2 = k_3 = k_4 = k_5 = k$$

To be compared with the LPM, the transient (output angular speed) and the frequency response characteristics of the FEM can be calculated as shown below

$$\omega(s) = s[\boldsymbol{J}s^2 + \boldsymbol{C}s + \boldsymbol{K}]^{-1}[T_i(s), 0,0,0,0,0]^T \tag{3.19}$$

Where, in equation (3.19)

$$\omega(s) = [\omega_1(s), \bar{\omega}_2(s), \dots, \omega_2(s)]^T$$

And J, K and C are from equations (3.18).

Following inversion of equation (3.19) and then multiplication with the input vector $T_i(s)$, both the transfer functions can be derived from as following

$$\frac{\omega_1(s)}{T_i(s)} = \frac{num1}{\Delta_1(s)} \tag{3.20}$$

$$\frac{\omega_2(s)}{T_i(s)} = \frac{k^5}{\Delta_1(s)} \tag{3.21}$$

Note that the above equations (3.20) & (3.21) have the same $\Delta(s)$ (since it is single input-multiple output)and can be written in details as

$$num1 = s^{10}J^4J_2 + s^9J^4c_2 + s^8(8kJ^3J_2 + kJ^4) + s^78kJ^3c_2 + s^6(7J^3k^2 + 21k^2J^2J_2) + s^521k^2J^2c_2 + s^4(15k^3J^2 + 20k^3JJ_2) + s^320k^3Jc_2 + s^2(5k^4J_2 + 10k^4J) + 5k^4c_2s + k^5 \quad (3.22)$$

$$\Delta_1(s) = J_1J^4J_2s^{11} + s^{10}(c_1J^4J_2 + J_1J^4c_2) + s^9(kJ^4J_2 + 8kJ_1J^3J_2 + kJ_1J^4 + c_1J^4c_2) + s^8(kc_1J^4 + 8kc_1J^3J_2 + 8kJ_1J^3c_2) + s^7(7J_1J^3k^2 + 21k^2J_1J^2J_2 + k^2J^4 + 8kc_1J^3c_2 + 7k^2J^3J_2) + s^6(21k^2J_1J^2c_2 + 7c_1J^3k^2 + 21k^2c_1J^2J_2 + 7k^2J^3c_2) + s^5(15k^3J^2J_2 + 20k^3J_1JJ_2 + 6J^3k^3 + 15k^3J_1J^2 + 21k^2c_1J^2c_2) + s^4(15k^3c_1J^2 + 15k^3J^2c_2 + 20k^3c_1J^2JJ_2 + 20k^3J_1Jc_2) + s^3(5k^4J_1J_2 + 20k^3c_1Jc_2 + 10k^4J_1J + 10J^2k^4 + 10k^4JJ_2) + s^2(5k^4c_1J_2 + 10k^4Jc_2 + 5k^4J_1c_2 + 10k^4c_1J) + s(k^5J_2 + 4k^5J + k^5J_1 + 5k^4c_1c_2) + k^5c_1 + k^5c_2 \quad (3.23)$$

Then FEM resonant frequencies (ω) will be derived following the same procedure for lumped parameter model(LPM) putting $s = i\omega$ in equation (3.23). Since

$$\Delta_1(i\omega) = Re\big(\Delta_1(i\omega)\big) + Img\big(\Delta_1(i\omega)\big) \tag{3.24}$$

Where in equation (3.24)

$$\begin{aligned} Re\big(\Delta_1(i\omega)\big) = \{&(-c_1JJ_2 - J_1J^4c_2)\omega^{10} \\ &+ (kc_1J^4 + 8kc_1J^3J_2 + 8kJ_1J^4c_2 + kJ^4c_2)\omega^8 \\ &+ (-7c_1J^3k^2 - 21k^2J_1J^2c_2 - 7k^2J^3c_2 \\ &- 21k^2c_1J^2J_2)\omega^6 \\ &+ (15k^3c_1J^2 + 15k^3J^2c_2 + 20k^3c_1JJ_2 \\ &+ 20k^3J_1Jc_2)\omega^4 \\ &+ (-10k^4c_1J - 5k^4c_1J_2 - 10k^4Jc_2 - 5k^4J_1c_2)\omega^2 \\ &+ k^5c_1 + k^5c_2\} \end{aligned}$$

$$\begin{aligned} Img\big(\Delta_1(i\omega)\big) = i\omega\{&-J_1J^4J_2\omega^{10} + (8kJ_1J^3J_2 + kJ^4J_2 \\ &+ kJ_1J^4 + c_1J^4c_2)\,\omega^8 + (-7k^2J^3J_2k^2J^4 - 7J_1J^3k^2 \\ &- 21k^2J_1J^2J_2 + 8kc_1J^3c_2)\omega^6 + (21k^2c_1J^2c_2 \\ &+ 6J^3k^3 + 15k^3J_1J^2 + 15k^3J^2J_2 + 20k^3J_1JJ_2)\omega^4 \\ &+ (-20k^3c_1Jc_2 - 10k^4JJ_2 - 5k^4J_1J_2 - 10J^2k^4 \\ &- 10k^4J_1J)\omega^2 + k^5J_2 + k^5J_1 + 4k^5J + 5k^4c_1c_2\} \end{aligned}$$

Then,similar to LPM at the resonance, the load end rotor phase (φ_2) can be calculated by

$$\varphi_2 = -tan^{-1}\left(\frac{Img\left(\Delta_1(i\omega)\right)}{Re\left(\Delta_1(i\omega)\right)}\right) = -\pi/2$$

Thus

$$Re\left(\Delta_1(i\omega)\right) = 0$$

As it can be seen from equation (3.20) to (3.24),compared with the LPM, there will be a huge growing in the model complexity while modeling the two rotor-shaft system, using FEM method.

Compared with lumped parameter model, five sections finite element model shown in equation (3.23) produces eleven eigenvalues, while the LPM produces three only.

The lure, heartening more prediction accuracy, utilizing more finite element segments, will plainly cause computational errors. using ten shaft sections model, the equivalent system of equation (3.23) would rise to order 21 generating equivalent number of eigenvalues and eigenvectors.

3.3.3. Distributed-Lumped (Hybrid) Modeling Technique

In this part a hybrid (consisting of distributed-lumped) model-HM of the system comprised of dual rotor and shaft studied previously will be derived. As discussed earlier, the rotors (gearboxes and blades) and bearings (dampers) is modeled as rigid, lumped parameter(point-wise) elements .

Beacause of the tall and slim shaft dimensions, this element will be modeled as a distributed parameter element, and both the stiffness and

inertia and will be continuous functions of the length of shaft. The parameters and model of this system are shown in figure 3.11 below

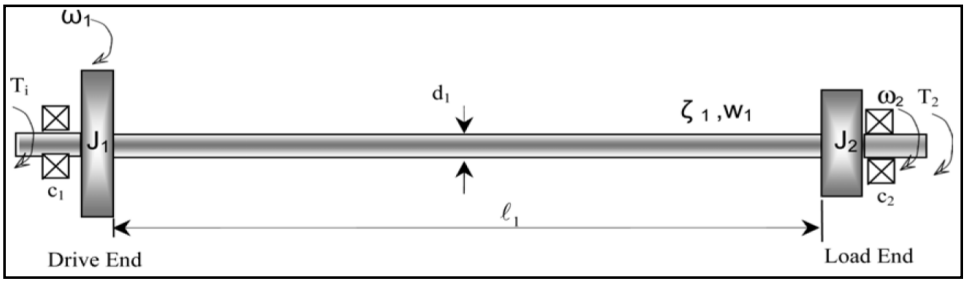

Figure 3.11 Distributed-Lumped Parameter model

(Whalley, Ebrahimi, & Jamil, 2005)

❖ **The distributed parameter shaft model torsional response**

In this inference, a shaft as uniformly distributed parameter, having diameter d and length l, is examined. The shaft consisting an infinte series of infiniesimal segments dx, in the length, which are undego torque inputs and outputs of $T(t,x)$ and $T(t,x+dx)$, respectively at a distance x and $x+dx$ along the shaft (Whalley, Ebrahimi, & Jamil, 2005).

Similarly, the corresponding inputs and outputs of angular velocity are $\omega(t,x)$ and $\omega(t,x+dx)$ respectively. Every segment has related series inductance $T(t,x)$ and L, which is an equipollent to the inertia per unit length of the shaft. Furthermore, A shunt capacitance $T(t,x)$ and C, is an equipollent to cpmpliance per unit length of the shaft. The internal friction of the shaft material can be supposed to be very small and will be neglected enabling all fricrional dissipation to be considered as generated from the bearings and windage only (Whalley, Ebrahimi, & Jamil, 2005).

Here

$$L = \frac{\rho \pi d^4}{32} \text{ (shaft inartia/m),}$$

and

$$C = \frac{1}{GJ_s} \text{ (shaft compliance/m).}$$

For analysis purposes the shaft consists of an infinte series of elements, as shown in firgure 3.12

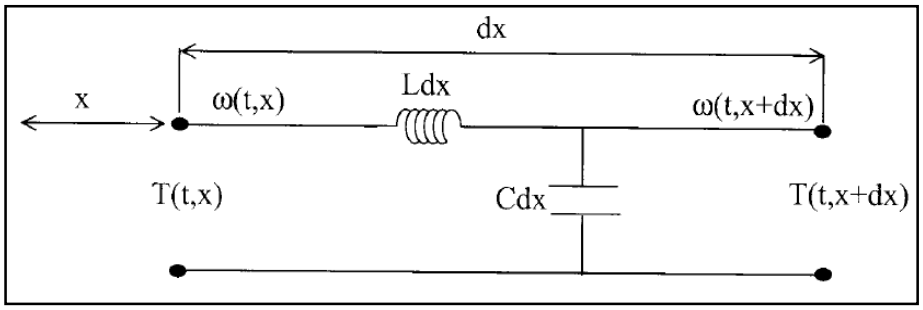

Figure 3.12 Incremental shaft element

(Whalley, Ebrahimi, & Jamil, 2005)

For equations

$$T(t, x + dx) - T(t, x) = -L \frac{\partial \omega}{\partial t}(t, x + dx)dx \tag{3.25}$$

$$\omega(t, x + dx) - \omega(t, x) = -L \frac{\partial T}{\partial t}(t, x + dx)dx \tag{3.26}$$

In the limit as $dx \to 0$ equations (3.25) and (3.26) become

$$\frac{\partial T}{\partial t}(t, x) = -L \frac{\partial \omega}{\partial t}(t, x) \tag{3.27}$$

$$\frac{\partial \omega}{\partial t}(t, x) = -C \frac{\partial T}{\partial t}(t, x) \tag{3.28}$$

Following Laplace transformations with respect to the time, assuming all initial conditions to be zero, then equations (3.27) and (3.28) can be rewritten as

$$\frac{\partial T}{dx} = -Ls\omega \tag{3.29}$$

$$\frac{\partial \omega}{dx} = -CsT \tag{3.30}$$

Where in equations (3.29) and (3.30)

$$T = T(s, x)$$

And

$$\omega = \omega(s, x).$$

After that, differentiating both equations with respect to x , equations (3.29) and (3.30) may be written as following

$$\frac{d^2T}{dx^2} = -Ls\frac{\partial \omega}{\partial x}$$

and

$$\frac{d^2\omega}{dx^2} = -Cs\frac{\partial T}{\partial x}$$

Hence

$$\frac{d^2T}{dx^2} = LCs^2T \tag{3.31}$$

And

$$\frac{d^2\omega}{dx^2} = LCs^2\omega \tag{3.32}$$

Equations (3.31) and (3.32) have the same form ans identical general solutions.

If a propagation function is defined as

$$\Gamma(s) = s\sqrt{LC}$$

Then the general solutions required are

$$T(s,x) = A\cosh\Gamma(s)x + \sinh\Gamma(s)x \tag{3.33}$$

$$\omega(s,x) = \bar{C}\sinh\Gamma(s)x + D\cosh\Gamma(s)x \tag{3.34}$$

When $x = 0$

$$A = T(s,0)$$

$$D = \omega(s,0)$$

Differentiang equations (3.32) and (3.34) with respect to x and equatin to (3.29) and (3.30) gives

$$-Ls\omega(s,x) = A\Gamma(s)\sinh\Gamma(s)x + B\Gamma(s)\cosh\Gamma(s)x \tag{3.35}$$

$$-CsT(s,x) = \bar{C}\Gamma(s)\cosh\Gamma(s)x + D\Gamma(s)\sinh\Gamma(s)x \tag{3.36}$$

Equation (3.34) with $x = 0$ becomes

$$-Ls\omega(s,0) = B\Gamma(s)$$

So that

$$B = \left(\frac{-Ls}{\Gamma(s)}\right)\omega(s,0) = -\sqrt{\frac{L}{C}}\,\omega(s,0) \tag{3.37}$$

And from equation (3.36) with $x = 0$

$$\bar{C} = \left(\frac{-Cs}{\Gamma(s)}\right)T(s,0) \tag{3.38}$$

Since the characteristic impedance can be defined as

$$\xi = \sqrt{\frac{L}{C}}$$

Then, using equations (3.37) and (3.38) yield

$$B = -\xi\omega(s,0)$$

And

$$\bar{C} = -\xi^{-1}T(s,0)$$

Hence, equations (3.33) and (3.34) become

$$T(s,x) = \cosh\Gamma(s)x\; T(s,0) - \xi\,\sinh\Gamma(s)x\;\omega(s,0)$$

$$\omega(s,x) = -\xi^{-1}\sinh\Gamma(s)x\; T(s,0) + \cosh\Gamma(s)x\;\omega(s,0)$$

At distance l along the shaft

$$\begin{bmatrix} T(s,l) \\ \omega(s,l) \end{bmatrix} = \begin{bmatrix} \cosh\Gamma(s)l & -\xi\sinh\Gamma(s)l \\ -\xi^{-1}\sinh\Gamma(s)l & \cosh\Gamma(s)l \end{bmatrix} \times \begin{bmatrix} T(s,0) \\ \omega(s,0) \end{bmatrix} \tag{3.39}$$

Then equation (3.39) can be written in the impedance form as below

$$\begin{bmatrix} T(s,l) \\ T(s,0) \end{bmatrix} = \begin{bmatrix} -\xi ctnh\,\Gamma(s)l & \xi(s)\,\mathrm{csch}\,\Gamma(s)l \\ -\xi\,\mathrm{csch}\,\Gamma(s)l & \xi(s)ctnh\,\Gamma(s) \end{bmatrix} \times \begin{bmatrix} \omega(s,l) \\ \omega(s,0) \end{bmatrix} \tag{3.40}$$

Where

$$ctnh\,\Gamma(s)l = \frac{\left(e^{2\Gamma(s)l}+1\right)}{\left(e^{2\Gamma(s)l}-1\right)} = w(s)$$

And

$$\text{csch}\,\Gamma(s)l = (ctn\,h^2\Gamma(s)l - 1)^{1/2} = (w(s)^2 - 1)^{1/2}$$

With this notation equation (3.40) becomes with

$$T(s,0) = T_1(s)$$

$$T(s,l) = T_2(s)$$

$$\omega(s,0) = \omega_1(s)$$

$$\omega(s,l) = \omega_2(s)$$

$$\begin{bmatrix} T_1(s) \\ T_2(s) \end{bmatrix} = \begin{bmatrix} \xi w(s) & -\xi(w(s)^2-1)^{1/2} \\ \xi(w(s)^2-1)^{1/2} & -\xi w(s) \end{bmatrix} \times \begin{bmatrix} \omega_1(s) \\ \omega_2(s) \end{bmatrix} \quad (3.41)$$

If now $T_2(s) = R\omega_2(s)$

Then

$$\begin{bmatrix} T_1(s) \\ 0 \end{bmatrix} = \begin{bmatrix} \xi w(s) & -\xi(w(s)^2-1)^{1/2} \\ \xi(w(s)^2-1)^{1/2} & -\xi w(s) - R \end{bmatrix} \times \begin{bmatrix} \omega_1(s) \\ \omega_2(s) \end{bmatrix}$$

So that

$$\begin{bmatrix} \omega_1(s) \\ \omega_2(s) \end{bmatrix} = \frac{\begin{bmatrix} \xi w(s) + R \\ \xi(w(s)^2-1)^{1/2} \end{bmatrix}}{\xi(w(s)R + \xi)} T_1(s) \quad (3.42)$$

According to figure 3.8, the distributed-lumped parameter model can be described in Laplace transformation format as

$$\begin{bmatrix} T_1(s) - J_1 s\omega_1(s) - c_1\omega_1(s) \\ J_2 s\omega_2(s) + c_2\omega_2(s) + T_2(s) \end{bmatrix}$$

$$= \begin{bmatrix} \xi w(s) & -\xi(w(s)^2 - 1)^{\frac{1}{2}} \\ \xi(w(s)^2 - 1)^{\frac{1}{2}} & -\xi w(s) \end{bmatrix} \begin{bmatrix} \omega_1(s) \\ \omega_2(s) \end{bmatrix}$$

Same as earlier, $T_2(s)$ will be considerd zero, so, the impedance description becomes

$$\begin{bmatrix} T_1(s) \\ 0 \end{bmatrix} = \begin{bmatrix} \xi w(s) + \gamma_1(s) & -\xi(w(s)^2 - 1)^{\frac{1}{2}} \\ \xi(w(s)^2 - 1)^{\frac{1}{2}} & -\xi w(s) - \gamma_2(s) \end{bmatrix} \times \begin{bmatrix} \omega_1(s) \\ \omega_2(s) \end{bmatrix} \quad (3.43)$$

Note that in equation (3.43)

$$\gamma_1(s) = J_1 s + c_1$$

$$\gamma_2(s) = J_2 s + c_2$$

$$L = \rho J_s$$

$$C = 1/(GJ_s)$$

Hence

$$\sqrt{(LC)} = \sqrt{(\rho G)}$$

$$\xi = \sqrt{(LC)} = J_s\sqrt{(\rho G)}$$

And since

$$w(s) = \frac{e^{2l\Gamma(s)} + 1}{e^{2l\Gamma(s)} - 1} \quad (3.44)$$

Where in equation (3.44)

$$\Gamma(s) = s\sqrt{(LC)} = s\sqrt{(\rho/G)}$$

In the frequency domain, if

$$\varphi_1(\omega) = 2l\omega\sqrt{(LC)}$$

Then equation (3.44) becomes

$$w(i\omega) = \frac{(e^{i\varphi_1(\omega)} + 1)}{(e^{i\varphi_1(\omega)} - 1)} \tag{3.45}$$

For steel with $G = 80 \times 10^9 \frac{N}{m^2}, \rho = 7980\ kg/m^3$,

$$\sqrt{(LC)} = \sqrt{(\rho/G)} = 3.16 \times 10^{-4} \tag{3.46}$$

using routine manipulation it is clear that

$$w(i\omega) = \frac{-i \sin \varphi_1(\omega)}{1 - \cos \varphi_1(\omega)} \tag{3.47}$$

The function

$$f\big(\varphi_1(\omega)\big) = \frac{\sin \varphi_1(\omega)}{1 - \cos \varphi_1(\omega)} \tag{3.48}$$

Of equation (3.48) generates various curves in the intervals

$$2n\pi \le \varphi_1(i\omega) \le 2(n+1)\pi, \qquad n = 0,1,2$$

Then, following the inversion of equation (3.43)

$$\begin{bmatrix}\omega_1(s)\\ \omega_2(s)\end{bmatrix} = \begin{bmatrix}\xi w(s) + \gamma_2(s)\\ \xi(w(s)^2 - 1)^{\frac{1}{2}}\end{bmatrix} T_1(s)/\Delta(s) \tag{3.49}$$

Where in equation (3.49)

$$\Delta(s) = \xi\big(\gamma_1(s) + \gamma_2(s)\big)w(s) + \gamma_1(s)\gamma_2(s) + \xi^2$$

The hybrid model-HM functions of the frequency response will now be compared. Substituting $w(s) = -if(\varphi_1(\omega))$ yields

$$\begin{bmatrix}\omega_1(s)\\ \omega_2(s)\end{bmatrix} = \begin{bmatrix} c_2 + \big(J_2\omega - \xi f(\varphi_1(\omega))\big)i \\ i\xi\big(f\big(\varphi_1(\omega)\big)^2 + 1\big)^{\frac{1}{2}} \end{bmatrix} \frac{T_1(i\omega)}{\Delta(i\omega)} \tag{3.50}$$

Where in equation (3.50)

$$\Delta(i\omega) = [(J_1c_2 + J_2c_1)\omega - \xi f(\varphi_1(\omega))(c_1 + c_2)]i + [\xi f(\varphi_1(\omega))(J_1 + J_2)\omega + c_1c_2 + \xi^2 - J_1J_2\omega^2]$$

So at resonance, the values of ω satisfying

$$[(J_1c_2 + J_2c_1)\omega - \xi f(\varphi_1(\omega))(c_1 + c_2)] = 0 \tag{3.51}$$

Should be determined. For the hybrid model there will be unlimited number of (ω) values satisfying equation (3.51), identical to the unlimited number of the resonant peaks which take place. It can be seen from equation (3.50) that if equation (3.51) is written as

$$f(\varphi_1(\omega)) - g(\varphi_1(\omega)) = 0 \tag{3.52}$$

Then

$$g(\varphi_1(\omega)) = \left[\frac{(J_1c_2 + J_2c_1)\varphi_1(\omega)}{2\xi(c_1 + c_2)l\sqrt{(LC)}}\right]$$

Resonant amplification can happen when the rotor's load end phase lags by an odd number only of multiples of $(-\pi/2)$ radians with $f(\varphi_1(\omega))$ and $g(\varphi_1(\omega))$ shows similar characteristics to those presented in figure 3.10. According to the figure, there would be an unlimited number of the interceptions of $f(\varphi_1(\omega))$ and $g(\varphi_1(\omega))$ curves. Resonant frequencies can be identified by these equalities.

Referring to equation (3.42), the subassemblies of $w(s)$ and $(w(s)^2-1)^{\frac{1}{2}}$ can be simulated as it is shown below:

1- Subassembly Simulation of $w(s)$

Using equation (3.44)

$$w(s)=\frac{e^{2l\Gamma(s)}+1}{e^{2l\Gamma(s)}-1}$$

And hence $\Gamma(s)=s\sqrt{(LC)}$

So, before designing $w(s)$ in Simulink, it need to be expressed in the delay form as it is shown below

$$w(s)=\frac{1+e^{-2l\Gamma(s)}}{1-e^{-2l\Gamma(s)}}=\frac{1+e^{-2ls\sqrt{(LC)}}}{1-e^{-2ls\sqrt{(LC)}}}=\frac{1+e^{-Ts}}{1-e^{-Ts}} \quad (3.53)$$

Where $T=2l\sqrt{(LC)}$

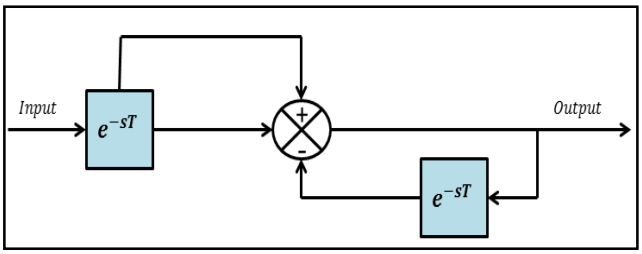

Figure 3.13 Block diagram of subassembly of $w(s)$

2- Subassembly Simulation of $(w(s)^2-1)^{\frac{1}{2}}$

Substituting equation (3.53) in the expression$(w(s)^2-1)^{\frac{1}{2}}$, the resulted equation is as following: -

$$(w(s)^2-1)^{\frac{1}{2}}=\frac{2e^{-l\Gamma(s)}}{1-e^{-2l\Gamma(s)}}=\frac{2e^{-ls\sqrt{(LC)}}}{1-e^{-2ls\sqrt{(LC)}}}=\frac{e^{-0.5Ts}}{1-e^{-Ts}} \quad (3.54)$$

Where $T = 2l\sqrt{(LC)}$

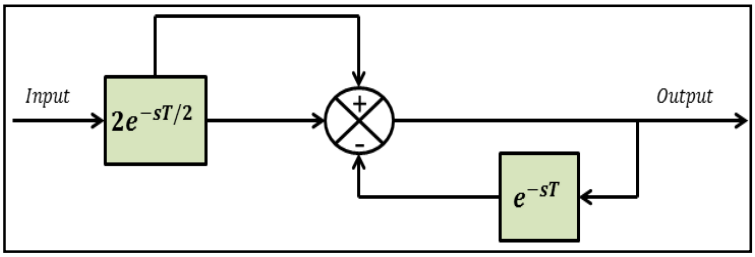

Figure 3.14 Block diagram of subassembly of $(w(s)^2 - 1)^{\frac{1}{2}}$

Chapter IV

Simulation Results and Discussions

4.1. Introduction

Matlab will be utilized here to show how new computer computational tools can be used in systems dynamics (torsional response). Matlab software was selected for the simulations here since it is one of the most extensively hired softwares in the system dynamics analysis courses and by researchers and practitioners working in the area and in so many different areas. Simulink, which is actually based on the matlab is a diagram-based interface, it is growing in publicity due to many reasons, for example, its power, effectiveness and finally its ease of use.

Time domain can be defined as the analysis of any data with respect to time, these data can be physical signals, mathematical functions, or time series of environmental or economic data. In the this domain, the function's or signal value is recognized for all the real numbers, in case of continuous time, or at different separate moments if it is discrete time. The time domain plots shows how is the studied signal is changing with time, while the frequency domain plots showing how much of the signal located within a specified frequency band along with range of frequencies.

Steady state response as defined by Drof and Bishop is the response that persist for long time according to any given input signal (Dorf & Bishop, 2009).

Unlikely, the transient or dynamic responses are the response of the system, starting from the initial to the final system states (Ogata, 2010).

Both the above responses are required after the system undergo initiating signals, to investigate the design generated, and performance extracted from the modeled system.

Accordingly, the following sections will repersent the full details of the simulation results of the modeled helicopter (Schweizer 300C) rotot systems modeled using the three modeling methods lumped parameter-LPM, finite element-FEM and distributed-lumped parameter technique-DLPMT are used inline with the details given previously in Chapter-III.

Discussions in details will be presented, highlighting the advantages incorporated with each method according to the earlier discussion in previous chapters and the results obtained in this chapter.

Table 4.1 General specification of system elements

Seq	Quantity		Value	Unit
	Name	symbol		
1	Shear modulus	G	80×10^9	N/m^2
2	Density	ρ	7980	kg/m^3
3	Gear ratio in main transmission gear	MTG	$20/60$	
4	Gear ratio in tail-main shaft transmission gear	MRG	$60/225$	

Table 4.2 Tail rotor elements identification (Hughes Schweizer 269 helicopter maintenance instructions 2, 2014)

Quantity		value	unit
Name	symbol		
Length of tail shaft	l_t	5.5	m
Diameter of tail shaft	d_{st}	0.09	m
Diameter of gearbox at the drive end of tail shaft	d_{t1}	0.31	m
Diameter of gearbox at the load end of tail shaft	d_{t2}	0.35	m
Viscous damping at the drive end of tail shaft	c_{t1}	4	$N.m.s/rad$
Viscous damping at the load end of tail shaft	c_{t2}	20	$N.m.s/rad$

Table 4.3 Main rotor elements identification (Hughes Schweizer 269 helicopter maintenance instructions 2, 2014)

Quantity		value	unit
Name	symbol		
Length of main shaft	l_m	1.1	m
Diameter of main shaft	d_{sm}	0.07	m
Diameter of gearbox at the drive end of main shaft	d_{m1}	0.46	m
Diameter of gearbox at the load end of main shaft	d_{m2}	0.35	m
Viscous damping at the drive end of main shaft	c_{m1}	4	$N.m.s/rad$
Viscous damping at the load end of main shaft	c_{m2}	20	$N.m.s/rad$

4.2. Lumped Parameter Model (LPM)

Referring to section (3.3), the lumped model was derived and the transfer function matrix can be expressed as

$$\begin{bmatrix}\omega_1(s)\\ \omega_2(s)\end{bmatrix} = \frac{\begin{bmatrix}J_2s^2+c_2s+k & k\\ k & J_1s^2+c_1s+k\end{bmatrix}}{\Delta(s)}\begin{bmatrix}T_1(s)\\ 0\end{bmatrix}$$

Note that in the above equation the denominator is

$$\Delta(s) = J_1J_2s^3 + (J_1c_2 + J_2c_1)s^2 + (J_1k + J_2k + c_1c_2)s + (c_1 + c_2)k$$

Note that the above transfer function matrix will be used twice for both tail and main rotors considering the gear ratios for both of them (in the above table).

According to the above transfer function matrix the block diagram of lumped parameter model (LPM) was constructed for both tail and main rotors of the helicopter as following

4.2.1. LPM Tail Rotor Derivation

Lumped parameter, tail shaft rotor configuration of Schweizer 300C is shown below in figure 4.1

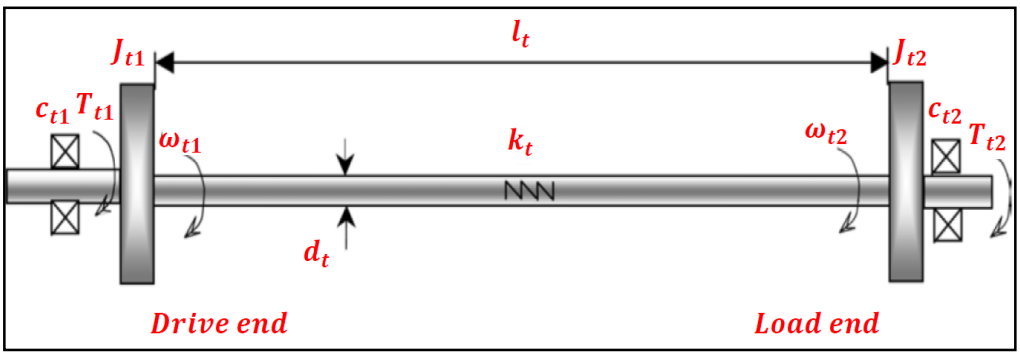

Figure 4.1 Lumped parameter, tail shaft configuration of Schweizer 300C

According to model shown above, the parameters table is provided below. Note that some parameters are constant values and some of them need to be calculated, the calculations are explained in details in this section and can be compared with the calculations done automatically by Matlab (Shown in Appendix A-4)

Calculations

1- $J_{st} = \frac{\pi {d_{st}}^4}{32} = \frac{\pi(0.09^4)}{32} = 6.44 \times 10^{-6}\ m^4$

2- $J_{t1} = \frac{\pi {d_{t1}}^4}{32} = \frac{\pi(0.31^4)}{32} = 9.06 \times 10^{-4}\ m^4$

3- $J_{t2} = \frac{\pi {d_{t2}}^4}{32} = \frac{\pi(0.35^4)}{32} = 1.5 \times 10^{-3}\ m^4$

4- $k_t = \frac{G \times J_{st}}{l_t} = \frac{(80\times10^9)\times(6.44\times10^{-6})}{5.5} = 9.36 \times 10^4\ N.m/rad$

Hence

$$\begin{bmatrix}\omega_{t1}(s)\\ \omega_{t2}(s)\end{bmatrix} = \frac{\begin{bmatrix} J_{t2}s^2 + c_{t2}s + k_t & k_t \\ k_t & J_{t1}s^2 + c_{t1}s + k_t \end{bmatrix}}{\Delta(s)} \begin{bmatrix} T_{t1}(s) \\ 0 \end{bmatrix}$$

And

$$\Delta(s) = J_{t1}J_{t2}s^3 + (J_{t1}c_{t2} + J_{t2}c_{t1})s^2 + (J_{t1}k_t + J_{t2}k_t + c_{t1}c_{t2})s + (c_{t1} + c_{t2})k_t$$

So $\omega_{t1}(s)$and $\omega_{t2}(s)$ can be expressed as

$\omega_{t1}(s)\{Symbolically\}$

$$= \frac{J_{t2}s^2 + c_{t2}s + k_t}{J_{t1}J_{t2}s^3 + (J_{t1}c_{t2} + J_{t2}c_{t1})s^2 + (J_{t1}k_t + J_{t2}k_t + c_{t1}c_{t2})s + (c_{t1} + c_{t2})k_t}$$

More details of the numerical calculation of this transfer function is attached in appendix-A7

$$\omega_{t1}(s)\{Numerically\} = \frac{0.001472s^2 + 20s + (9.36 \times 10^4)}{(1.33 \times 10^{-6})s^3 + 0.024s^2 + 302.7s + 2.25}$$

$$\omega_{t2}(s)\{Symbolically\}$$

$$= \frac{k_t}{J_{t1}J_{t2}s^3 + (J_{t1}c_{t2} + J_{t2}c_{t1})s^2 + (J_{t1}k_t + J_{t2}k_t + c_{t1}c_{t2})s + (c_{t1} + c_{t2})k_t}$$

$$\omega_{t2}(s)\{Numerically\} = \frac{(9.36 \times 10^4)}{(1.33 \times 10^{-6})s^3 + 0.024s^2 + 302.7s + 2.25}$$

4.2.2. LPM Main Rotor Derivation

Similarly, Lumped parameter, main shaft rotor configuration of Schweizer 300C is shown below in figure 4.2

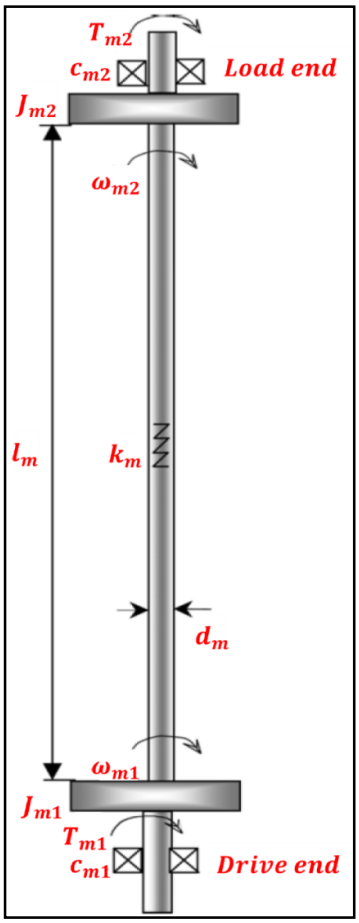

Figure 4.2 Lumped parameter, main shaft configuration of Schweizer 300C

According to model shown above, the parameters table is provided below. Note that some parameters are constant values and some of them need to be calculated, the calculations are explained in details in this section and can be compared with the calculations done automatically by Matlab (Shown in Appendix A-4)

Calculations

1- $J_{sm} = \frac{\pi {d_{sm}}^4}{32} = \frac{\pi(0.07^4)}{32} = 2.36 \times 10^{-6}\ m^4$

2- $J_{m1} = \frac{\pi {d_{m1}}^4}{32} = \frac{\pi(0.46^4)}{32} = 4.4 \times 10^{-3}\ m^4$

3- $J_{m2} = \frac{\pi {d_{m2}}^4}{32} = \frac{\pi(0.35^4)}{32} = 1.5 \times 10^{-3}\ m^4$

4- $k_m = \frac{G \times J_{sm}}{l_m} = \frac{(80 \times 10^9) \times (2.36 \times 10^{-6})}{1.1} = 1.71 \times 10^5\ N.m/rad$

Hence

$$\begin{bmatrix}\omega_{m1}(s)\\ \omega_{m2}(s)\end{bmatrix} = \frac{\begin{bmatrix}J_{m2}s^2 + c_{m2}s + k_m & k_m\\ k_m & J_{m1}s^2 + c_{m1}s + k_m\end{bmatrix}}{\Delta(s)} \begin{bmatrix}T_{m1}(s)\\ 0\end{bmatrix}$$

And

$$\Delta(s) = J_{m1}J_{m2}s^3 + (J_{m1}c_{m2} + J_{m2}c_{m1})s^2 + (J_{m1}k_t + J_{m2}k_t + c_{m1}c_{m2})s + (c_{m1} + c_{m2})k_m$$

So $\omega_{m1}(s)$and $\omega_{m2}(s)$ can be derived as

$$\omega_{m1}(s)\{Symbolically\} = \frac{J_{m2}s^2 + c_{m2}s + k_m}{J_{m1}J_{m2}s^3 + (J_{m1}c_{m2} + J_{m2}c_{m1})s^2 + (J_{m1}k_t + J_{m2}k_t + c_{m1}c_{m2})s + (c_{m1} + c_{m2})k_m}$$

$$\omega_{m1}(s)\{Numerically\} = \frac{0.00147s^2 + 20s + (1.71 \times 10^5)}{(6.47 \times 10^{-6})s^3 + 0.094s^2 + 1085s + 4.11}$$

$$\omega_{m2}(s)\{Symbolically\} = \frac{k_m}{J_{m1}J_{m2}s^3 + (J_{m1}c_{m2} + J_{m2}c_{m1})s^2 + (J_{m1}k_t + J_{m2}k_t + c_{m1}c_{m2})s + (c_{m1} + c_{m2})k_m}$$

$$\omega_{m2}(s)\{Numerically\} = \frac{(1.71 \times 10^5)}{(6.47 \times 10^{-6})s^3 + 0.094s^2 + 1085s + 4.11}$$

Then, the simulation block diagram for the lumped parameter model (LPM) of the whole system was built as following

(The block diagram in Simulink for the LPM of the whole system is shown in appendix A-4)

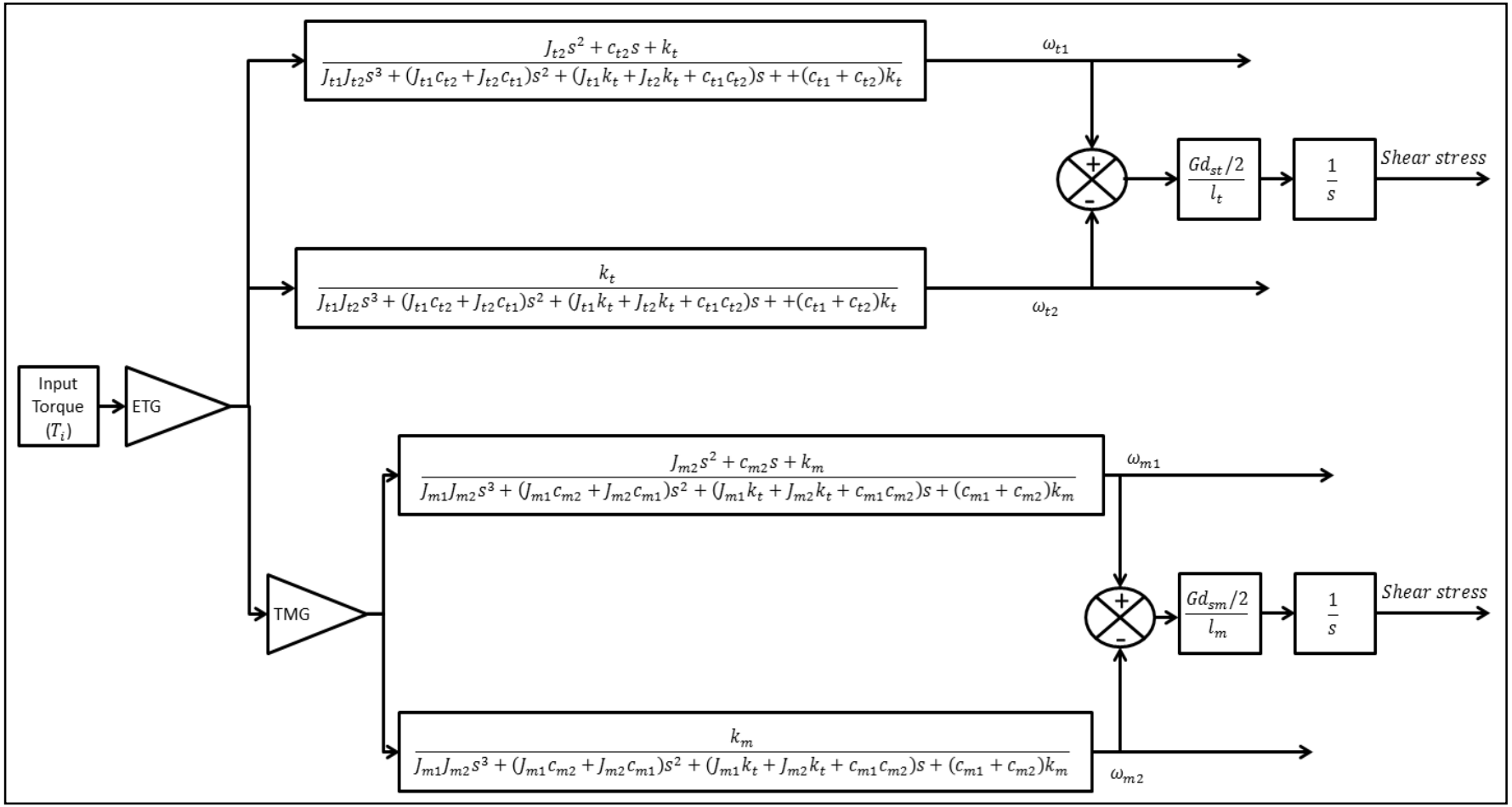

Figure 4.3 LPM simulation block diagram of the dual rotor-shaft system

4.2.3. LPM Time Domain (Transient Response) Analysis

To show the influence of applying unit step input changes on the system input (input torque) in the selected system (comprising rotors, shafts and inertias), the output angular speed (ω) for the lumped parameter model (LPM) will be simulated in this section for both the tail and main rotors. The supplied torque intput $T_i(t) = 3250\ \mathrm{N.m}$ is used to generate the steady state response of tail rotor output angular speed $\omega_{t1} = \omega_{t2} = 100\ \mathrm{rad/s}$ and $\omega_{m1} = \omega_{m2} = 27\ \mathrm{rad/s}$.

Figures (4.4) to (4.6) shown bellow illustrates the LPM time domain transient responses for tail rotor with drive end $\omega_{t1}(t)$ and the load end $\omega_{t2}(t)$, respectively. Similarly Figures (4.7) to (4.9) shown bellow illustrates the LPM time domain transient responses for the main rotor with drive end $\omega_{m1}(t)$ and the load end $\omega_{m2}(t)$, respectively. Note that all of the simulations are computed for 0.025 (s).

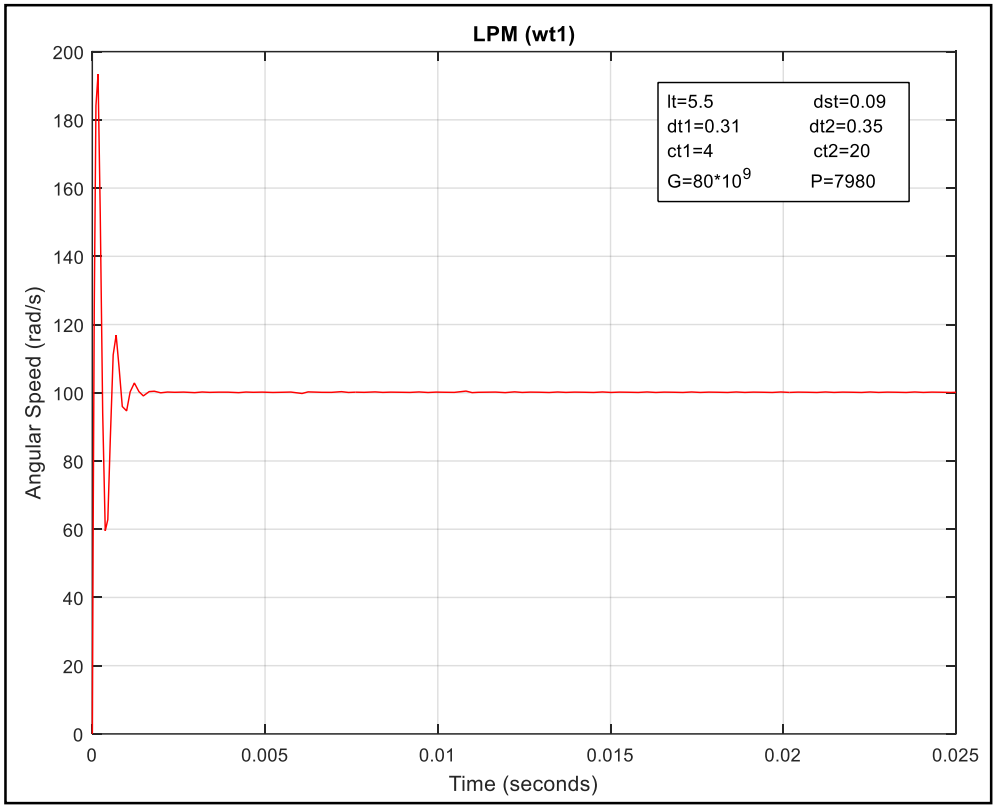

Figure 4.4 Step response of LPM (tail rotor-drive end)

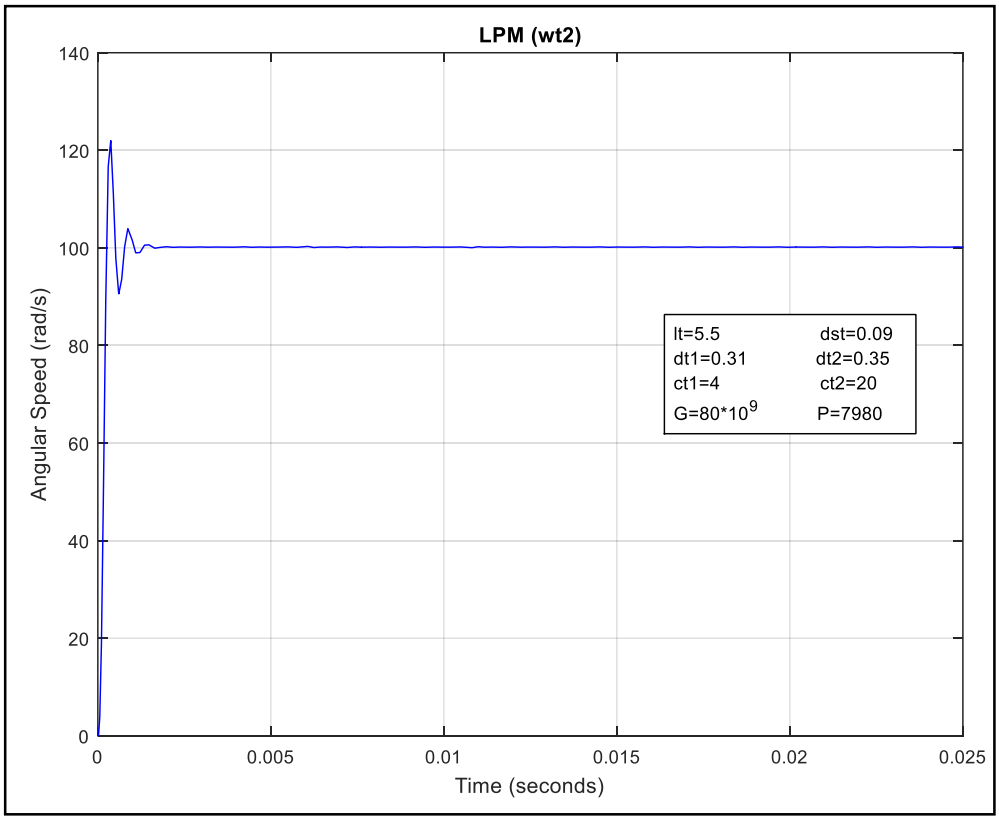

Figure 4.5 Step response of LPM (tail rotor-load end)

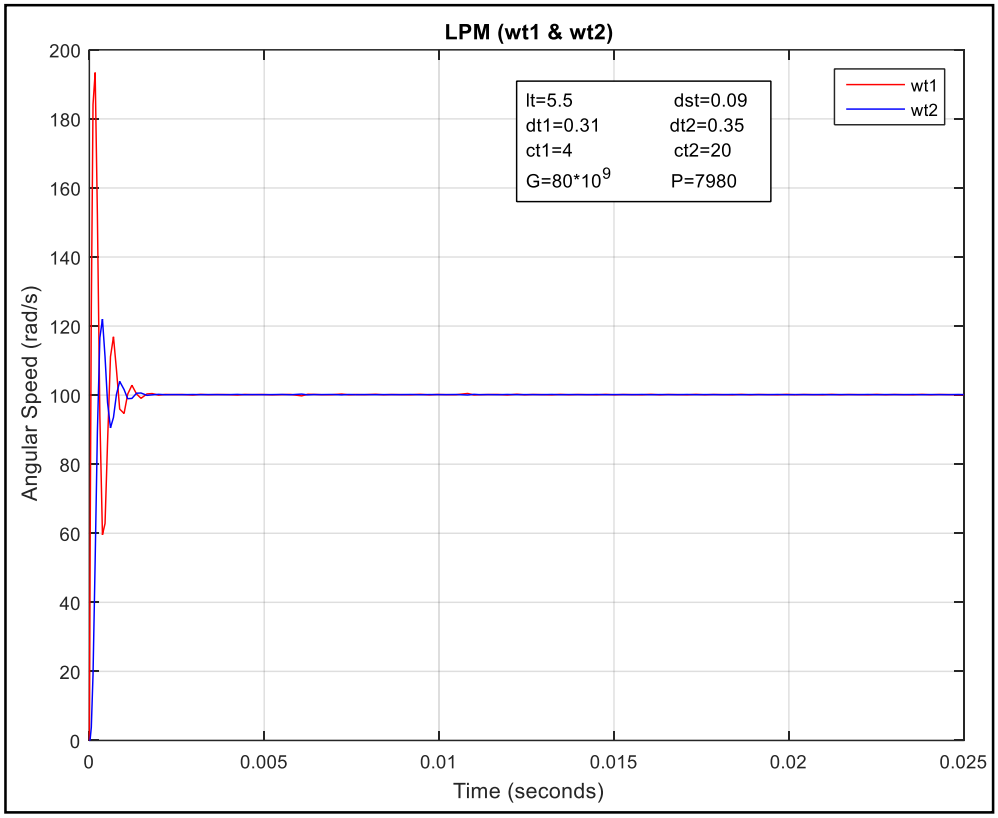

Figure 4.6 LPM step responses of tail rotor (drive and load ends)

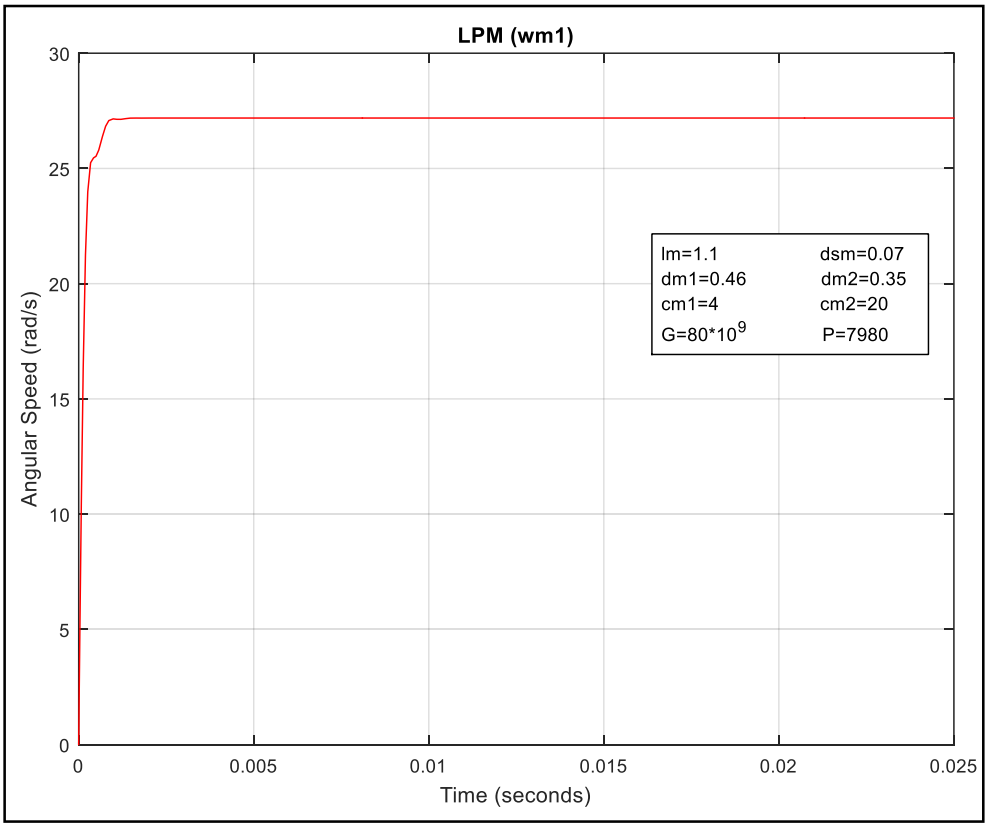

Figure 4.7 Step response of LPM (main rotor-drive end)

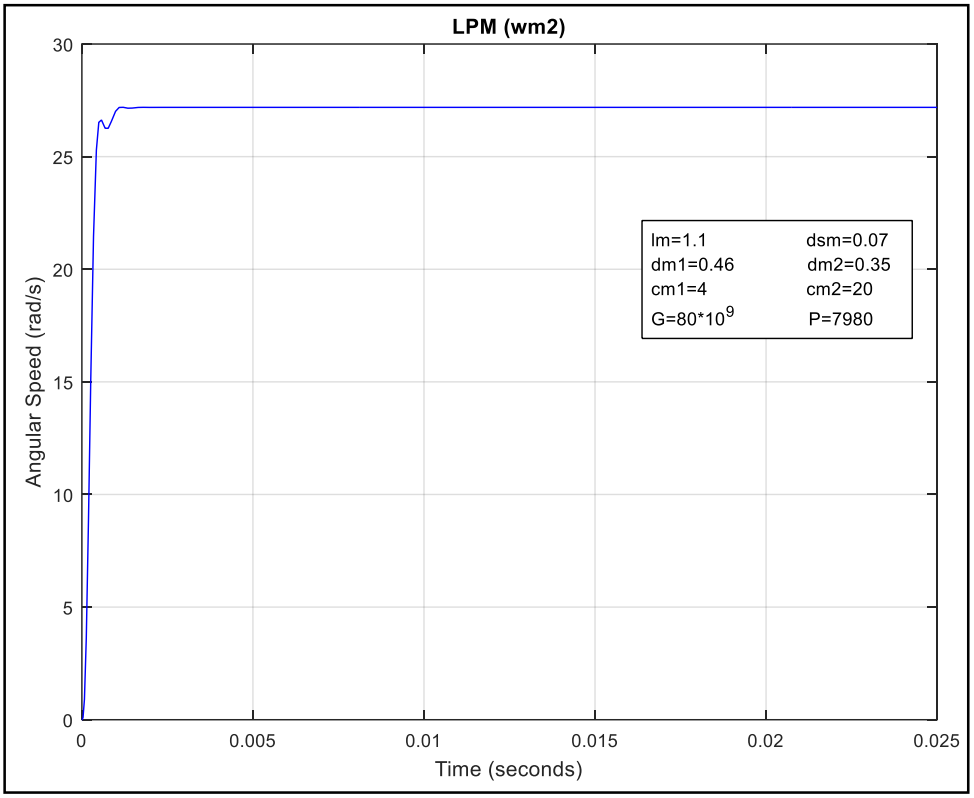

Figure 4.8 Step response of LPM (main rotor-load end)

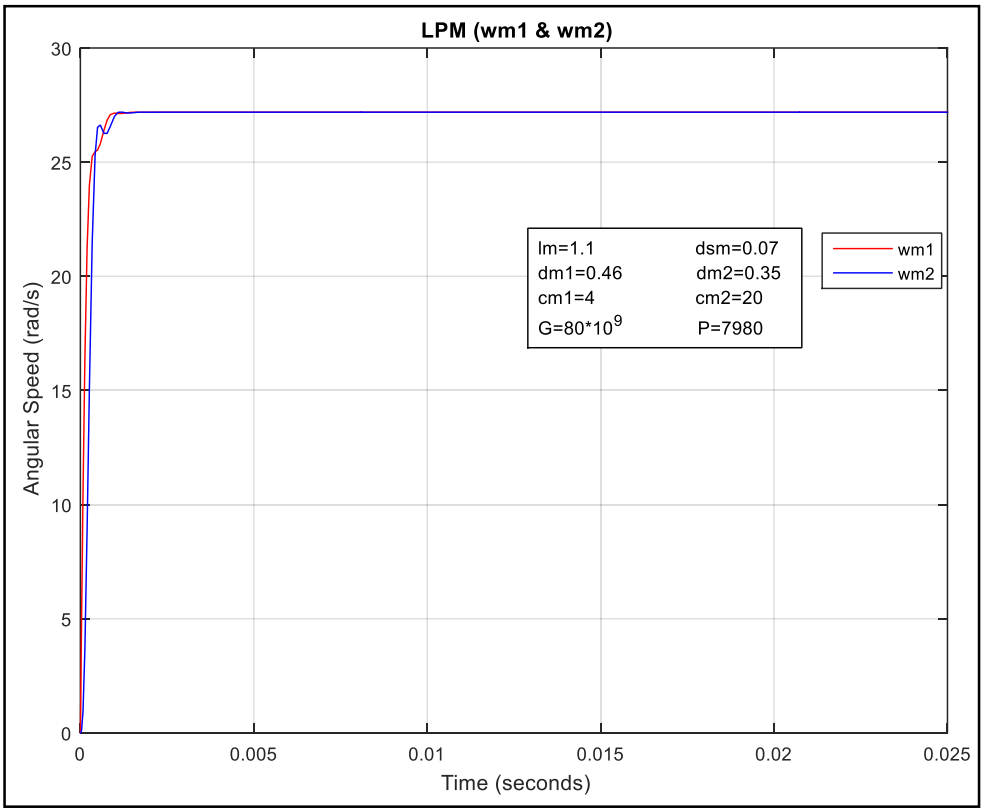

Figure 4.9 LPM step responses of main rotor (drive and load ends)

At the end, all the step responses of the LPM are shown in one graph for better illustration. Figure 4.10 showing the four LPM responses for both tail and main rotors with drive and load ends.

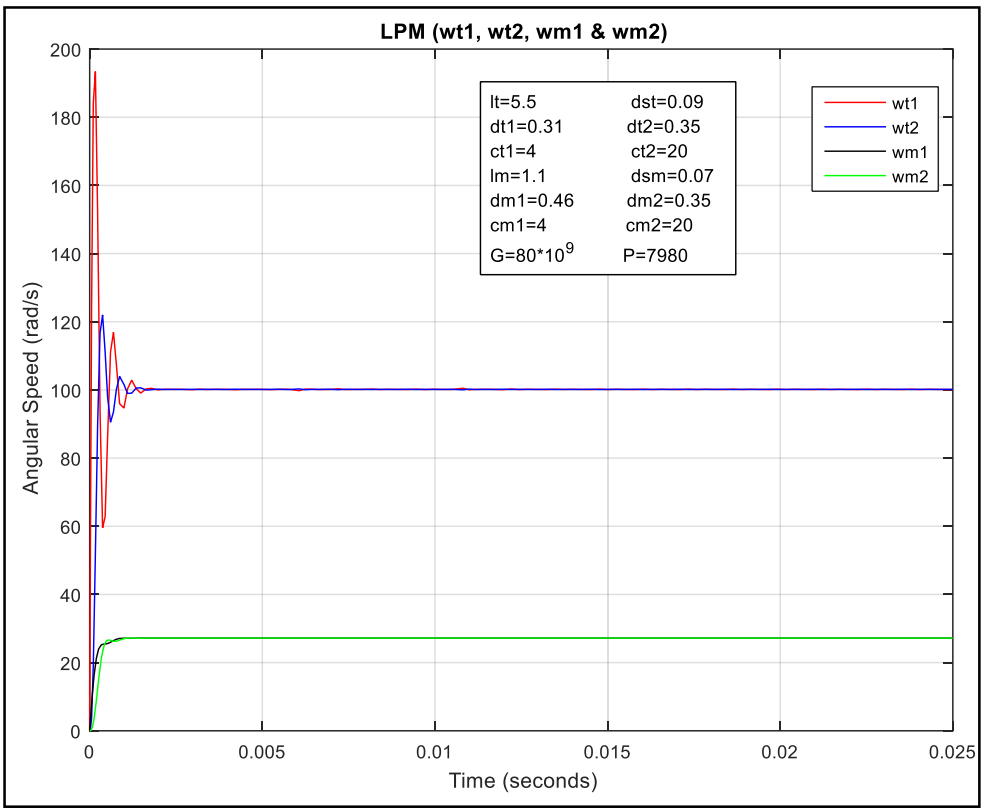

Figure 4.10 LPM step responses of both tail and main rotors (drive and load ends)

Then the shear stress of the LPM is simulated and results are shown below for both tail and main rotors in figures (4.11) and (4.12) respectively.

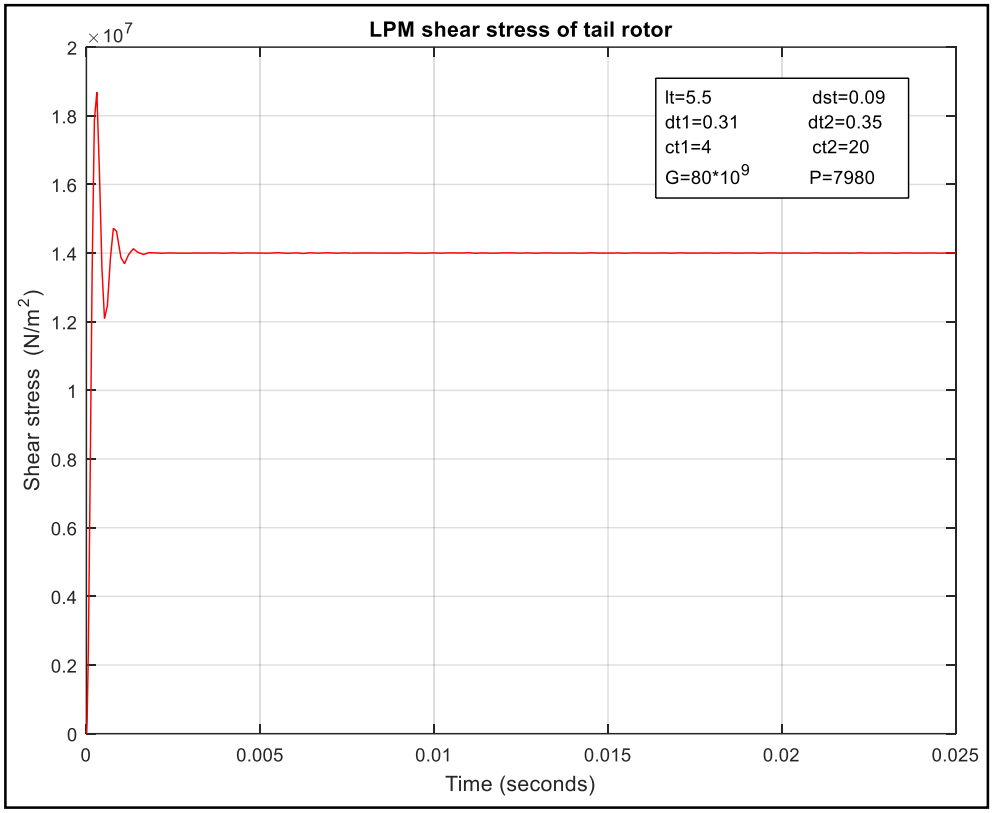

Figure 4.11 LPM shear stress of tail rotor

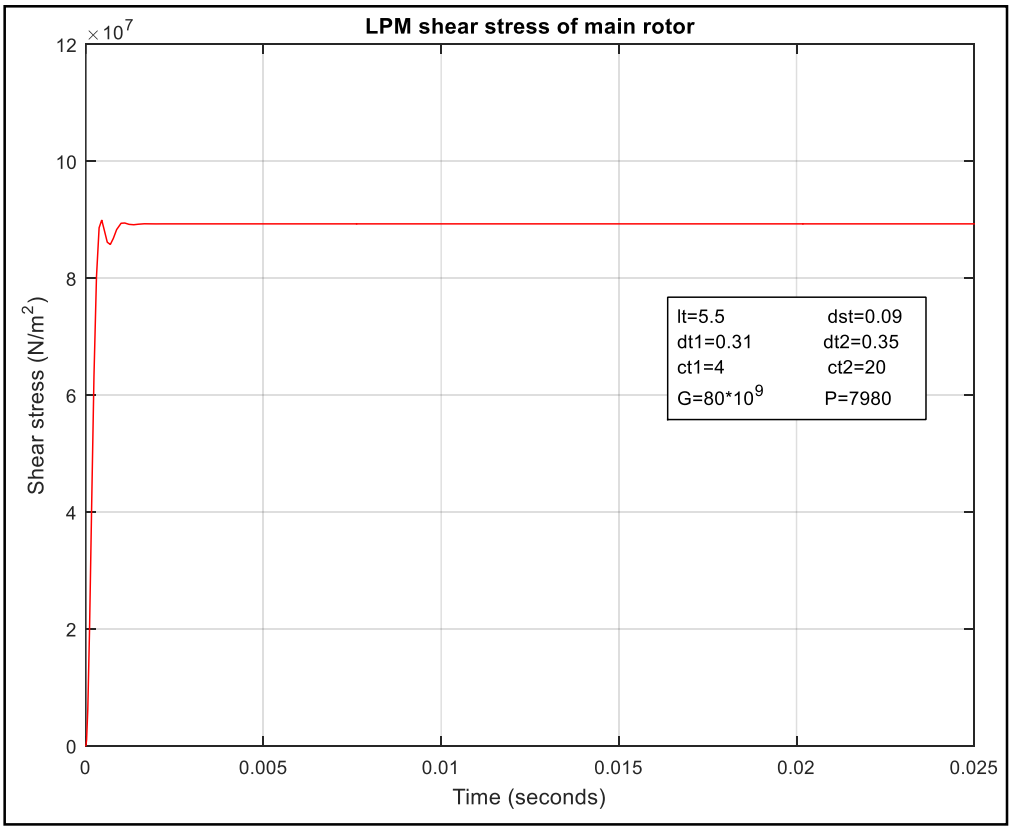

Figure 4.12 LPM shear stress of main rotor

4.2.4. LPM Frequency Domain Analysis

An alternative method for analyzing problem is to consider the frequency domain analysis rather than the system time domain response.

Frequency domain analysis approach allowing the phase and modulus features of the acquired output(s) to be calculated for some range of frequencies (ω), as shown below. After that, frequency response (Bode) plots can be utilized in order to estimate the time domain characteristics (transient rsponse) of the studied application.

Here the frequency domain analysis will be done to compare between the calculated resonant frequency using the equations from chapter III and those from the Bode graphs for both tail and main rotors and each rotor will be investigated for the three modeling techniques used; LPM, FEM and DLPM.

Referring to equation (3.11), the resonant frequency can be expressed as

$$\omega_t^2 = \frac{k_t(c_{t1} + c_{t2})}{J_{t1}c_{t2} + J_{t2}c_{t1}}$$

Using the parameters of the tail rotor given in table (4.2) and the calculated parameters for the tail rotor in section (4.2.1) and substituting in the above equation

$$\omega_t^2 = \frac{(9.36 \times 10^4)(4 + 20)}{(9.06 \times 10^{-4})(20) + (1.5 \times 10^{-3})(4)}$$

$$\omega_t^2 = 9.3 \times 10^7$$

$$\omega_t = 9651\, rad/s$$

Now the resonant frequency (ω_t) calculated for the LPM tail rotor is shown above, and it can be noticed that the calculated value is smaller than the value extracted from the frequency domain analysis (Bode plots), which are provided in figures (4.13) and (4.14), where its value at the drive end, is $11700\, rad/s$ and at the load end is $10500\, rad/s$.

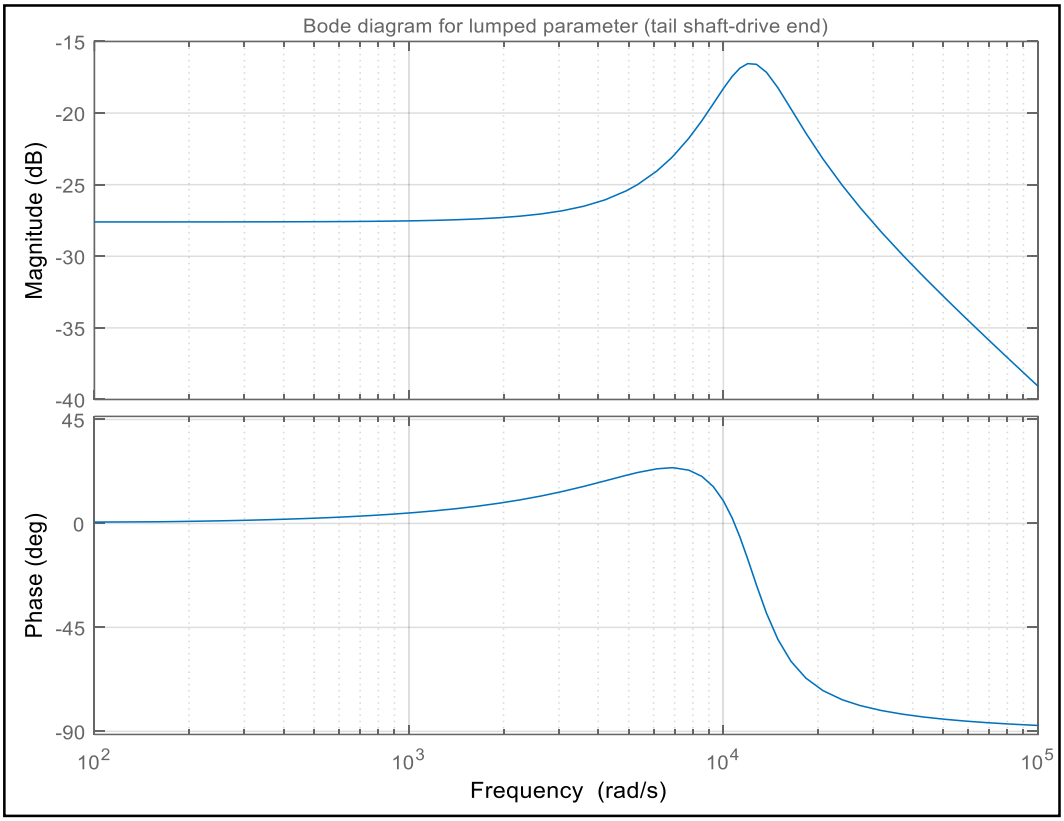

Figure 4.13 Bode plot of LPM (tail shaft-drive end)

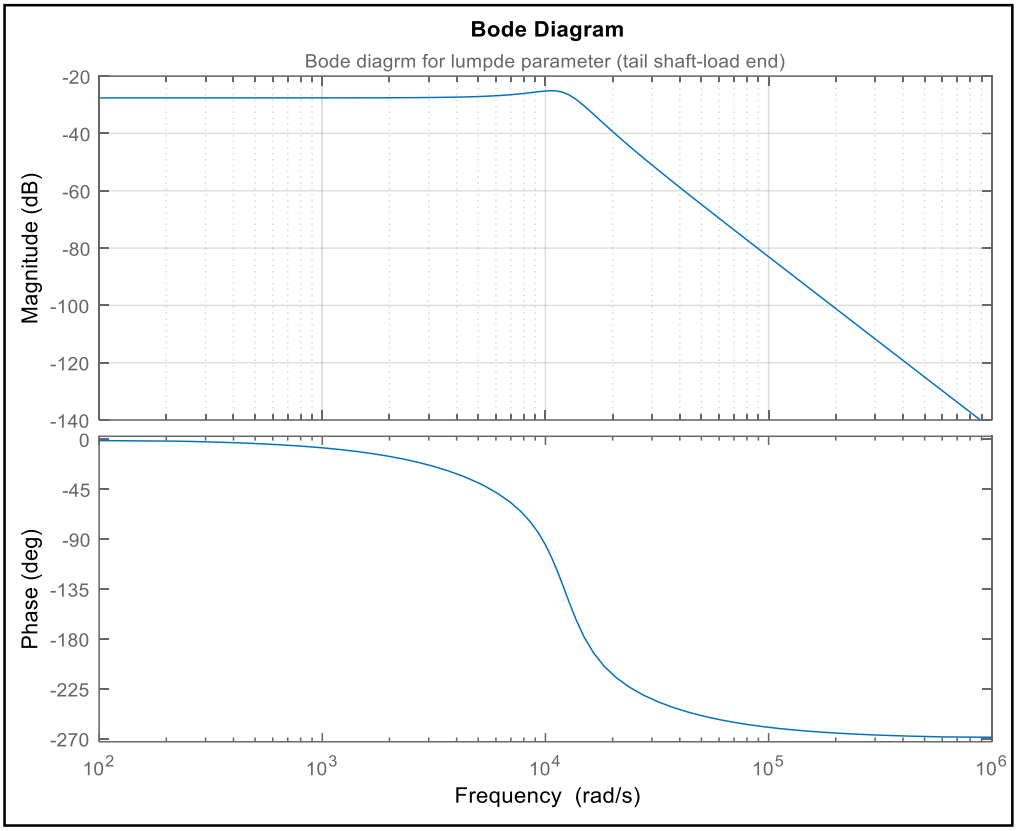

Figure 4.14 Bode plot of LPM (tail shaft-load end)

Similarly, referring to the same equation (3.11), the resonant frequency of the main rotor can be expressed as

$$\omega_m^2 = \frac{k_m(c_{m1} + c_{m2})}{J_{m1}c_{m2} + J_{m2}c_{m1}}$$

Using the parameters of the main rotor given in table (4.3) and the calculated parameters for the main rotor in section (4.2.2) and substituting in the above equation

$$\omega_m^2 = \frac{(1.71 \times 10^5)(4 + 20)}{(4.4 \times 10^{-3})(20) + (1.5 \times 10^{-3})(4)}$$

$$\omega_m^2 = 4.4 \times 10^7$$

$$\omega_m = 6608\, rad/s$$

Again comparing the resonant frequency (ω_m) calculated for the LPM main rotor shown above with the value extracted from the frequency domain analysis (Bode plots), which are provided in figures (4.15) and (4.16), it can be noticed that the calculated value is smaller than the value extracted graphically (Bode plots) where its value at the drive end, is 10070 rad/s and at the load end is 10180 rad/s.

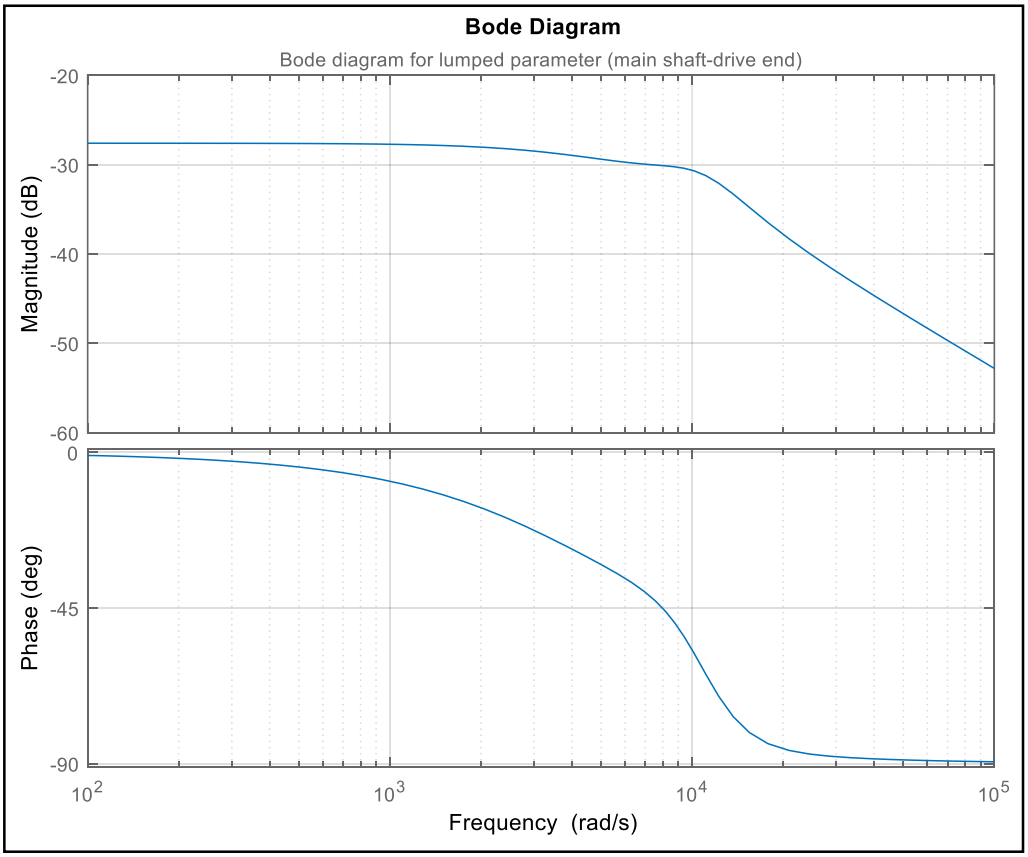

Figure 4.15 Bode plot of LPM (main shaft-drive end)

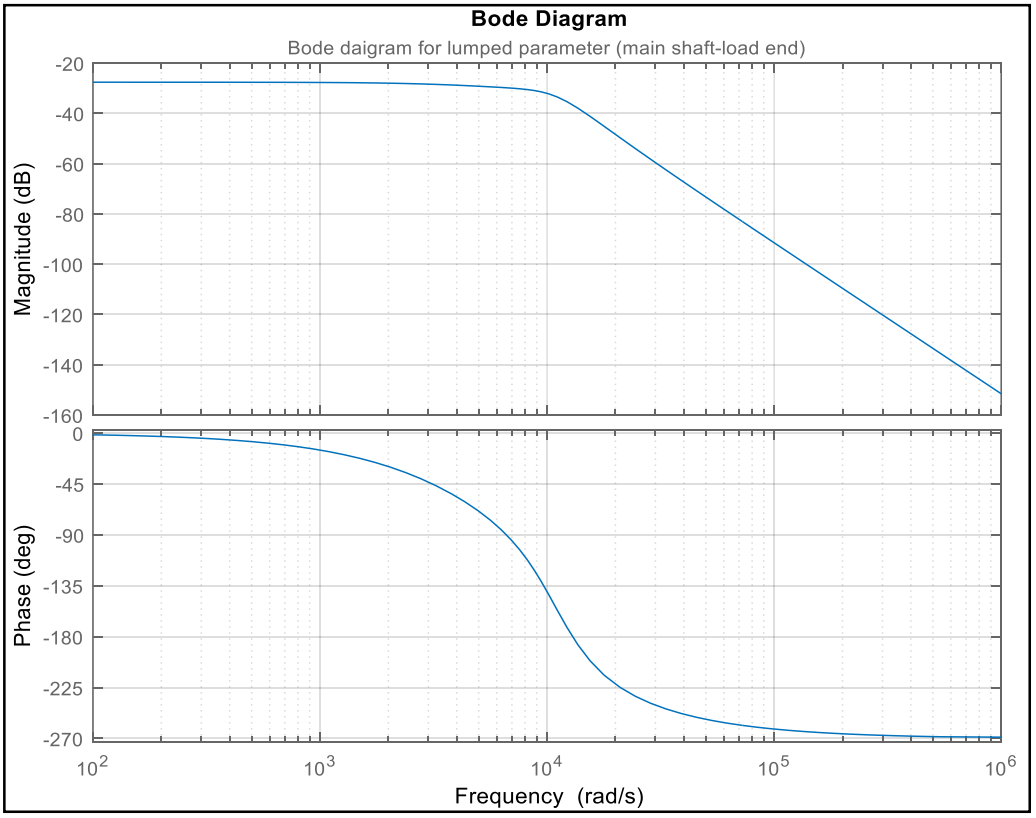

Figure 4.16 Bode plot of LPM (main shaft-load end)

4.3. Finite Element Model (FEM)

Referring to section (3.3), the finite element model of the selected system was derived and the transfer function matrix can be expressed as

$$num1 = s^{10}J^4J_2 + s^9J^4c_2 + s^8(8kJ^3J_2 + kJ^4) + s^78kJ^3c_2$$
$$+ s^6(7J^3k^2 + 21k^2J^2J_2) + s^521k^2J^2c_2$$
$$+ s^4(15k^3J^2 + 20k^3JJ_2) + s^320k^3Jc_2$$
$$+ s^2(5k^4J_2 + 10k^4J) + 5k^4c_2s + k^5$$

Note that in the above equation the denominator is

$$\Delta_1(s) = J_1J^4J_2s^{11} + s^{10}(c_1J^4J_2 + J_1J^4c_2)$$
$$+ s^9(kJ^4J_2 + 8kJ_1J^3J_2 + kJ_1J^4 + c_1J^4c_2)$$
$$+ s^8(kc_1J^4 + 8kc_1J^3J_2 + 8kJ_1J^3c_2)$$
$$+ s^7(7J_1J^3k^2 + 21k^2J_1J^2J_2 + k^2J^4 + 8kc_1J^3c_2$$
$$+ 7k^2J^3J_2)$$
$$+ s^6(21k^2J_1J^2c_2 + 7c_1J^3k^2 + 21k^2c_1J^2J_2 + 7k^2J^3c_2)$$
$$+ s^5(15k^3J^2J_2 + 20k^3J_1JJ_2 + 6J^3k^3 + 15k^3J_1J^2$$
$$+ 21k^2c_1J^2c_2)$$
$$+ s^4(15k^3c_1J^2 + 15k^3J^2c_2 + 20k^3c_1J^2JJ_2 + 20k^3J_1Jc_2)$$
$$+ s^3(5k^4J_1J_2 + 20k^3c_1Jc_2 + 10k^4J_1J + 10J^2k^4$$
$$+ 10k^4JJ_2)$$
$$+ s^2(5k^4c_1J_2 + 10k^4Jc_2 + 5k^4J_1c_2 + 10k^4c_1J) + s(k^5J_2$$
$$+ 4k^5J + k^5J_1 + 5k^4c_1c_2) + k^5c_1 + k^5c_2$$

Note that the above transfer function matrix will be used twice for both tail and main rotors considering the gear ratios for both of them (in the above table).

4.3.1. FEM Tail Rotor Derivation

Finite element (five sections), tail rotor shaft configuration of Schweizer 300C is shown above in figure (3.7) and according to that model, the parameters are provided in table (4.2). Note that some parameters are constant values and some of them need to be calculated, the calculations are explained in details in this section and can be compared with the calculations done automatically by Matlab (Shown in Appendix A-5)

Recall that

$$\bar{J}_{t1} = \bar{J}_{t2} = \bar{J}_{t3} = \bar{J}_{t4} = J_t$$

And

$$k_{t1} = k_{t2} = k_{t3} = k_{t4} = k_{t5} = k_t$$

Calculations

1- $J_{st} = \frac{\pi {d_{st}}^4}{32} = \frac{\pi(0.09^4)}{32} = 6.44 \times 10^{-6}\ m^4$

2- $J_{t1} = \frac{\pi {d_{t1}}^4}{32} = \frac{\pi(0.31^4)}{32} = 9.06 \times 10^{-4}\ m^4$

3- $J_{t2} = \frac{\pi {d_{t2}}^4}{32} = \frac{\pi(0.35^4)}{32} = 1.5 \times 10^{-3}\ m^4$

4- $k_t = \frac{G \times J_{st}}{l_t} = \frac{(80 \times 10^9) \times (6.44 \times 10^{-6})}{5.5} = 9.36 \times 10^4\ N.m/rad$

So $\omega_{t1}(s)$and $\omega_{t2}(s)$ can be expressed as

$\omega_{t1}(s)\{Symbolically\}$

$$= \frac{\begin{matrix} s^{10}{J_{st}}^4 J_{t2} + s^9{J_{st}}^4 c_{t2} + s^8\left(8k_t{J_{st}}^3 J_{t2} + k_t{J_{st}}^4\right) \\ +s^7 8k_t{J_{st}}^3 c_{t2} + \\ s^6\left(7{J_{st}}^3{k_t}^2 + 21{k_t}^2{J_{st}}^2 J_{t2}\right) + s^5 21{k_t}^2{J_{st}}^2 c_{t2} \\ +s^4\left(15{k_t}^3{J_{st}}^2 + 20{k_t}^3 J_{st} J_{t2}\right) + \\ s^3 20{k_t}^3 J_{st} c_{t2} + s^2\left(5{k_t}^4 J_{t2} + 10{k_t}^4 J_{st}\right) + 5{k_t}^4 c_{t2} s + {k_t}^5 \end{matrix}}{\begin{matrix} J_{t1}{J_{st}}^4 J_{t2} s^{11} + s^{10}\left(c_{t1}{J_{st}}^4 J_{t2} + J_{t1}{J_{st}}^4 c_{t2}\right) + \\ s^9\left(k_t{J_{st}}^4 J_{t2} + 8k_t J_{t1}{J_{st}}^3 J_{t2} + k_t J_{t1}{J_{st}}^4 + c_{t1}{J_{st}}^4 c_{t2}\right) \\ +s^8\left(k_t c_{t1}{J_{st}}^4 + 8k_t c_{t1}{J_{st}}^3 J_{t2} + 8k_t J_{t1}{J_{st}}^3 c_{t2}\right) \\ +s^7\begin{pmatrix} 7J_{t1}{J_{st}}^3{k_t}^2 + 21{k_t}^2 J_{t1}{J_{st}}^2 J_{t2} + {k_t}^2{J_{st}}^4 + 8k_t c_{t1}{J_{st}}^3 c_{t2} \\ +7{k_t}^2{J_{st}}^3 J_{t2} \end{pmatrix} \\ +s^6\begin{pmatrix} 21{k_t}^2 J_{t1}{J_{st}}^2 c_{t2} + 7c_{t1}{J_{st}}^3{k_t}^2 \\ +21{k_t}^2 c_{t1}{J_{st}}^2 J_{t2} + 7{k_t}^2{J_{st}}^3 c_{t2} \end{pmatrix} + \\ s^5\left(15{k_t}^3{J_{st}}^2 J_{t2} + 20{k_t}^3 J_{t1} J_{st} J_{t2} + 6{J_{st}}^3{k_t}^3 + 15{k_t}^3 J_{t1}{J_{st}}^2 + 21{k_t}^2 c_{t1}{J_{st}}^2 c_{t2}\right) \\ +s^4\left(15{k_t}^3 c_{t1}{J_{st}}^2 + 15{k_t}^3{J_{st}}^2 c_{t2} + 20{k_t}^3 c_{t1}{J_{st}}^2 J_{t2} + 20{k_t}^3 J_{t1} J_{st} c_{t2}\right) \\ +s^3\left(5{k_t}^4 J_{t1} J_{t2} + 20{k_t}^3 c_{t1} J_{st} c_{t2} + 10{k_t}^4 J_{t1} J_{st} + 10{J_{st}}^2{k_t}^4 + 10{k_t}^4 J_{st} J_{t2}\right) \\ +s^2\left(5{k_t}^4 c_{t1} J_{t2} + 10{k_t}^4 J_{st} c_{t2} + 5{k_t}^4 J_{t1} c_{t2} + 10{k_t}^4 c_{t1} J_{st}\right) + \\ s\left({k_t}^5 J_{t2} + 4{k_t}^5 J_{st} + {k_t}^5 J_{t1} + 5{k_t}^4 c_{t1} c_{t2}\right) + {k_t}^5 c_{t1} + {k_t}^5 c_{t2} \end{matrix}}$$

$\omega_{t1}(s)\{Numerically\}$

$$= \frac{\begin{matrix} 2.5 \times 10^{-24} s^{10} + 3.4 \times 10^{-20} s^9 + (2.95 \times 10^{-13}) s^8 \\ +(4 \times 10^{-9}) s^7 + 0.011 s^6 + 152.7 s^5 + (1.56 \times 10^8) s^4 \\ +2.11 \times 10^{12} s^3 + (5.7 \times 10^{17}) s^2 + (7.7 \times 10^{21}) s \\ +7.2 \times 10^{24} \end{matrix}}{\begin{matrix} (2.29 \times 10^{-27}) s^{11} + (4.12 \times 10^{-23}) s^{10} \\ +(2.67 \times 10^{-16}) s^9 + (4.8 \times 10^{-12}) s^8 \\ +(1.02 \times 10^{-5}) s^7 + 0.1837 s^6 \\ +(1.43 \times 10^5) s^5 + (2.55 \times 10^9) s^4 \\ +(5.33 \times 10^{14}) s^3 + (9.35 \times 10^{18}) s^2 \\ +(4.8 \times 10^{22}) s + (1.7 \times 10^{26}) \end{matrix}}$$

$$\omega_{t2}(s)\{Symbolically\}$$

$$= \frac{{k_t}^5}{\begin{matrix} J_{t1}{J_{st}}^4 J_{t2} s^{11} + s^{10}\left(c_{t1}{J_{st}}^4 J_{t2} + J_{t1}{J_{st}}^4 c_{t2}\right) + \\ s^9\left(k_t{J_{st}}^4 J_{t2} + 8k_t J_{t1}{J_{st}}^3 J_{t2} + k_t J_{t1}{J_{st}}^4 + c_{t1}{J_{st}}^4 c_{t2}\right) \\ +s^8\left(k_t c_{t1}{J_{st}}^4 + 8k_t c_{t1}{J_{st}}^3 J_{t2} + 8k_t J_{t1}{J_{st}}^3 c_{t2}\right) \\ +s^7\begin{pmatrix} 7J_{t1}{J_{st}}^3{k_t}^2 + 21{k_t}^2 J_{t1}{J_{st}}^2 J_{t2} + {k_t}^2{J_{st}}^4 + 8k_t c_{t1}{J_{st}}^3 c_{t2} \\ +7{k_t}^2{J_{st}}^3 J_{t2} \end{pmatrix} \\ +s^6\begin{pmatrix} 21{k_t}^2 J_{t1}{J_{st}}^2 c_{t2} + 7c_{t1}{J_{st}}^3{k_t}^2 \\ +21{k_t}^2 c_{t1}{J_{st}}^2 J_{t2} + 7{k_t}^2{J_{st}}^3 c_{t2} \end{pmatrix} + \\ s^5\left(15{k_t}^3{J_{st}}^2 J_{t2} + 20{k_t}^3 J_{t1} J_{st} J_{t2} + 6{J_{st}}^3{k_t}^3 + 15{k_t}^3 J_{t1}{J_{st}}^2 + 21{k_t}^2 c_{t1}{J_{st}}^2 c_{t2}\right) \\ +s^4\left(15{k_t}^3 c_{t1}{J_{st}}^2 + 15{k_t}^3{J_{st}}^2 c_{t2} + 20{k_t}^3 c_{t1}{J_{st}}^2 J_{t2} + 20{k_t}^3 J_{t1} J_{st} c_{t2}\right) \\ +s^3\left(5{k_t}^4 J_{t1} J_{t2} + 20{k_t}^3 c_{t1} J_{st} c_{t2} + 10{k_t}^4 J_{t1} J_{st} + 10{J_{st}}^2{k_t}^4 + 10{k_t}^4 J_{st} J_{t2}\right) \\ +s^2\left(5{k_t}^4 c_{t1} J_{t2} + 10{k_t}^4 J_{st} c_{t2} + 5{k_t}^4 J_{t1} c_{t2} + 10{k_t}^4 c_{t1} J_{st}\right) + \\ s({k_t}^5 J_{t2} + 4{k_t}^5 J_{st} + {k_t}^5 J_{t1} + 5{k_t}^4 c_{t1} c_{t2}) + {k_t}^5 c_{t1} + {k_t}^5 c_{t2} \end{matrix}}$$

$$\omega_{t2}(s)\{Numerically\} = \frac{(7.2 \times 10^{24})}{\begin{matrix} (2.29 \times 10^{-27})s^{11} + (4.12 \times 10^{-23})s^{10} \\ +(2.67 \times 10^{-16})s^9 + (4.8 \times 10^{-12})s^8 \\ +(1.02 \times 10^{-5})s^7 + 0.1837s^6 \\ +(1.43 \times 10^5)s^5 + (2.55 \times 10^9)s^4 \\ +(5.33 \times 10^{14})s^3 + (9.35 \times 10^{18})s^2 \\ +(4.8 \times 10^{22})s + (1.7 \times 10^{26}) \end{matrix}}$$

4.3.2. FEM Main Rotor Derivation

Finite element (five sections), main rotor shaft configuration of Schweizer 300C is shown above in figure (3.7) and according to that model, the parameters are provided in table (4.3). Note that some parameters are constant values and some of them need to be calculated, the calculations are explained in details in this section and can be compared with the calculations done automatically by Matlab (Shown in Appendix A-5)

Recall that

$$\bar{J}_{m1} = \bar{J}_{m2} = \bar{J}_{m3} = \bar{J}_{m4} = J_m$$

And

$$k_{m1} = k_{m2} = k_{m3} = k_{m4} = k_{m5} = k_m$$

Calculations

1- $J_{sm} = \frac{\pi {d_{sm}}^4}{32} = \frac{\pi(0.07^4)}{32} = 2.36 \times 10^{-6}\ m^4$

2- $J_{m1} = \frac{\pi {d_{m1}}^4}{32} = \frac{\pi(0.46^4)}{32} = 4.4 \times 10^{-3}\ m^4$

3- $J_{m2} = \frac{\pi {d_{m2}}^4}{32} = \frac{\pi(0.35^4)}{32} = 1.5 \times 10^{-3}\ m^4$

4- $k_m = \frac{G \times J_{sm}}{l_m} = \frac{(80 \times 10^9) \times (2.36 \times 10^{-6})}{1.1} = 1.71 \times 10^5\ N.m/rad$

So $\omega_{m1}(s)$and $\omega_{m2}(s)$ can be expressed as

$\omega_{m1}(s)\{Symbolically\}$

$$= \frac{\begin{matrix} s^{10}J_{sm}{}^{4}J_{m2} \\ +s^{9}J_{sm}{}^{4}c_{m2} \\ +s^{8}\left(8k_{m}J_{sm}{}^{3}J_{m2}+k_{m}J_{sm}{}^{4}\right) \\ +s^{7}8k_{m}J_{sm}{}^{3}c_{m2}+ \\ s^{6}\left(7J_{sm}{}^{3}k_{m}{}^{2}+21k_{m}{}^{2}J_{sm}{}^{2}J_{m2}\right) \\ +s^{5}21k_{m}{}^{2}J_{sm}{}^{2}c_{m2} \\ +s^{4}\left(15k_{m}{}^{3}J_{sm}{}^{2}+20k_{m}{}^{3}J_{sm}J_{m2}\right)+ \\ s^{3}20k_{m}{}^{3}J_{sm}c_{m2}+ \\ s^{2}\left(5k_{m}{}^{4}J_{m2}+10k_{m}{}^{4}J_{sm}\right) \\ +5k_{m}{}^{4}c_{m2}s \\ +k_{m}{}^{5} \end{matrix}}{\begin{matrix} J_{m1}J_{sm}{}^{4}J_{m2}s^{11} \\ +s^{10}\left(c_{m1}J_{sm}{}^{4}J_{m2}+J_{m1}J_{sm}{}^{4}c_{m2}\right)+ \\ s^{9}\begin{pmatrix} k_{m}J_{sm}{}^{4}J_{m2}+8k_{m}J_{m1}J_{sm}{}^{3}J_{m2} \\ +k_{m}J_{m1}J_{sm}{}^{4}+c_{m1}J_{sm}{}^{4}c_{m2} \end{pmatrix} \\ +s^{8}\left(k_{m}c_{m1}J_{sm}{}^{4}+8k_{m}c_{m1}J_{sm}{}^{3}J_{m2}+8k_{m}J_{m1}J_{sm}{}^{3}c_{m2}\right) \\ +s^{7}\begin{pmatrix} 7J_{m1}J_{sm}{}^{3}k_{m}{}^{2}+21k_{m}{}^{2}J_{m1}J_{sm}{}^{2}J_{m2} \\ +k_{m}{}^{2}J_{sm}{}^{4}+8k_{m}c_{m1}J_{sm}{}^{3}c_{m2} \\ +7k_{m}{}^{2}J_{sm}{}^{3}J_{m2} \end{pmatrix} \\ +s^{6}\begin{pmatrix} 21k_{m}{}^{2}J_{m1}J_{sm}{}^{2}c_{m2}+7c_{m1}J_{sm}{}^{3}k_{m}{}^{2} \\ +21k_{m}{}^{2}c_{m1}J_{sm}{}^{2}J_{m2}+7k_{m}{}^{2}J_{sm}{}^{3}c_{m2} \end{pmatrix}+ \\ s^{5}\begin{pmatrix} 15k_{m}{}^{3}J_{sm}{}^{2}J_{m2}+20k_{m}{}^{3}J_{m1}J_{mt}J_{m2}+6J_{sm}{}^{3}k_{m}{}^{3} \\ +15k_{m}{}^{3}J_{m1}J_{sm}{}^{2}+21k_{m}{}^{2}c_{m1}J_{sm}{}^{2}c_{m2} \end{pmatrix} \\ +s^{4}\begin{pmatrix} 15k_{m}{}^{3}c_{m1}J_{sm}{}^{2}+15k_{m}{}^{3}J_{sm}{}^{2}c_{m2} \\ +20k_{m}{}^{3}c_{m1}J_{sm}{}^{2}J_{m2}+20k_{m}{}^{3}J_{m1}J_{sm}c_{m2} \end{pmatrix} \\ +s^{3}\begin{pmatrix} 5k_{m}{}^{4}J_{m1}J_{m2}+20k_{m}{}^{3}c_{m1}J_{sm}c_{m2} \\ +10k_{m}{}^{4}J_{m1}J_{sm}+10J_{sm}{}^{2}k_{m}{}^{4}+10k_{m}{}^{4}J_{sm}J_{m2} \end{pmatrix} \\ +s^{2}\begin{pmatrix} 5k_{m}{}^{4}c_{m1}J_{m2}+10k_{m}{}^{4}J_{sm}c_{m2} \\ +5k_{m}{}^{4}J_{m1}c_{m2}+10k_{m}{}^{4}c_{m1}J_{sm} \end{pmatrix}+ \\ s(k_{m}{}^{5}J_{m2}+4k_{m}{}^{5}J_{sm}+k_{m}{}^{5}J_{m1} \\ +5k_{m}{}^{4}c_{m1}c_{m2}) \\ +k_{m}{}^{5}c_{m1}+k_{m}{}^{5}c_{m2} \end{matrix}}$$

$$\omega_{m1}(s)\{Numerically\} = \frac{\begin{array}{c}(6.3\times10^{-26})s^{10}+(6.2\times10^{-22})s^{9}\\+(3.7\times10^{-14})s^{8}+(3.6\times10^{-10})s^{7}\\+0.007s^{6}+68.44s^{5}\\+(4.9\times10^{8})s^{4}+(4.7\times10^{12})s^{3}\\+(8.8\times10^{18})s^{2}+(8.6\times10^{22})s\\+(1.5\times10^{26})\end{array}}{\begin{array}{c}(5.7\times10^{-29})s^{11}+(8.1\times10^{-25})s^{10}\\+(3.3\times10^{-17})s^{9}+(4.7\times10^{-13})s^{8}\\+(6.4\times10^{-6})s^{7}+0.09s^{6}\\+(4.4\times10^{5})s^{5}+(6.2\times10^{9})s^{4}\\+(8.1\times10^{15})s^{3}+(1.1\times10^{20})s^{2}\\+(7.8\times10^{23})s+(3.5\times10^{27})\end{array}}$$

$$\omega_{m2}(s)\{Symbolically\}$$

$$= \frac{{k_m}^5}{\begin{matrix} J_{m1}{J_{sm}}^4 J_{m2} s^{11} \\ +s^{10}\left(c_{m1}{J_{sm}}^4 J_{m2} + J_{m1}{J_{sm}}^4 c_{m2}\right) + \\ s^9\begin{pmatrix} k_m{J_{sm}}^4 J_{m2} + 8k_m J_{m1}{J_{sm}}^3 J_{m2} \\ +k_m J_{m1}{J_{sm}}^4 + c_{m1}{J_{sm}}^4 c_{m2} \end{pmatrix} \\ +s^8\left(k_m c_{m1}{J_{sm}}^4 + 8k_m c_{m1}{J_{sm}}^3 J_{m2} + 8k_m J_{m1}{J_{sm}}^3 c_{m2}\right) \\ +s^7\begin{pmatrix} 7J_{m1}{J_{sm}}^3{k_m}^2 + 21{k_m}^2 J_{m1}{J_{sm}}^2 J_{m2} \\ +{k_m}^2{J_{sm}}^4 + 8k_m c_{m1}{J_{sm}}^3 c_{m2} \\ +7{k_m}^2{J_{sm}}^3 J_{m2} \end{pmatrix} \\ +s^6\begin{pmatrix} 21{k_m}^2 J_{m1}{J_{sm}}^2 c_{m2} + 7c_{m1}{J_{sm}}^3{k_m}^2 \\ +21{k_m}^2 c_{m1}{J_{sm}}^2 J_{m2} + 7{k_m}^2{J_{sm}}^3 c_{m2} \end{pmatrix} + \\ s^5\begin{pmatrix} 15{k_m}^3{J_{sm}}^2 J_{m2} + 20{k_m}^3 J_{m1} J_{mt} J_{m2} + 6{J_{sm}}^3{k_m}^3 \\ +15{k_m}^3 J_{m1}{J_{sm}}^2 + 21{k_m}^2 c_{m1}{J_{sm}}^2 c_{m2} \end{pmatrix} \\ +s^4\begin{pmatrix} 15{k_m}^3 c_{m1}{J_{sm}}^2 + 15{k_m}^3{J_{sm}}^2 c_{m2} \\ +20{k_m}^3 c_{m1}{J_{sm}}^2 J_{m2} + 20{k_m}^3 J_{m1} J_{sm} c_{m2} \end{pmatrix} \\ +s^3\begin{pmatrix} 5{k_m}^4 J_{m1} J_{m2} + 20{k_m}^3 c_{m1} J_{sm} c_{m2} \\ +10{k_m}^4 J_{m1} J_{sm} + 10{J_{sm}}^2{k_m}^4 + 10{k_m}^4 J_{sm} J_{m2} \end{pmatrix} \\ +s^2\begin{pmatrix} 5{k_m}^4 c_{m1} J_{m2} + 10{k_m}^4 J_{sm} c_{m2} \\ +5{k_m}^4 J_{m1} c_{m2} + 10{k_m}^4 c_{m1} J_{sm} \end{pmatrix} + \\ s({k_m}^5 J_{m2} + 4{k_m}^5 J_{sm} + {k_m}^5 J_{m1} \\ +5{k_m}^4 c_{m1} c_{m2}) \\ +{k_m}^5 c_{m1} + {k_m}^5 c_{m2} \end{matrix}}$$

$$\omega_{m2}(s)\{Numerically\} = \frac{(1.5 \times 10^{26})}{\begin{matrix} (5.7 \times 10^{-29})s^{11} + (8.1 \times 10^{-25})s^{10} \\ +(3.3 \times 10^{-17})s^9 + (4.7 \times 10^{-13})s^8 \\ +(6.4 \times 10^{-6})s^7 + 0.09s^6 \\ +(4.4 \times 10^5)s^5 + (6.2 \times 10^9)s^4 \\ +(8.1 \times 10^{15})s^3 + (1.1 \times 10^{20})s^2 \\ +(7.8 \times 10^{23})s + (3.5 \times 10^{27}) \end{matrix}}$$

Then, the simulation block diagram for the finite element model (FEM) of the whole system was built as it is shown in figure 4.17

(The block diagram in Simulink for the FEM of the whole system is shown in appendix A-5)

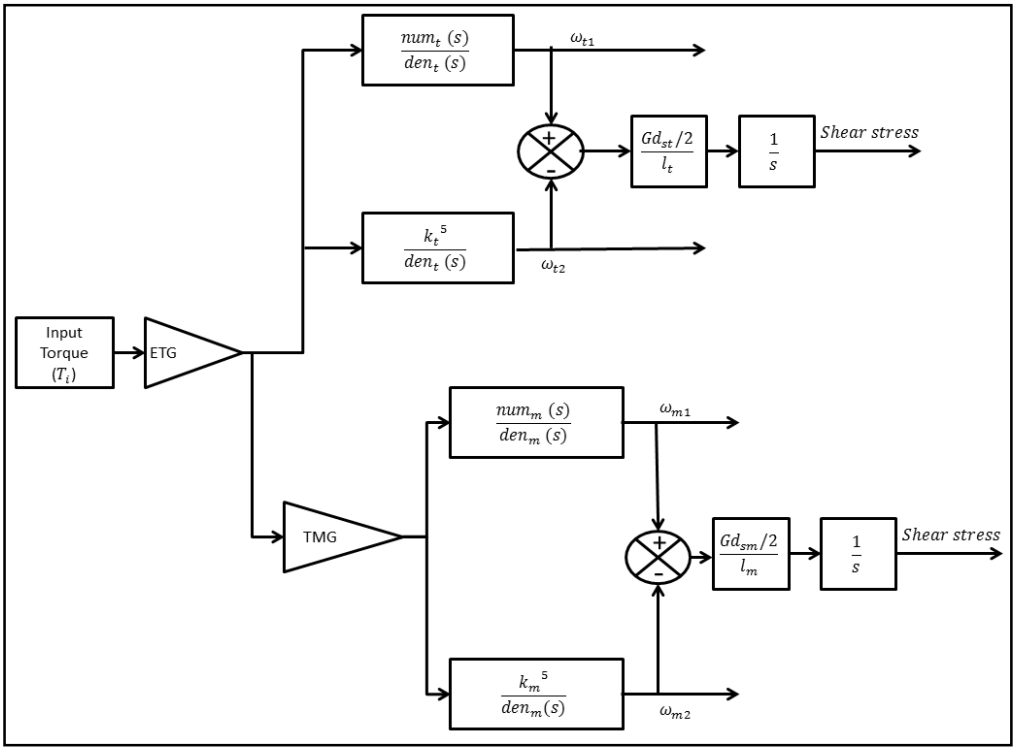

Figure 4.17 FEM simulation block diagram of the dual rotor-shaft system

4.3.3. FEM Time Domain (Transient Response) Analysis

Again a unit step input changes on the system input (input torque) is applied to the new model (FEM) to be compared with LPM shown earlier and also with DLPM which will be shown later.

the output angular speed (ω) for the finite element model (FEM) will be simulated in this section for both the tail and main rotors of the helicopter. The supplied torque intput is the same of that used with LPM ($T_i(t) = 3250\ N.m$) is used to generate the steady state response of tail rotor output angular speed $\omega_{t1} = \omega_{t2} = 100\ rad/s$ and $\omega_{m1} = \omega_{m2} = 27\ rad/s$.

Figures (4.18) to (4.20) shown bellow illustrates the FEM time domain transient responses for tail rotor with drive end $\omega_{t1}(t)$ and the load end $\omega_{t2}(t)$, respectively.

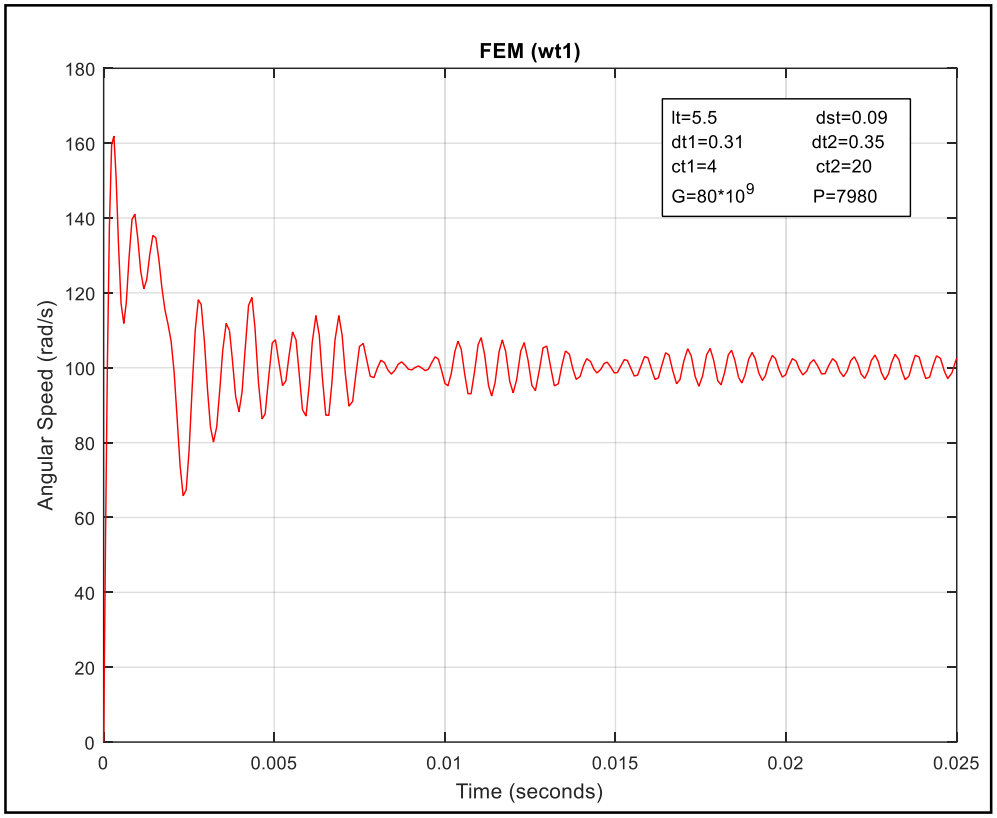

Figure 4.18 Step response of FEM (tail rotor-drive end)

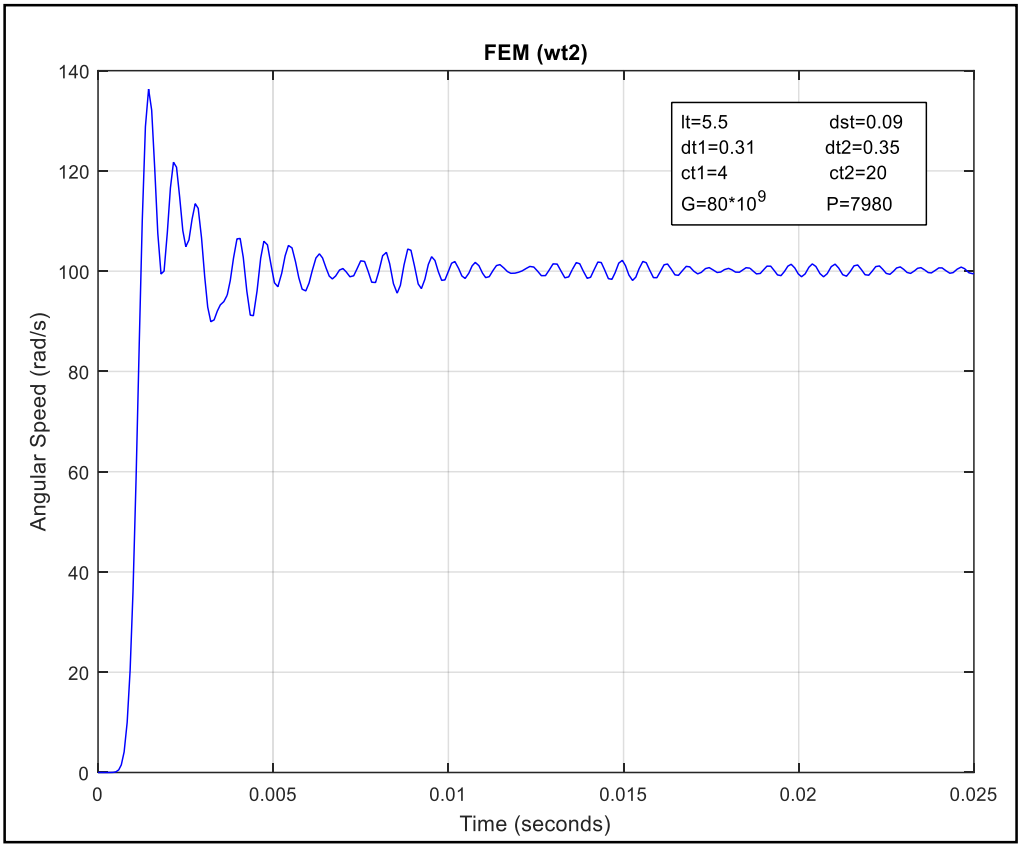

Figure 4.19 Step response of FEM (tail shaft-load end)

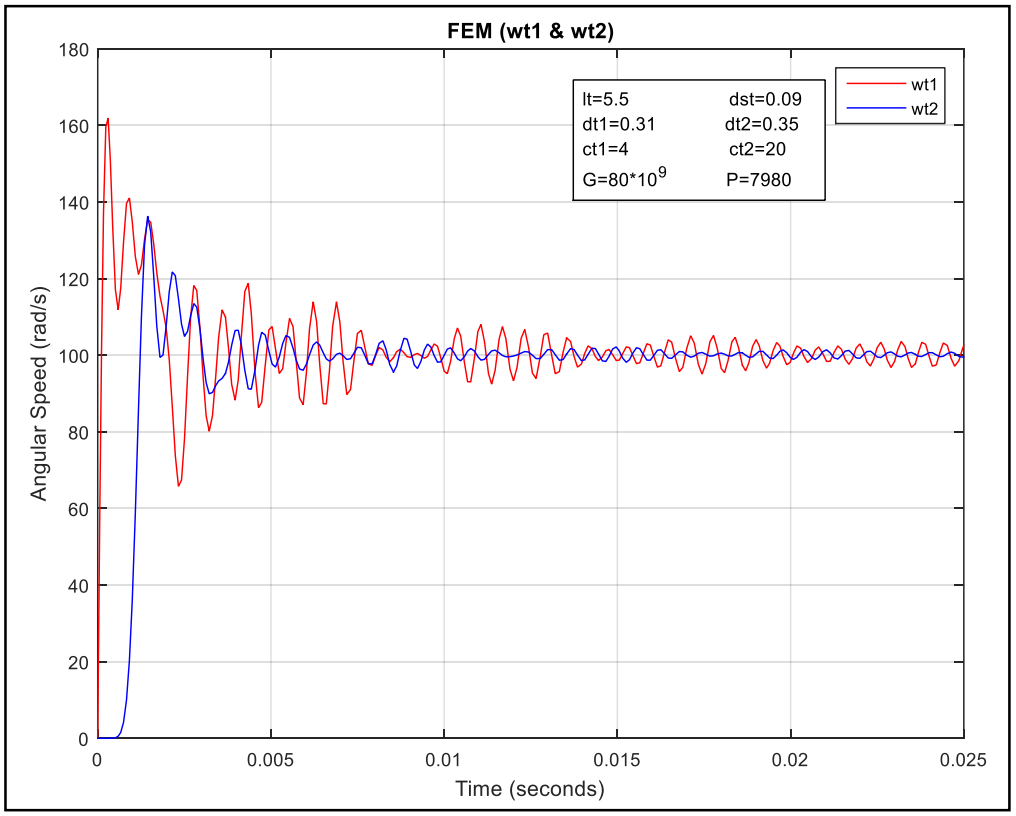

Figure 4.20 FEM step responses of tail rotor (drive and load ends)

Similarly Figures (4.21) to (4.23) shown bellow illustrates the FEM time domain transient responses for the main rotor with drive end $\omega_{m1}(t)$ and the load end $\omega_{m2}(t)$, respectively.

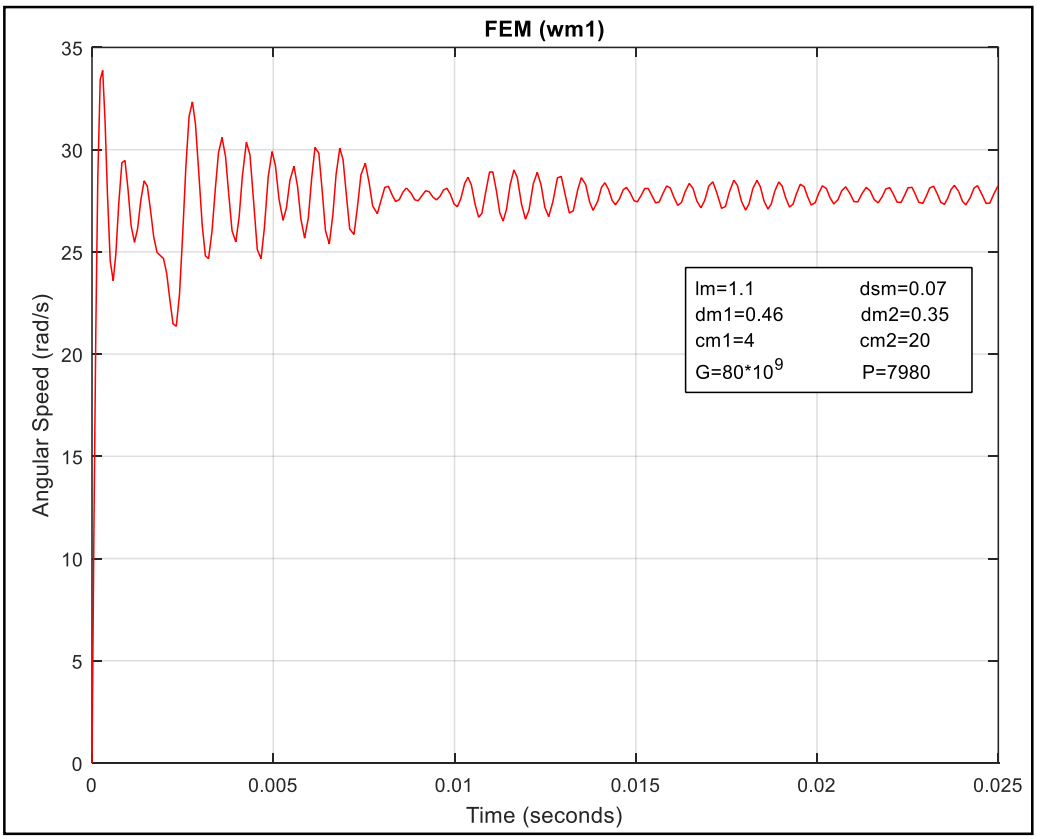

Figure 4.21 Step response of FEM (main rotor-drive end)

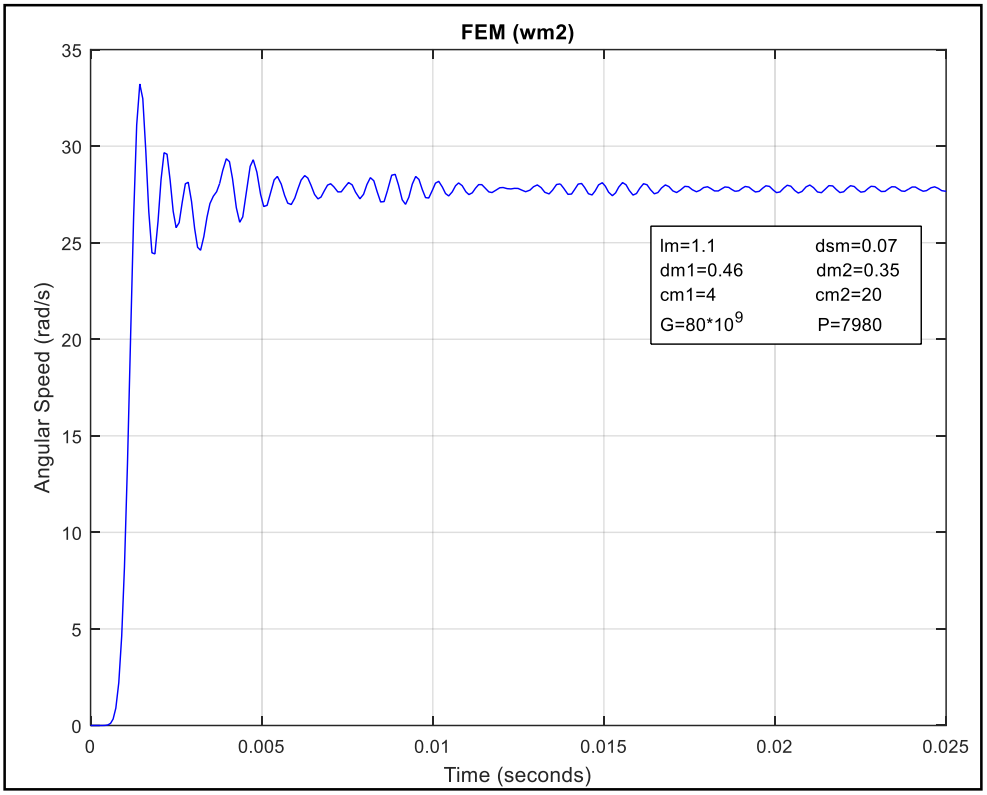

Figure 4.22 Step response of FEM (main rotor-load end)

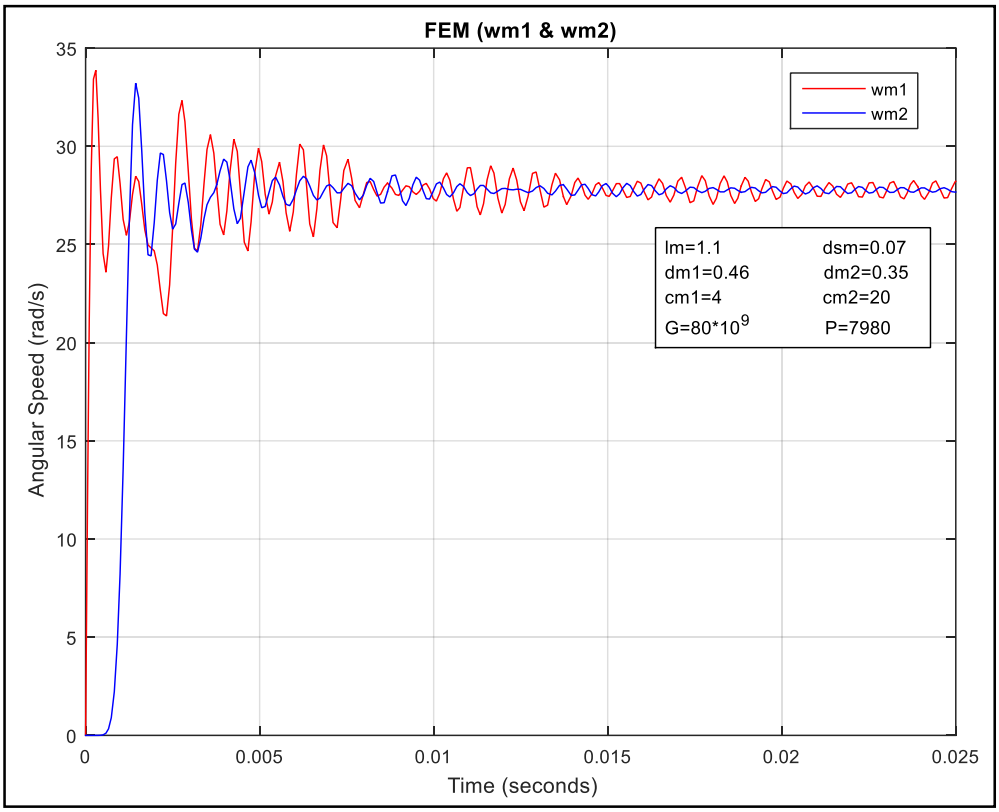

Figure 4.23 FEM step responses of main rotor (drive and load ends)

At the end, all the step responses of the FEM are shown in one graph for better illustration. Figure 4.24 showing the four FEM responses for both tail and main rotors with drive and load ends.

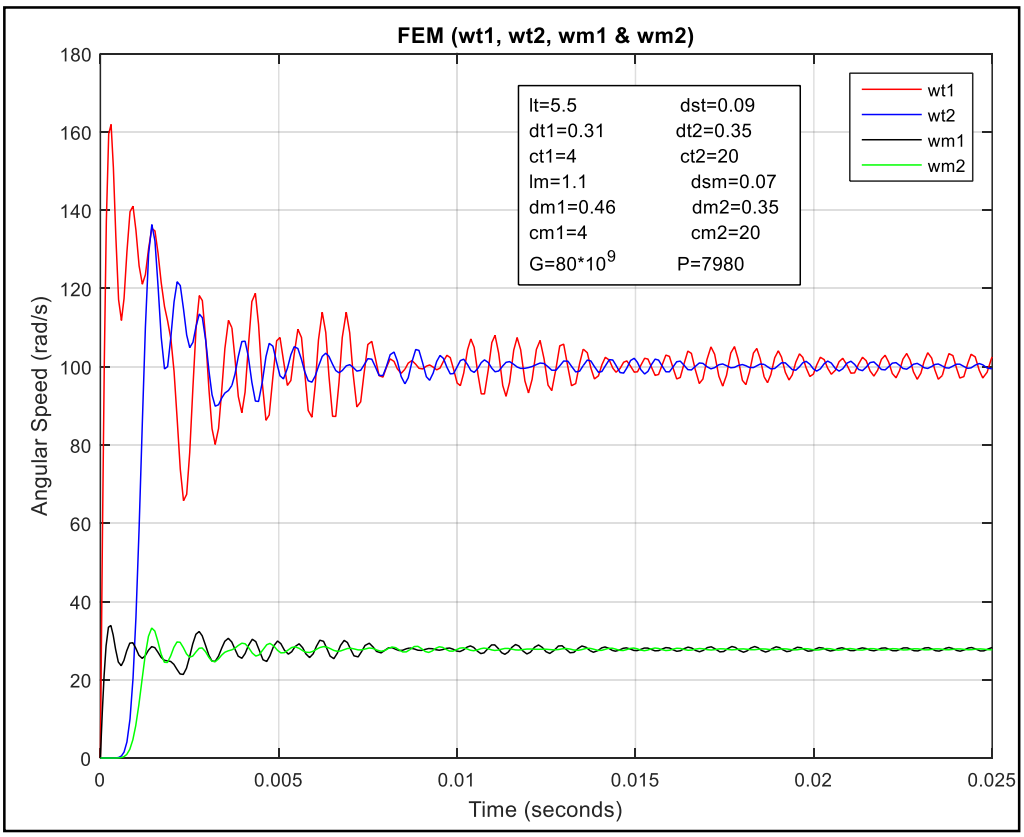

Figure 4.24 FEM step responses of both tail and main rotors (drive and load ends)

After that, the shear stress of the FEM is simulated and results are shown below for both tail and main rotors in figures (4.25) and (4.26) respectively.

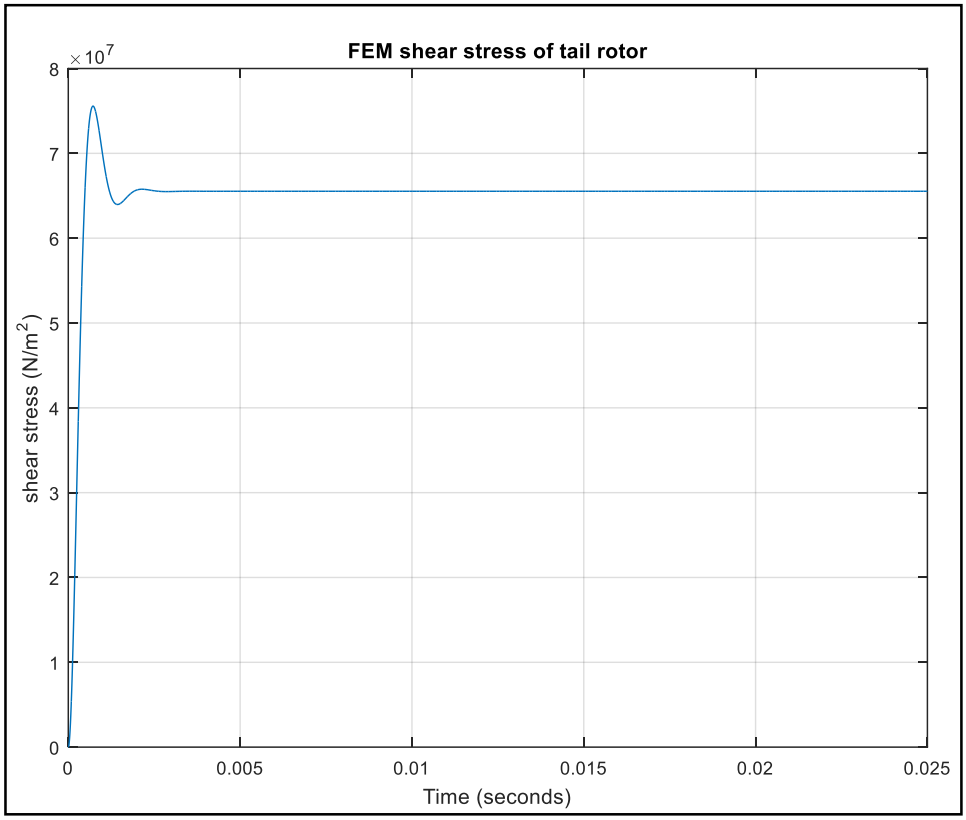

Figure 4.25 FEM shear stress of tail rotor

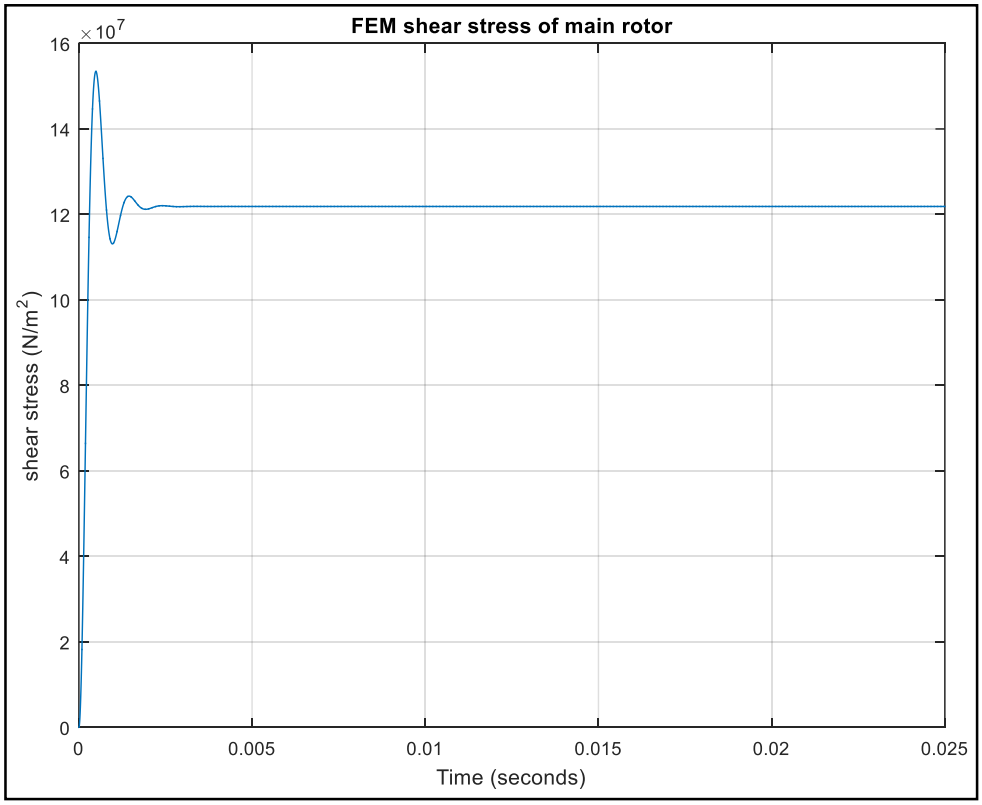

Figure 4.26 FEM shear stress of main rotor

4.3.4. FEM Frequency Domain Analysis

Similar to LPM, the FEM Bode plots are shown below in figure (4.27) and (4.28), and the tail rotor resonant frequencies (ω_t) can be estimated to be $2000,5000,8500,10050,10300\ rad/s$ at the drive end, and $10000,80000,15000,200000,230000\ rad/s$ at the load end.

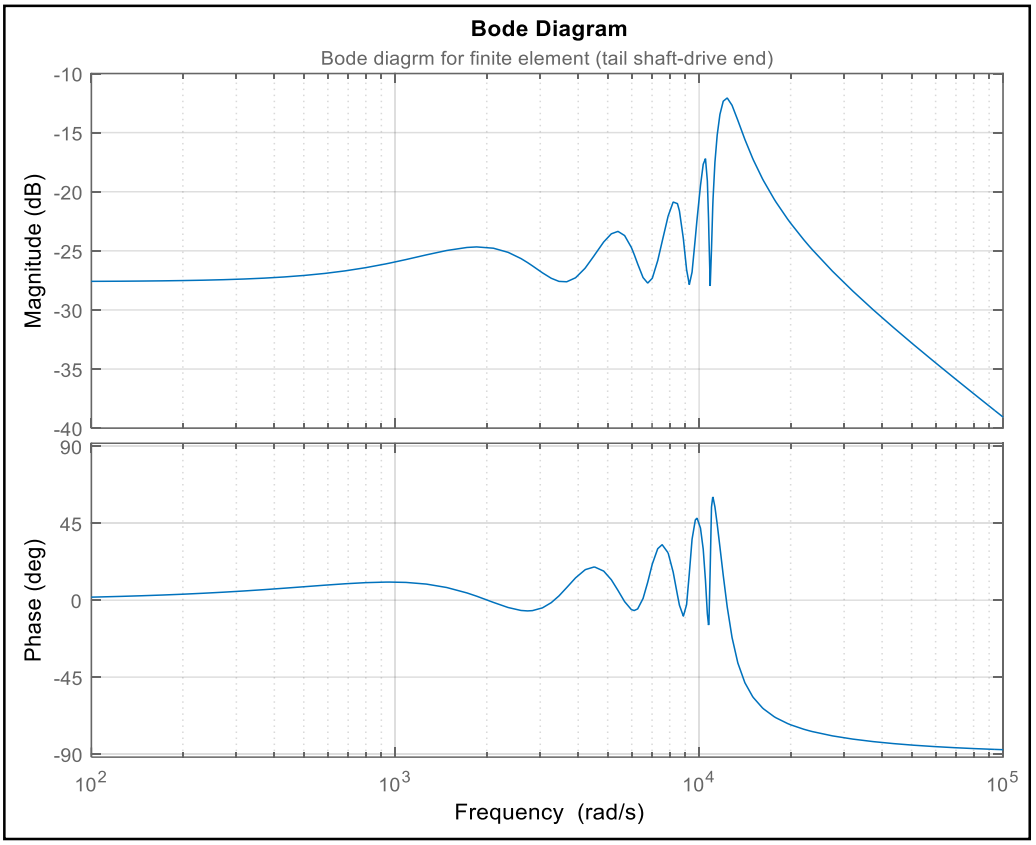

Figure 4.27 Bode plot of FEM (tail shaft-drive end)

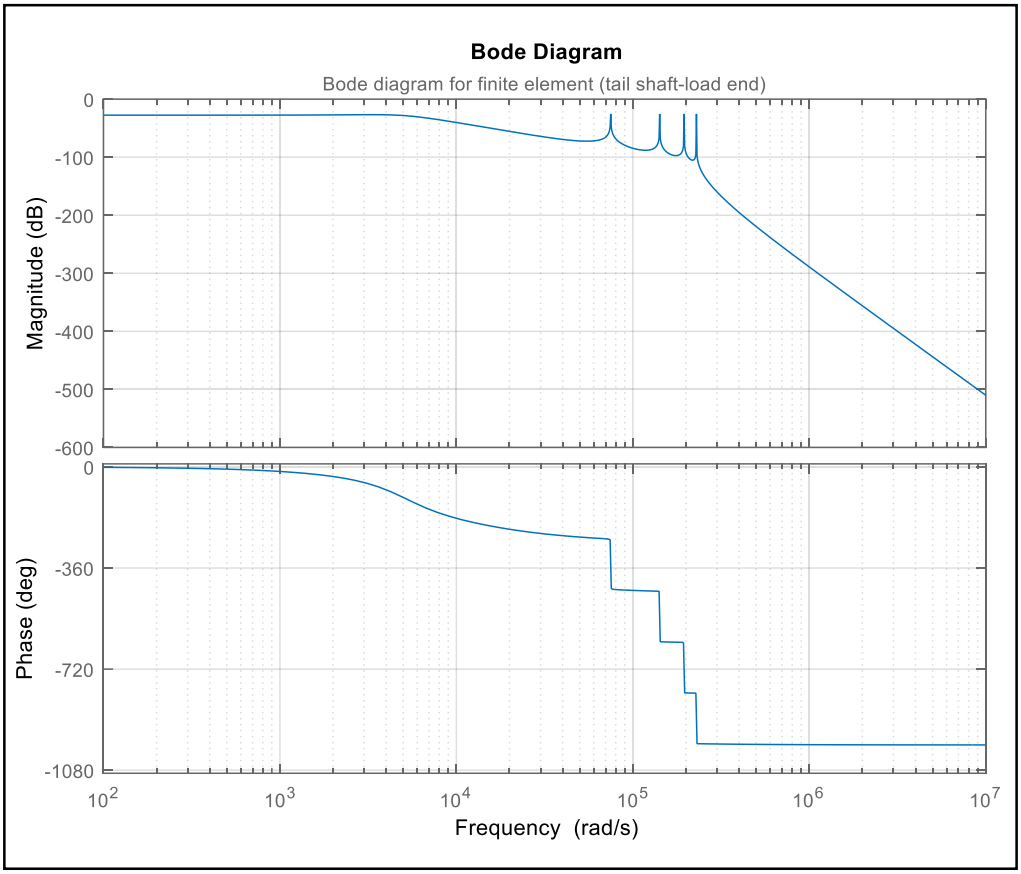

Figure 4.28 Bode plot of FEM (tail shaft-load end)

Again FEM main rotor Bode plots are shown below in figures (4.29) and (4.30) and according to plots, the resonant frequencies (ω_m) can be estimated to be $2000,5000,8500,10050,10300\ rad/s$ at the drive end, and $10000,80000,15000,200000,230000\ rad/s$ at the load end.

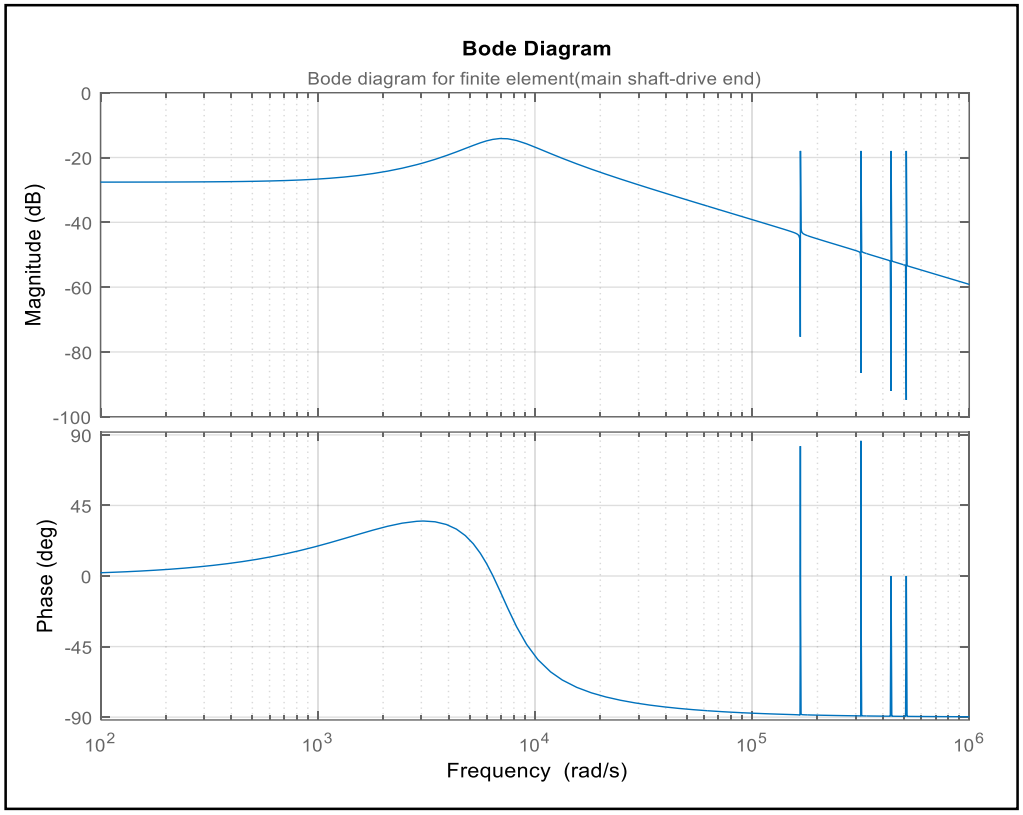

Figure 4.29 Bode plot of FEM (main shaft-drive end)

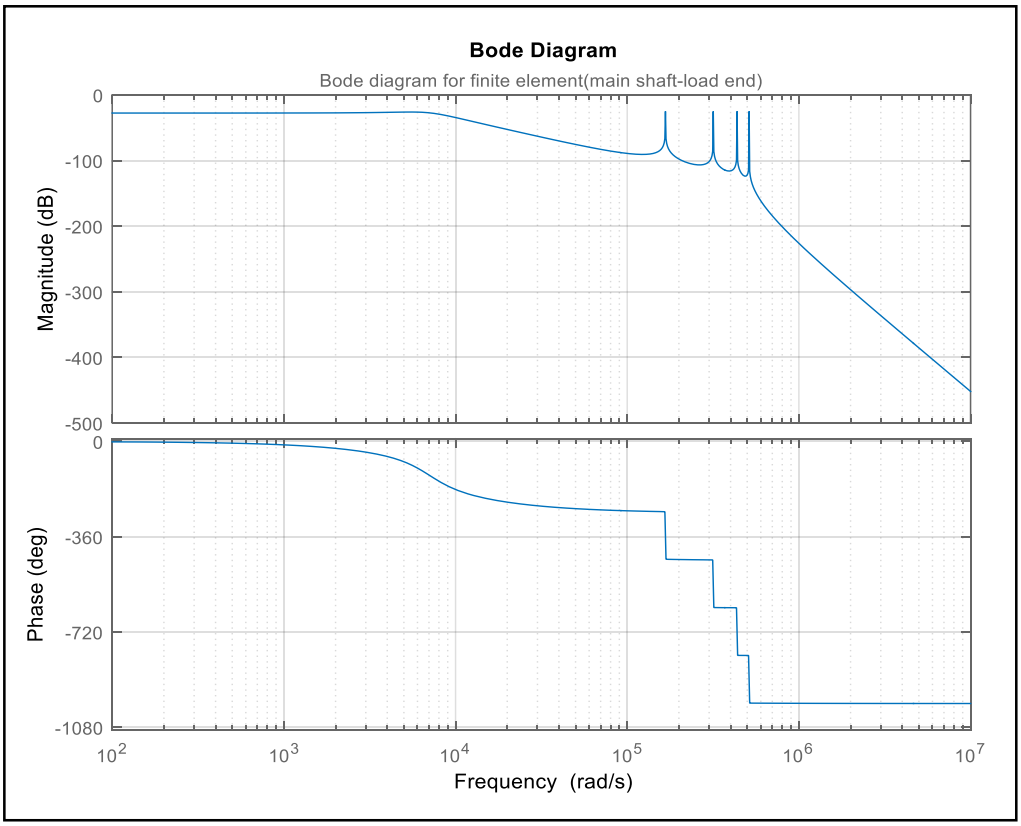

Figure 4.30 Bode plot of FEM (main shaft-load end)

4.4. Distributed-Lumped Parameter Model (DLPM)

Referring to section (3.3), the DLPM was derived and the transfer function matrix can be expressed as

$$\begin{bmatrix}\omega_1(s)\\ \omega_2(s)\end{bmatrix} = \begin{bmatrix}\xi w(s) + \gamma_2(s)\\ \xi(w(s)^2 - 1)^{\frac{1}{2}}\end{bmatrix} T_1(s)/\Delta(s)$$

Where

$$\Delta(s) = \xi\big(\gamma_1(s) + \gamma_2(s)\big)w(s) + \gamma_1(s)\gamma_2(s) + \xi^2$$

4.4.1. Tail Rotor Model Simulation

DLPM tail rotor shaft configuration of Schweizer 300C is shown earlier in figure (3.11) and according to that model; and the parameters listed in table (4.2), Note that some parameters are constant values and some of them need to be calculated, the calculations are explained in details in this section and can be compared with the calculations done automatically by Matlab (Shown in Appendix A-6)

Calculations

1- $J_{st} = \frac{\pi {d_{st}}^4}{32} = \frac{\pi(0.09^4)}{32} = 6.44 \times 10^{-6}\ m^4$

2- $J_{t1} = \frac{\pi {d_{t1}}^4}{32} = \frac{\pi(0.31^4)}{32} = 9.06 \times 10^{-4}\ m^4$

3- $J_{t2} = \frac{\pi {d_{t2}}^4}{32} = \frac{\pi(0.35^4)}{32} = 1.5 \times 10^{-3}\ m^4$

4- $L_t = \rho \times J_{st} = (7980) \times (6.44 \times 10^{-6}) = 0.0514\ m^4$

5- $C_t = \frac{1}{G \times J_{st}} = \frac{1}{(80\times10^9)\times(6.44\times10^{-6})} = 1.94 \times 10^{-6}\ \ N^{-1}\, m^{-2}$

6- $\xi_t = J_{st}\sqrt{(\rho \times G)} = (6.44 \times 10^{-6})\sqrt{(7980) \times (80 \times 10^9)} = 162.67\ kg.m^2/s^2$

7- $\Gamma_t = 2 \times l_t \times \sqrt{(L_t \times C_t)} = 2 \times 5.5 \times \sqrt{(0.0514 \times 1.94 \times 10^{-6})} = 0.0035$

8- $w(s) = \frac{1+e^{-\Gamma_t s}}{1-e^{-\Gamma_t s}} = \frac{1+e^{-0.0035s}}{1-e^{-0.0035s}}$

9- $(w(s)^2 - 1)^{\frac{1}{2}} = \frac{e^{-0.5\Gamma_t s}}{1-e^{-\Gamma_t s}} = \frac{e^{-0.50\times 0035s}}{1-e^{-0.0035s}} = \frac{e^{-0.00175s}}{1-e^{-0.0035s}}$

4.4.2. Main Rotor Model Simulation

DLPM main rotor shaft configuration of Schweizer 300C is shown earlier in figure (3.11) and according to that model, the parameters are provided in table (4.3). The calculations are explained in details in this section and can be compared with the calculations done automatically by Matlab (Shown in Appendix A-7)

Calculations

1- $J_{sm} = \frac{\pi {d_{sm}}^4}{32} = \frac{\pi(0.07^4)}{32} = 2.36 \times 10^{-6}\ m^4$

2- $J_{m1} = \frac{\pi {d_{m1}}^4}{32} = \frac{\pi(0.46^4)}{32} = 4.4 \times 10^{-3}\ m^4$

3- $J_{m2} = \frac{\pi {d_{m2}}^4}{32} = \frac{\pi(0.35^4)}{32} = 1.5 \times 10^{-3}\ m^4$

4- $L_m = \rho \times J_{sm} = (7980) \times (2.36 \times 10^{-6}) = 0.0188\ m^4$

5- $C_m = \frac{1}{G \times J_{sm}} = \frac{1}{(80\times 10^9)\times(2.36\times 10^{-6})} = 5.3 \times 10^{-6}\ N^{-1}\ m^{-2}$

6- $\xi_m = J_{sm}\sqrt{(\rho \times G)} = (2.36 \times 10^{-6})\sqrt{(7980) \times (80 \times 10^9)} = 59.63\ kg.m^2/s^2$

7- $\Gamma_m = 2 \times l_m \times \sqrt{(L_m \times C_m)} = 2 \times 1.1 \times \sqrt{(0.0188 \times 5.3 \times 10^{-6})} = 0.00069$

8- $w(s) = \frac{1+e^{-\Gamma_m s}}{1-e^{-\Gamma_m s}} = \frac{1+e^{-0.00069s}}{1-e^{-0.00069s}}$

9- $(w(s)^2 - 1)^{\frac{1}{2}} = \frac{e^{-0.5\Gamma_m s}}{1-e^{-\Gamma_m s}} = \frac{e^{-0.50\times 0.00069 s}}{1-e^{-0.00069 s}} = \frac{e^{-0.000345 s}}{1-e^{-0.0035 s}}$

Then, the simulation block diagram in Simulink for the distributed-lumped parameter model (DLPM) of the whole system was built as it is shown in figure (4.31)

(The block diagram in Simulink for the DLPM of the whole system is shown in appendix A-6).

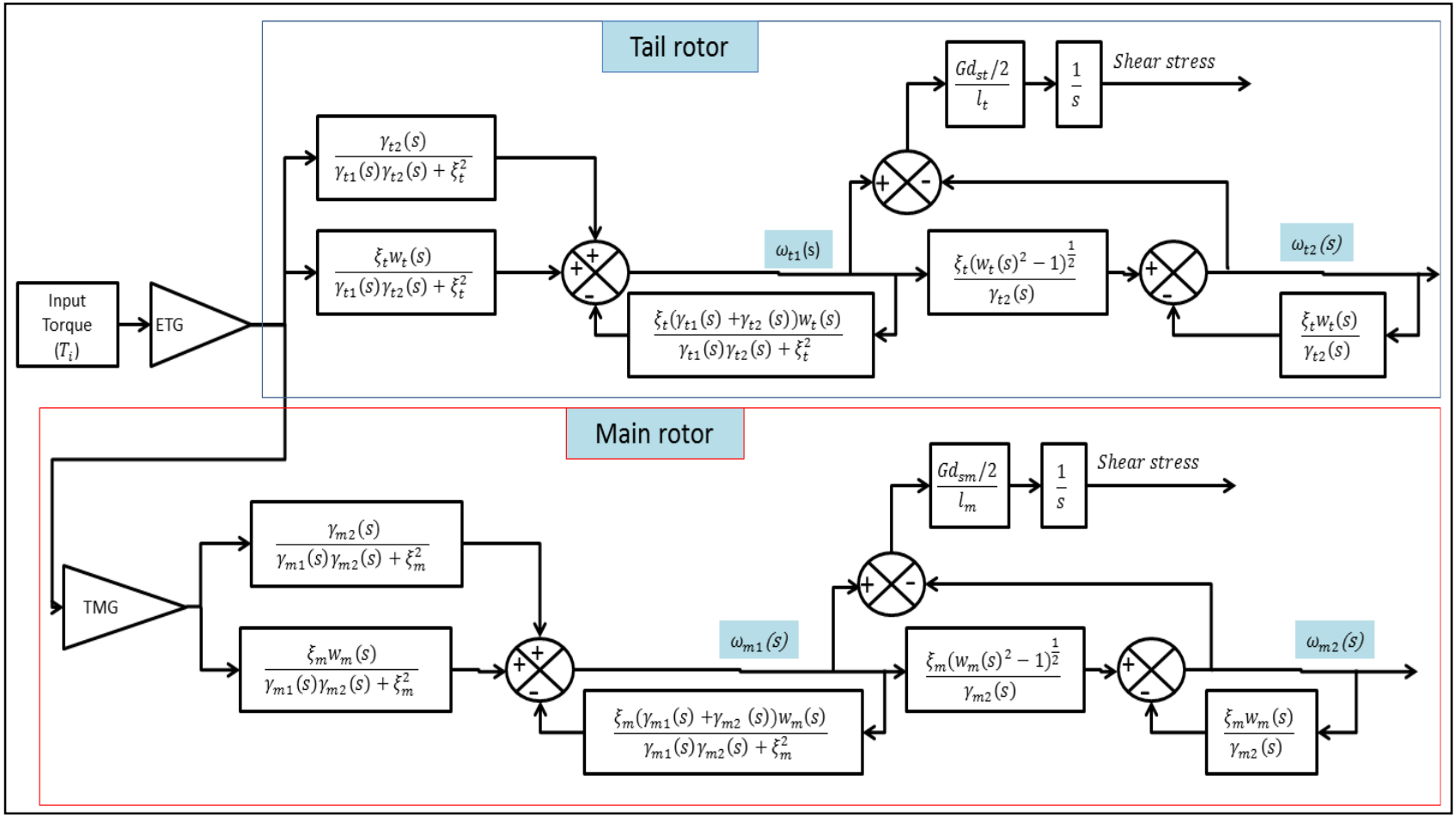

Figure 4.31 DLPM simulation block diagram of the dual rotor-shaft system

4.4.3. DLPM Time Domain (Transient Response) Analysis

Similar to LPM and FEM, the DLPM will be subjected to a unit step input change on the system input (input torque $T_i(t) = 3250\ N.m$) in order to study the steady state response of the DLPM and compare it with LPM and FEM.

Here the output angular speed (ω) for the distributed lumped parameter model (DLPM) is simulated again for both the tail and main rotors. The steady state response of tail rotor output angular speed $\omega_{t1} = \omega_{t2} = 100\ rad/s$ and $\omega_{m1} = \omega_{m2} = 27\ rad/s$.

Figures (4.32) to (4.34) shown bellow illustrates the DLPM time domain transient responses for tail rotor with drive end $\omega_{t1}(t)$ and the load end $\omega_{t2}(t)$, respectively.

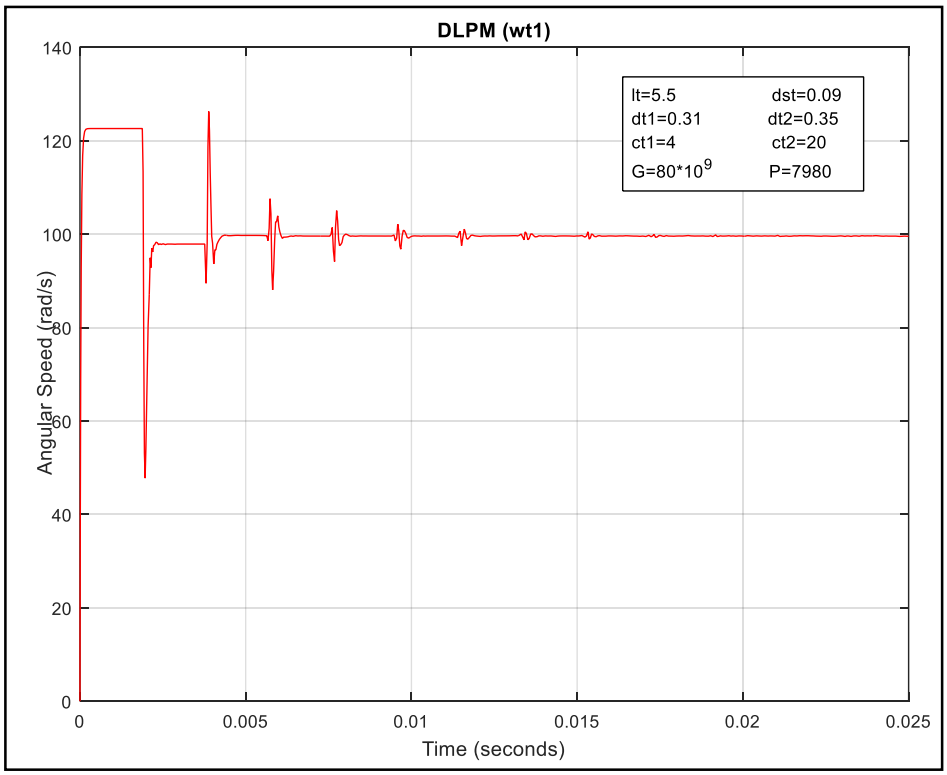

Figure 4.32 Step response of DLPM (tail shaft-drive end)

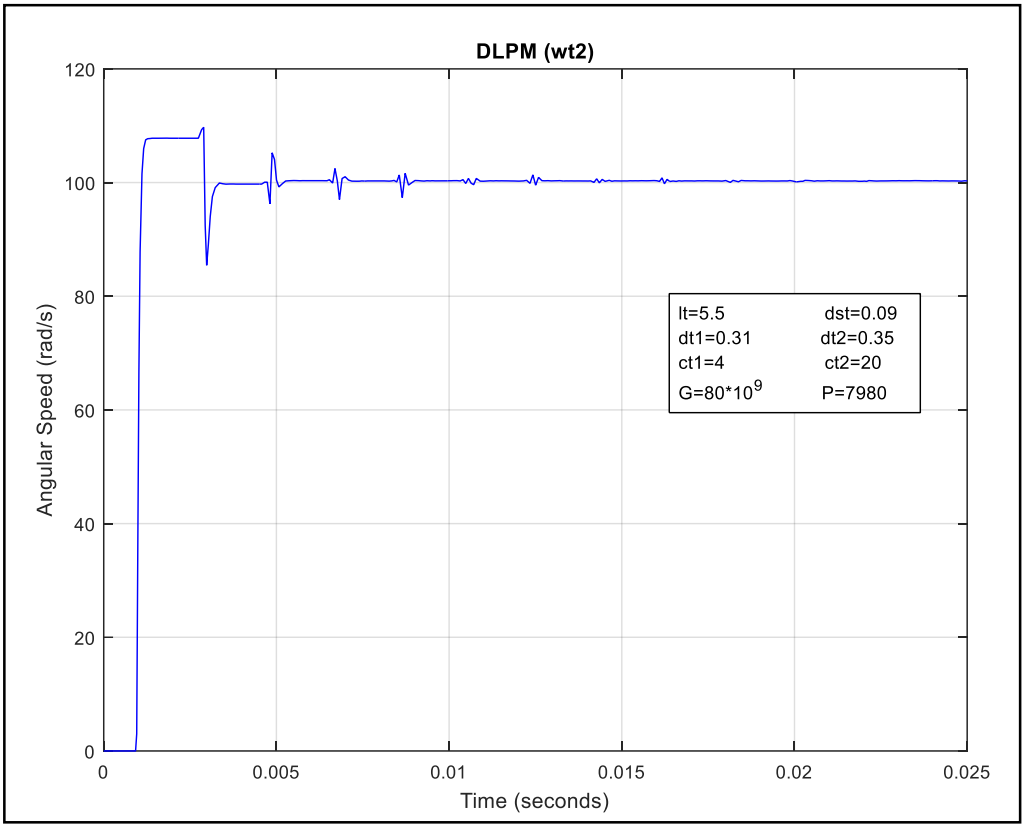

Figure 4.33 Step response of DLPM (tail shaft-load end)

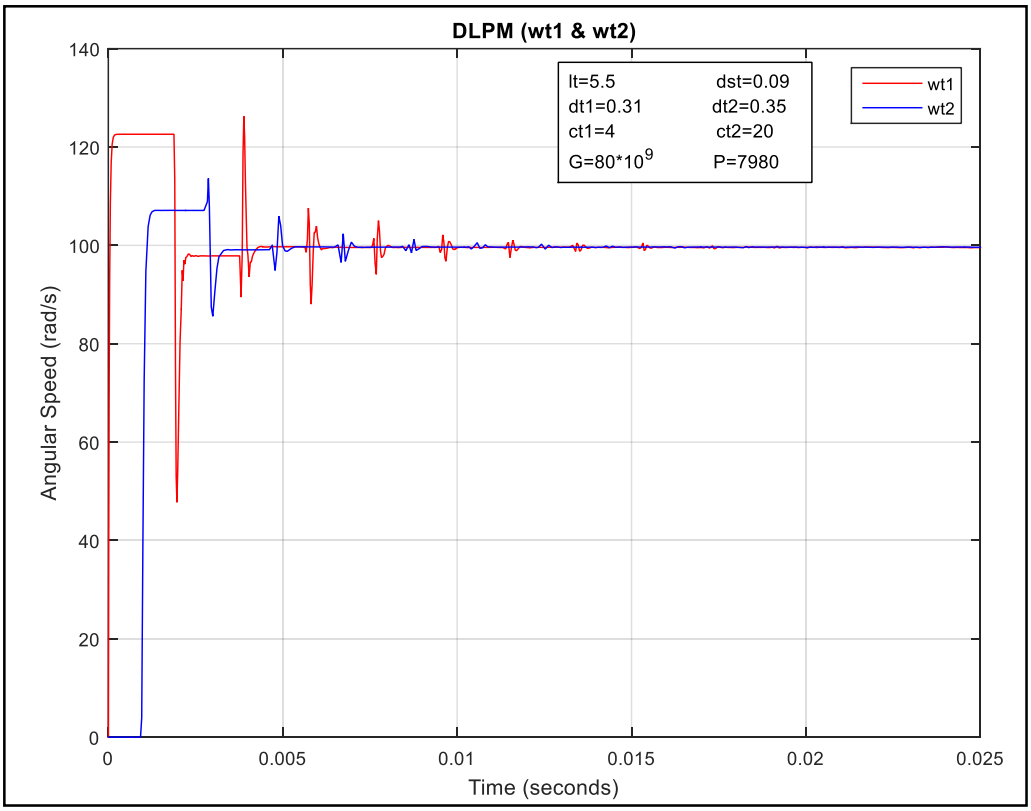

Figure 4.34 DLPM step responses of tail rotor (drive and load ends)

Similarly Figures (4.35) to (4.37) shown bellow illustrates the DLPM time domain transient responses for the main rotor with drive end $\omega_{m1}(t)$ and the load end $\omega_{m2}(t)$, respectively.

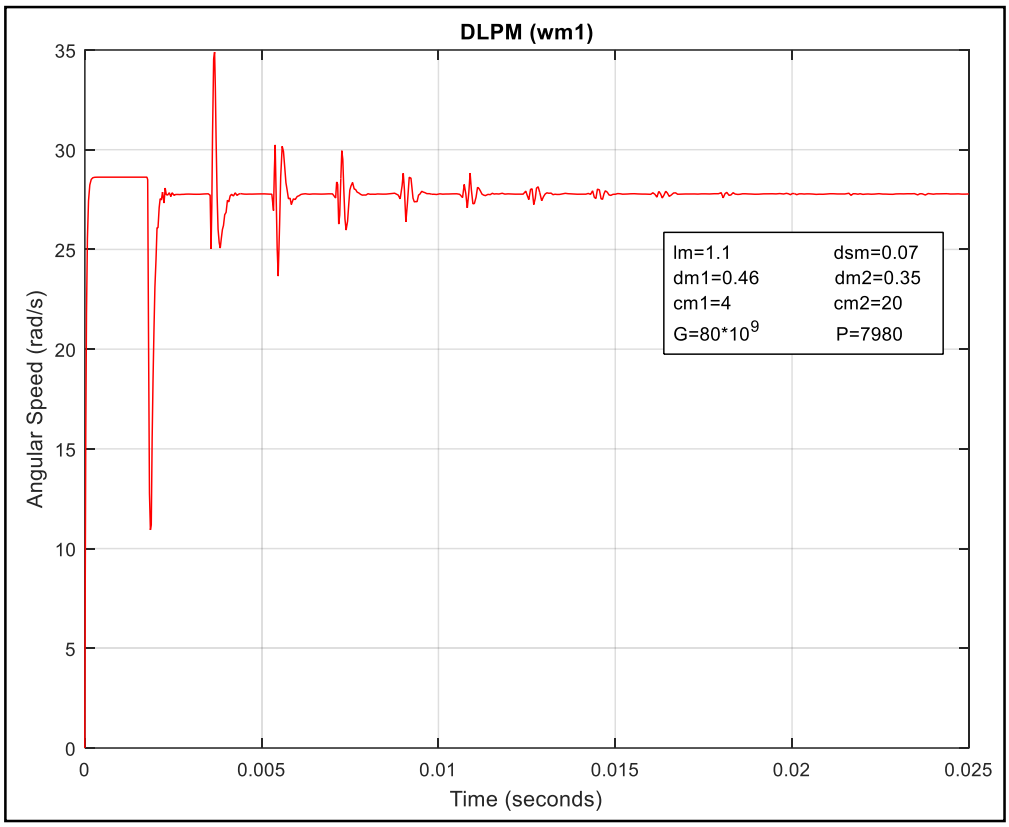

Figure 4.35 Step response of DLPM (main shaft-drive end)

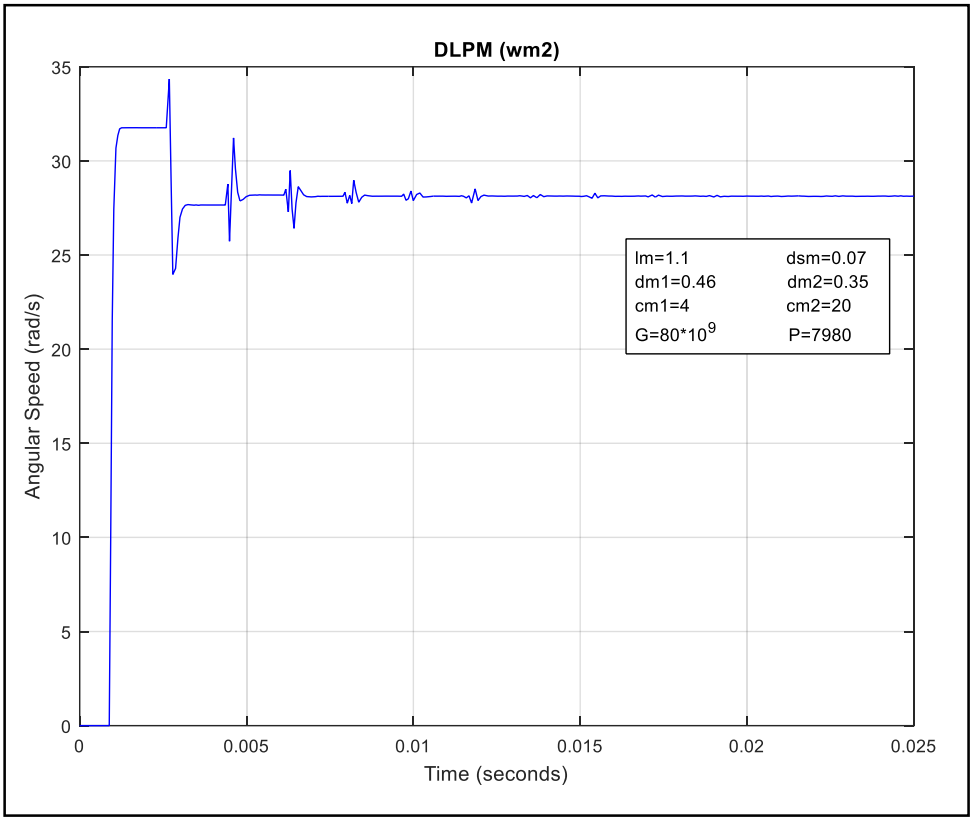

Figure 4.36 Step response of DLPM (main shaft-load end)

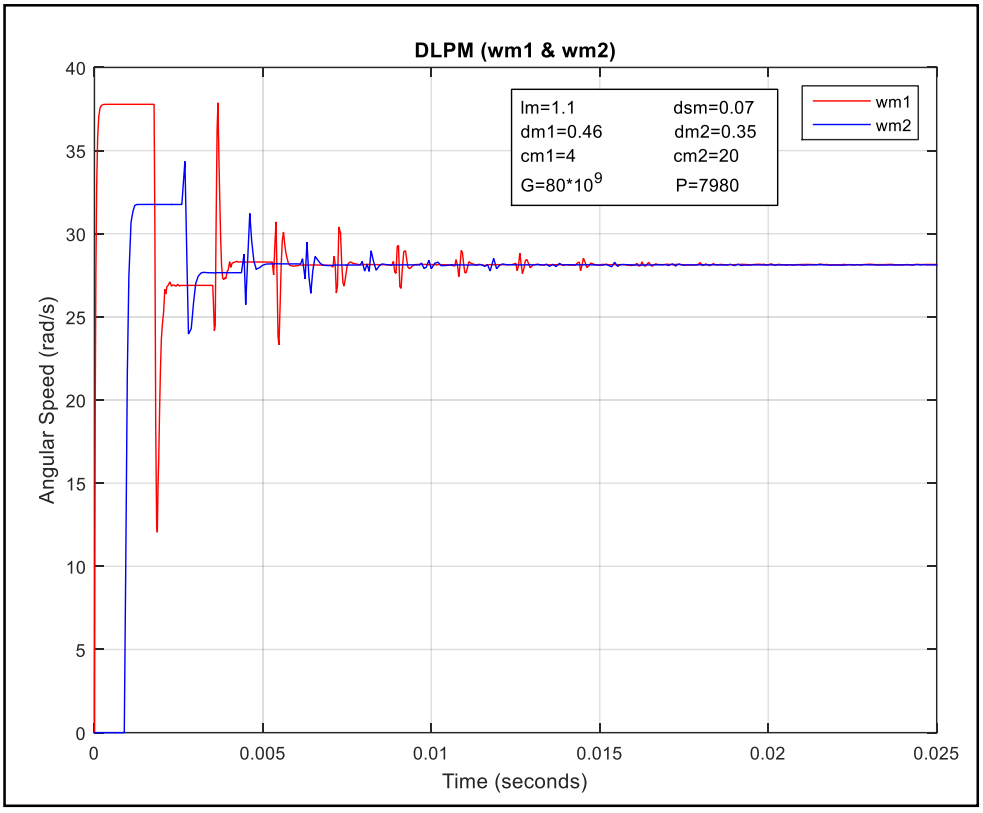

Figure 4.37 DLPM step responses of main rotor (drive and load ends)

At the end, all the step responses of the DLPM are shown in one graph for better illustration. Figure 4.38 showing the four DLPM responses for both tail and main rotors with drive and load ends.

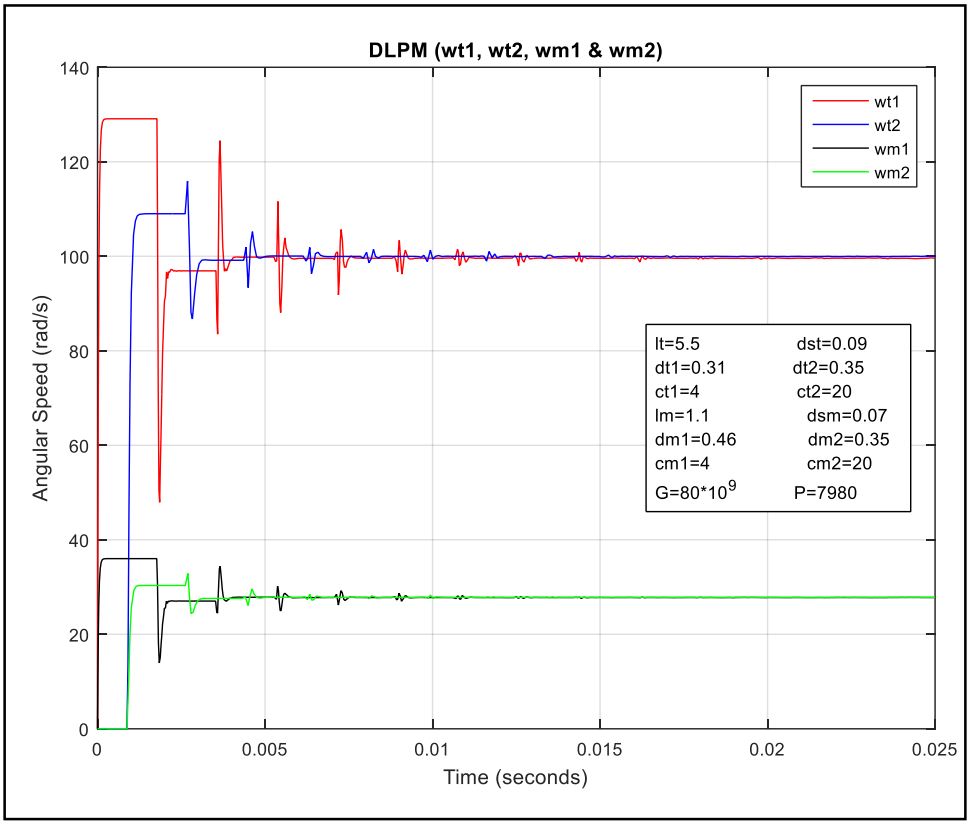

Figure 4.38 DLPM step responses of both tail and main rotors (drive and load ends)

After that, the shear stress of the DLPM is simulated and results are shown below for both tail and main rotors in figures (4.39) and (4.40) respectively.

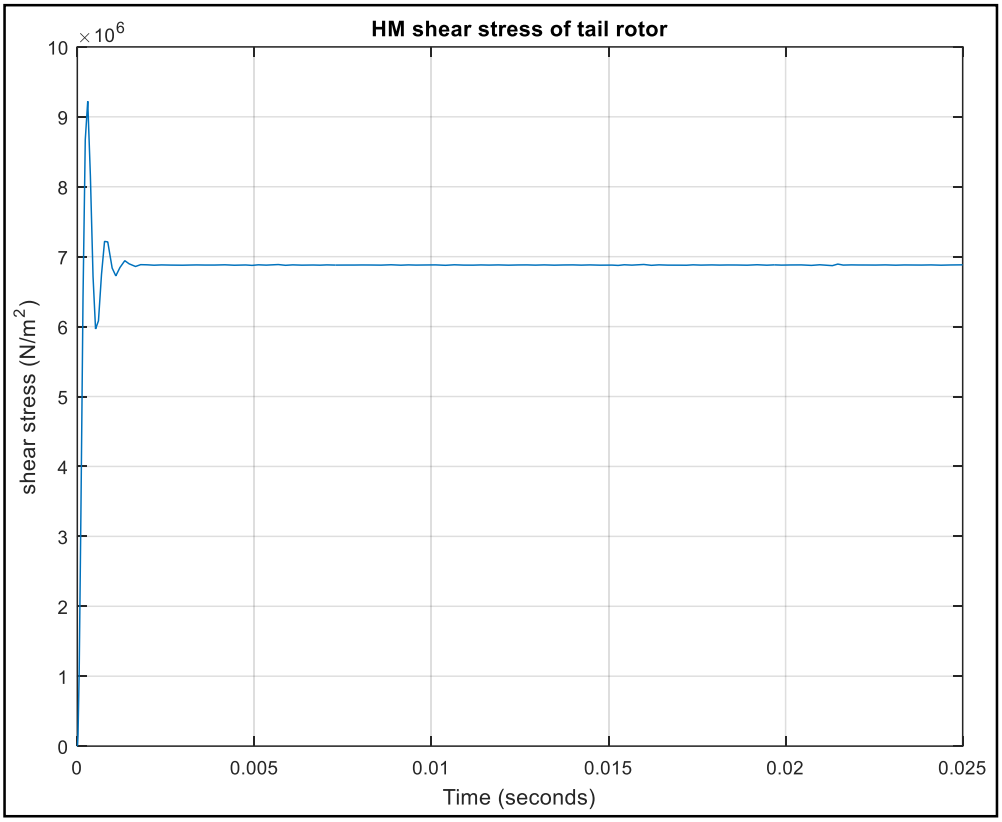

Figure 4.39 DLPM shear stress of tail rotor

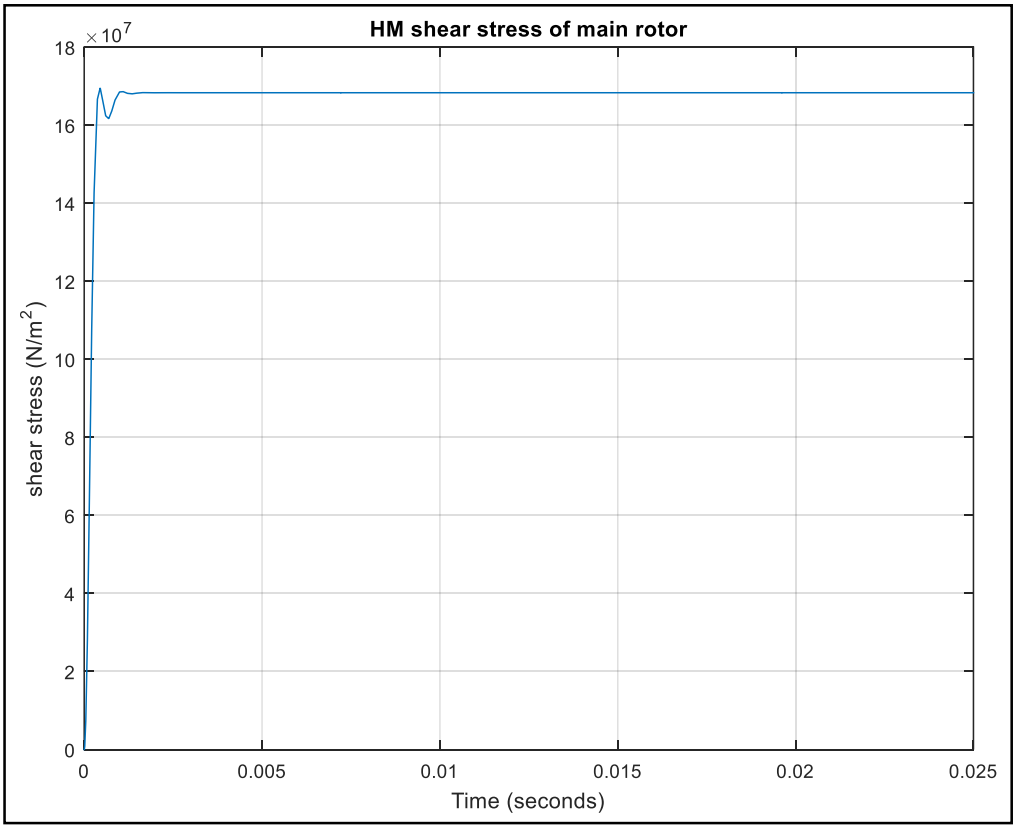

Figure 4.40 DLPM shear stress of main rotor

4.5. Comparison Study

Finally, as it is shown below in figures (4.41) to (4.44) the LPM, FEM responses are incorporated with the DLPM responses for the seek of comparison. These illustrates that the FEM performance begins to get closer to the DLPM response features but still will remain slightly different, and there will be no guarantee that I will be the same if the number of section in FEM is increased.

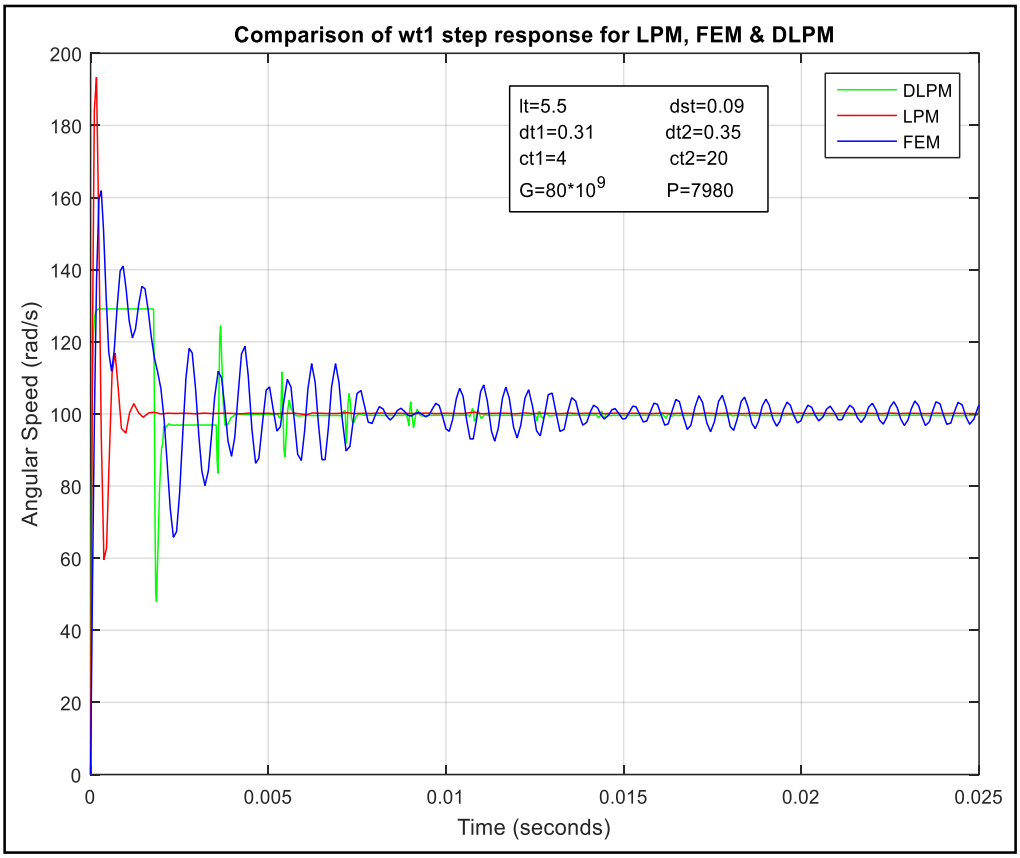

Figure 4.41 Comparison of LPM, FEM and DLPM step responses (tail shaft-drive end)

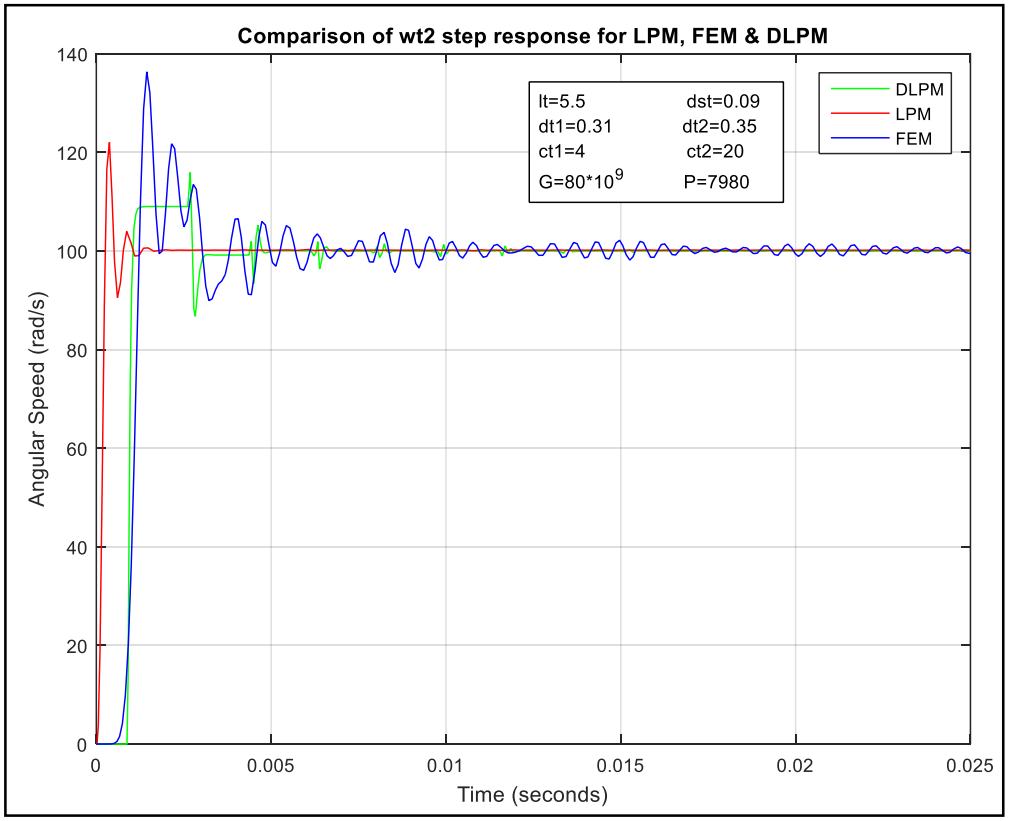

Figure 4.42 Comparison of LPM, FEM and DLPM responses (tail shaft-load end)

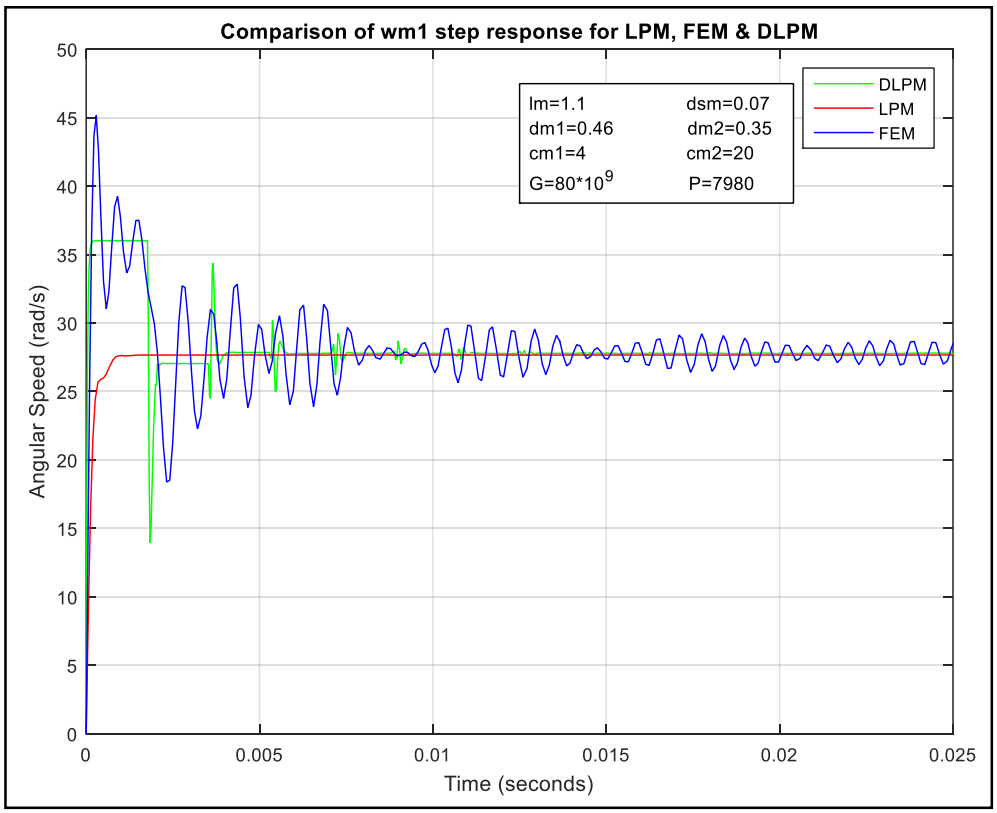

Figure 4.43 Comparison of LPM, FEM and DLPM responses (main shaft-drive end)

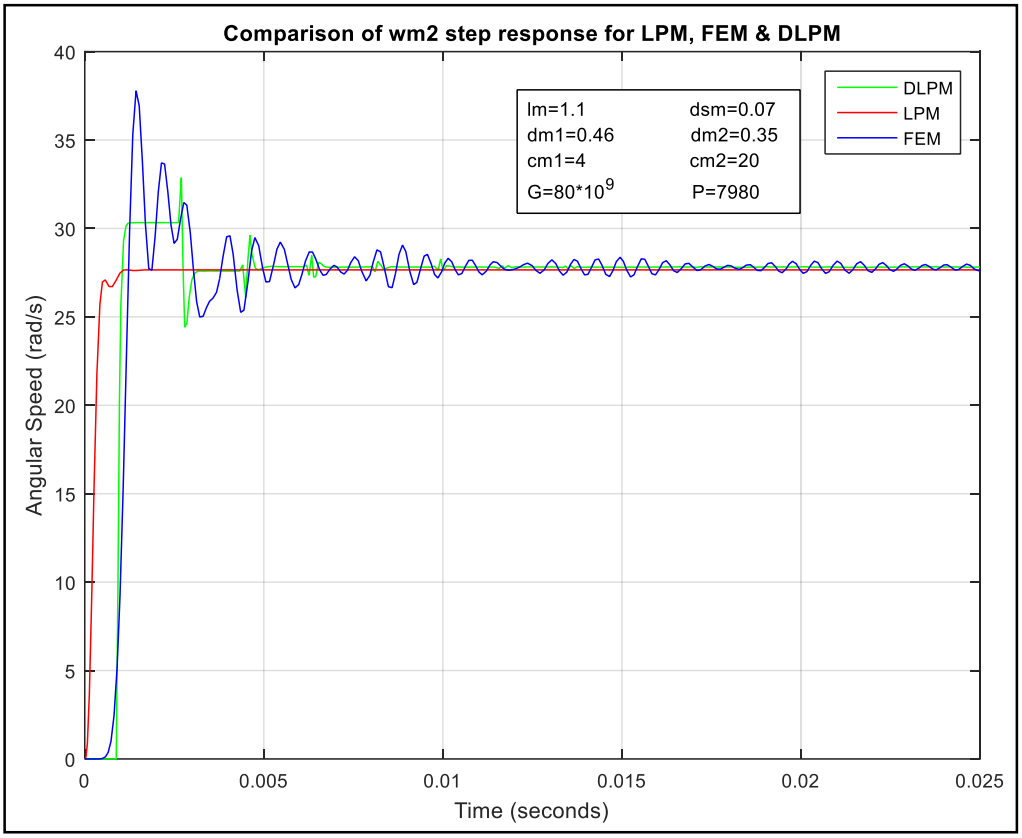

Figure 4.44 Comparison of LPM, FEM and DLPM responses (main shaft-load end)

Regardless the overwhelming utilization of LPM for such dynamic analyses, as it was shown in figures (4.4) to (4.10) there will be considerable variations between the expected and real transient response of the used system models. Here, both the LPM and FEM are assumed to be pointwise elements. The DLPM can be considered as high accuracy modeling technique since it is only eleminating the internal friction of the steel. According to that, the LPM transient response have little similarity with the outcomes from the DLPM performance.

Regarding the FEM, even with five segments used, there are considerable time domain differeneces. Furthermore,when the number of FEM sections used is increased, it will enlarge the dimension of the

transfer function matrix which will lead to more computational time and will encrease the possibility of errors generated from the inversion and still there will be an uncertainty in the simulations of results.

Chapter V

Conclusions and Recommendations

In this research the dynamical torsional response of the rotor systems of a helicopter were investigated. Lumped parameter-LPM, finite element-FEM and hybrid-HM (distributed-lumped) models for the selected systems consisting from shaft, rotors and bearings were derived and from that, the transient response of the rotors angular speed and the shear stress were simulated. After that, the equations for the calculations of the resonant frequencies (ω), for all models, were extracted.

Matlab software have been used in the simulations since it offers a lot of built-in mathematical functions which makes solving equations very easy. Alos it can be used in so many applications for example, math and computation, algorithm development scientific and engineering graphics and also modeling and simulation.

To compare the used modeling methodolgies the helicopter Schweizer 300C was considered as case study for the comparison purpose. Both tail and main rotors were considered for the dynamical analsys. The system can be asumed to be equivalent dynamical system consisting of two, rigid rotors (Gear boxes or blades), supported by bearings at each end, and linked by a long, slim drive shaft. According to the diameters, dampings, lengths, inertias and gear ratios parameters

for both main and tail rotors the systems can be modeled and analyzed with some further calculations depending on the modeling method considered (for example stiffness, polar moment of inertias, compliance, etc). Although the Lumped parameter model-LPM, is the simplest analytical investigation, it is expected to realize least accuracy of results and that is what the results shows.

Furthermore, Finite element models-FEM may be used to enhance the lumped parameter model's results, though the uncertainties according the accuracy of outcomes gained now start to appear. As it is illustrated in this research, the FEM is acquired at the expenditure of engaging computational errors, huge matrix complexity, dimensionality and uncertainty.

Using the third modeling technique (Distributed-lumped parameter modeling-DLPM- or as it is known sometimes as Hybrid modeling), analysis leads to unclear, accurate and attractive option. Utilizing this method, componenet that are assumed as being 'widely scattered' can be modeled easily utilizing continuous (finite) system representation. Furthermore, exhibiting relatively lumped characteristics will be recognized by classical concentrated, point-wise models, This is the hybrid modeling which is consisting of distributed-lumped parameter model.

Hybrid method (DLPM) as it was shown in chapter IV, results in admittance equation for the analysis purposes. Unlike FEM, the main

advantage is that there is not any doubt regarding final results acquired with DLPM.

For the seek of differentiation, according to the studied system, LPM shows massive frequency and time domain differences compred to the rest of methods. The simulation of transient response, shows inflating settling time and overshoots characteristics, which is not the case with the DLPM, which can be considered as high validity realization.

FEM method improved the LPM predictions of the time domain response, leading to conforming with the results obtained by the DLPM.

Evenly, it is clear from the prediction of the resonant frequency, for the FEM, that there were inconvenient differences in the results obtained by analytical results and graphical computation. Attempts pointed at rectifying these generated differences by means of differentiating to acquire the extremum values of the function, also there were numerical difficulties rised because of the huge inflation happens in the order (degree) of the polynomials of the (TF) and the shortage of the very well-known resonant peaks, at the load and drvie ends.

There is one more issue need to think about. What is the most appropriate number of sections to be used in the finite element models?

Considering that the moment that the computational errors will initiate to significantly mess up the results.

Without the DLPM, there are no bench-mark standard. Hence, This induce estimation and falsehood in the large scale. Additional confusion may propagate when we come to know that, both LPM and FEM results of the resonant frequencies, generated huge difference compared to the frequencies extracted using frequency response; meanly simulation results using Bode plots. Anyway, the overthrow for the DLPM, generates consistently perfect analysis and hence computer simulation connexion. This is including prediction of resonant frequencies from both the equations and analysis in chapter IV. This method is pragmatic in creating the graphical solution for similar resonance problems and subsequently in recognizing the requested resonance frequencies (ω), all of the above emphasize developed accuracy and also computational accuracy.

The FEM furthermore, fail to reveal high frequency manner of the studied application. Compared to this, the DLPM (distributed-lumped), investigation demonstrates that rotor systems are continuing to respond for high frequency disturbances. Generally, there are no peak values of the frequency amplitudes, and the dynamic decline, similar to that specified by the FEM as the DLPM prdouces resonance peaks if excited by high frequencies, cyclic pulsations.

It can be realized that LPM will not be sufficiently accurate especially for actual applications, whereas the FEM computation and analysis will be too inaccurate and too slow. Compared to this, the DLPM response analysis is accurate, rapid, and is the optimal method for real-time and actual problems.

Finally, it can be concluded that the response of DLPM is guaranteed regardless of the studied system as it was shown in chapter II. The system should be described mainly using the effects of lumped parameter, and then the used model will show this accurately. It was shown it the results and simulation that this technique is the most accurate and the closest to the reality among the three techniques used in this research. Furthermore, this technique can be applied in a similar way to a wide vriety of engineering applications and that is why this research is concluded by a recommendation of using this technique for the analysis purposes.

References

Abdul-Ameer,A. (2011). *Modeling of Fluid Power Transmission Systems*. International Symposium on Innovation in Intelligent Systems and Applications, 15-18 June, 2011, Istanbul – Turkey, pp 205-211.

Aleyaasin, M., & Ebrahimi, M. (2000). *Hybrid modeling for analysis and identification of rotors*, Elsevier Science S.A, pp 163-176.

Atsushi Ikai. (2017). *World of Nano-Biomechanics***.** 2nd edn.Elsevier.

Bandler,J,W. (1977). *Transmission Line Modeling and Sensitivity Evaluation for Lumped Network Simulation and Design in the Time Domain*. Journal of The Franklin Institute, pp 15-32.

Barati,E & Esfahani,J,A. (2010). *Mathematical modeling of convective drying Lumped temperature and spatially distributed mositure in slab*. Elsevier Ltd, pp 2294-2301.

Bartlett,H & Whalley,R. (1998). *Modeling and analysis of variable geometry exhaust gas systems*. Elsevier Science Inc, pp 545–567.

Bartlett,H. Whalley,R, Rizvi,S,S,I. (1998). *Hybrid Modeling of marine power transmission systems*. pp 97-108.

Chen,z. (2005). *Finite element methods and their applications*. Germany,Berlin: Springer.

Chistopoulos,C. (1993). *Transmission-Line Modeling (TLM): A brief introduction and recent advance*. IEEE, pp 1/1-1/6.

Christopoulos,C. (1991). *The Historical Development of TLM*. IEEE, pp 1/1–1/4.

Close,C,M & Frederick,D,K. (1993). Modeling and analysis of dynamic systems, 2nd edn, USA: Houghton Mifflin.

Close,C,M & Frederick,D,K. (1993). *Modeling and analysis of dynamic systems*. 2nd edn.USA: Houghton Mifflin.

Cook,R,D. (1995). *Finite element modeling for stress analysis*.Canada: John Wiley & Sons, Inc

Coyle,s. (2009). *Cyclic and Collective, more art and science of flying helicopters*. USA: Eagle Eye Solutions LLC.

Desai,Y.,Eldho,T., & Shah,A. (2011). *Finite element method with applications in engineering*.New Delhi. India: Dorling Kindersley.

Dorf,R,C & Bishop,R,H. (2009). *Modern Control Systems*. 11th edn. India, New Delhi: Pearson Prentice Hall.

Dynamic Models Distributed parameter systems, Chapter 7.

Engineering Design Handbook, Helicopter Design, part One, Preliminary Design.(1974). Headquarters, U.S. Army materiel Command.

European Rotorcraft Forum 2014, Conference Programme & Proceedings, 2-5 September 2014, UK, Southampton: Royal Aeronautical Society (RAeS)

Garciaa,G,A,R. M,R,R. & Kevrekidis,I,G. (1998). *Identification of distributed parameter systems: A neural net based approach*. Great Britain: Elsevier Science Ltd, Vol. 22, pp S965-S968.

Groppi,G. Belloli,A. Tronconi,E. Forzatti,P. (1995). *A Comparison of lumped and distributed models of monolith catalytic combustors*. Elsevier Science Ltd,Vol. 50, No. 17, pp 2705-2715,.

Heydweiller,J,C. Sincovec,R,F. Fan,L. (1977). *Dynamic Simulation of Chemical Processes Described by Distributed and Lumped Parameter Models*. Great Britain: Pergamon Press, Vol. I, pp 125-131.

Hughes Schweizer 269 helicopter maintenance instructions 2.(2014).

Hui S,Y,R & Christopoulos, C. 1991. The use of TLM-Based Discrete Transforms for General Numerical Analysis. pp 6/1 – 6/2.

Jalali,M,H. Ghayour,M. Ziaei-Rad,S. Shahriari,B. (2014). *Dynamic analysis of a high speed rotor-bearing system*, Measurement 53 (2014) 1–9

Jalali,M,H. Shahriari,B. Ghayour,M. Ziaei-Rad,S. Yousefi,S. (2014). *Evaluation of Dynamic Behavior of a Rotor-Bearing System in Operating Conditions*, International Journal of Mechanical, Aerospace, Industrial, Mechatronic and Manufacturing Engineering Vol:8, No:10, pp 1675-1679.

Johns,P,B. (1971). *Numerical calculation for scattering in waveguides using a transmission line matrix*. Volume 2, IEEE conference, pp D 1/2.

Johnson,W.(1980). *Helicopter Theory*. New York, USA:Dover publications inc

Kelly,s,G.(2009). *System Dynamics and Response*. USA:CENGAGE Learning.

Kulakowski, B. T. Gardner,J.F & Shearer,J.L.(2007). *Dynamic Modeling and Control of Engineering Systems*. Cambridge University Press.

Lalanne,C. (2014). *Mechanical Vibration and Shock Analysis, Sinusoidal Vibration (volume 1)*. USA,Hoboken: John Wiley & Sons, Inc.

Logan,D.L. (2012). *A fisrst course in the finite element method*. USA,Stamford: Cengage Learning.

McGowen,S,S. (2005). *Helicopters, an Illustrated History of Their Impact*. USA, California: ABC-CLIO, Inc.

Ogata,K. (2010). *Modern Control Engineering*. 5th edn, India, New Delhi: Pearson Prentice Hall.

Palm,W,G. (2010). *System Dynamics*.Singapore:McGraw Hill.

Pavlou, D.G.(2015). *Essentials of the Finite Element Method For Mechanical and Structural Engineers*. India: Elsevier.

Rao Singiresu,S.(2011). *The finite element method in engineering*. 5th edn. Chennai, India: Elsevier.

Ray,W,H. (1978). *Some Recent Applications of Distributed Parameter Systems Theory-A Survey*. Great Britain: Pergamon Press Ltd, Vol. 14, pp 281– 287.

Salazar,T. 2010. *Mathematical model and simulation for a helicopter with tail rotor*,CIMMACS'10 Proceedings of the 9th WSEAS iternasional conference on computational intelligance, man-machine systems cybernetics,pp27-33.

Schierwagen,A,K. (1990). *Identification Problems in Distributed Parameter Neuron Models*. Great Britain, International Federation of Automatic Control, Vol.26, No.4, pp 739 – 755.

Schweizer 300C Helicopter Technical information/SZR-004. (2008).

Tirupathi,R.C. Ashok,D.B. (2012). *Introduction to finite elements in engineering*. England:Pearson.

Venkatesan,C. (2015). *Fundamentals of Helicopter Dynamics*. USA:NewYork: CRC Press.

Villegas,J,A. Duncan,S,R. Wang,H,G. Yang,W,Q & Raghavan,R,S. (2009). *Distributed parameter control of a batch fluidised bed dryer*. pp 1096–1106.

Watton,J & Tadmori, M,J.(1988). *A comparison of techniques for the analysis of transmission line dynamics in electrohydraulic control systems*, Appl. Math.Modeling, Butterworth Publishers, Vol. 12,pp 457-466.

Whalley,R & Abdul-Ameer,A. (2010). *Heating, ventilation and air conditioning system Modeling*. Elsevier Ltd, pp 644–656.

Whalley,R. & Abdul-Ameer,A. (2010). *Heating, ventilation and air conditioning system Modeling*. Elsevier Ltd, pp 644–656.

Whalley,R. (1988), *The response of distributed-lumped parameter system*. Roc Instn Mech Engrs, Vol. 202, No C6, pp 421-429.

Whalley,R. Abdul-Ameer.A & Ebrahimi,K,M. (2011). *The axes response and resonance identification for a machine tool*. Elsevier Ltd, pp 1171–1192.

Whalley,R. Ebrahimi,M & Jamil,Z.(2005). *The torsional response of rotor systems*, Roc Instn Mech Engrs, Vol. 202, No C6, pp 357-380.

Yakimenko, O ,A. (2011). *Engineering Computations and Modeling in MATLAB/Simulink*. USA: American Institute of Aeronautics and Astronautics.

Appendices

Appendix-A1:

Defined parameter values for the system (Hughes Schweizer 269 helicopter maintenance instructions 2, 2014)

Specifications

Performance

Standard day, sea level, maximum gross weight unless otherwise noted
Maximum speed (VNE) . . . . . 95 kits... …..... 176 km/hr.
Maximum cruise speed (VH) . . . . . 86 kts . . .. 159 km/hr
Hover ceiling, In-Ground-Effect (1700 lb).. . . . . 10,800 ft. . . . . 3,292 m
Hover ceiling, Out-of-Ground-Effect (1700 lb) .. . . 8,600 ft. . . . . 2,621 m
Range (long range cruise* speed @ 4,000 feet) (no reserve)
- 32.5 gallon. . . . . 191 nm. . . . . 354 km
- 64.0 gallon. . . . . 375 nm. . . . . 694 km

Weights

Maximum takeoff gross weight. . . .. 2,050 lb . . . . . 930 kg
Empty weight, standard configuration . . . . . 1100 lb . . . . . 499 kg
Useful load . . . . . 950 lb . . . . . 431 kg

Dimensions

Fuselage length . . . . . 22.19 ft. . . . . 6.76 m
Fuselage width . . . . . 4.25 ft. . . . . 1.30 m
Fuselage height . . . . . 7.17 ft. . . . . 2.18 m
Overall length (rotors turning). . . . . 30.83 ft. . . . . 9.40 m
Overall height (to top of tail rotor). . . . . 8.72 ft. . . . . 2.65 m
Width (canopy) . . . . . 4.25 ft. . . . . 1.30 m
Main rotor diameter. . . . . 26.83 ft. . . . . 8.18 m
Tail rotor diameter. . . . . 4.25 ft. . . . . 1.30 m
Main landing gear tread (fully compressed). . . . . 6.54 ft. . . . . 1.99 m

Accommodation

Normal cabin seating (training) 2

Maximum certified cabin seating (utility). 3

Cabin length. . . . . 4.75 ft. . . . . 1.45 m

Cabin width . . . . . 4.92 ft. . . . . 1.50 m

Power plants

Type. . . . . Textron Lycoming HIO-360-D1A

Power plant ratings (per engine, standard day, sea level)

- Takeoff (5-minute) . . . . . 190 hp . . . . . 141 kw

- Maximum continuous . . . . . 190 hp . . . . . 141 kw

Fuel Capacity

Standard fuel capacity . . . . . 32.5 US gal . . . 123.03 l

Extended range capacity . . . . . 64.0 US gal . . . 242.27 I

Appendix-A2:

Project's Pictures

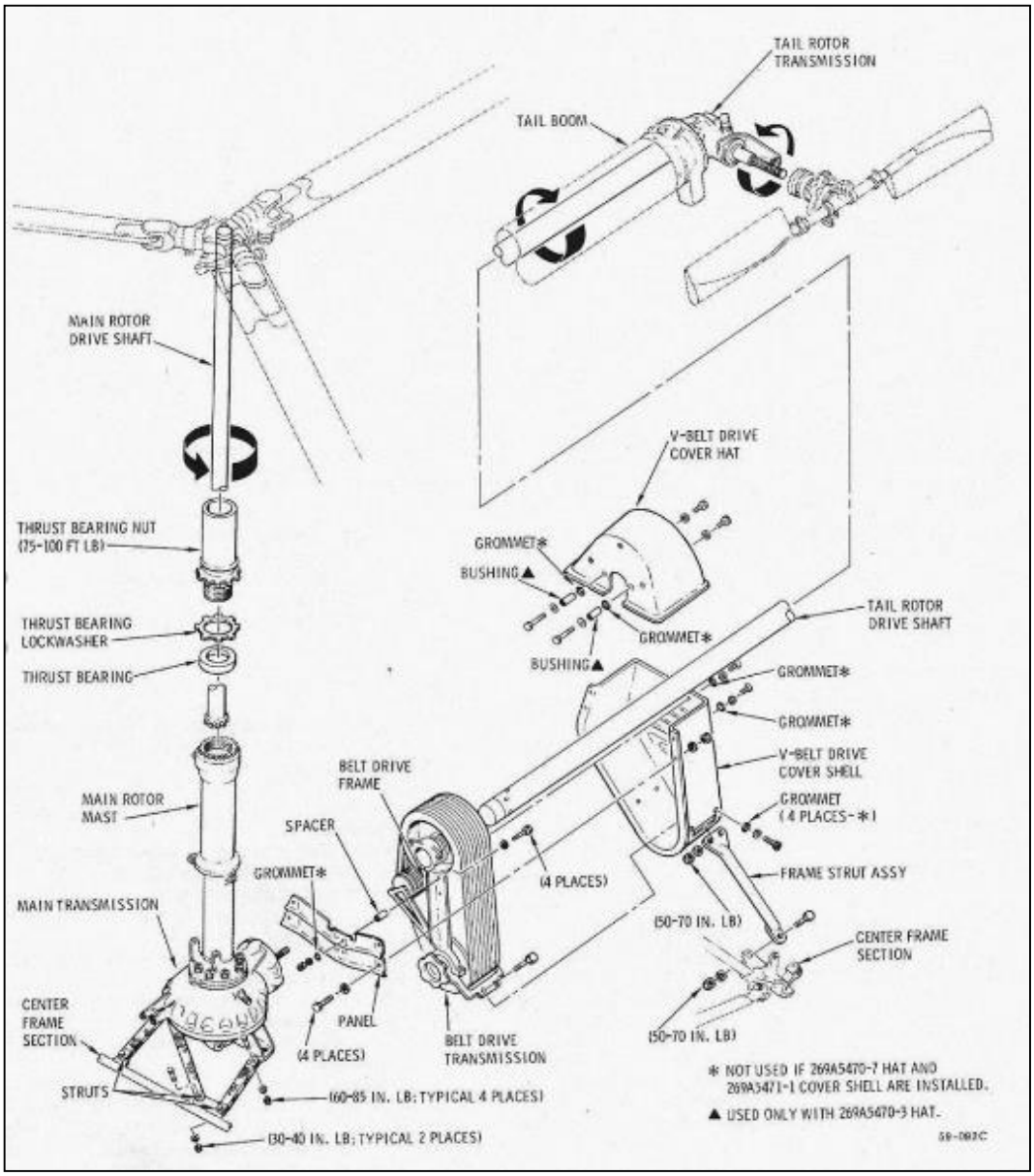

Figure A-1: Main transmission, tail transmission and drive system

(Hughes Schweizer 269 helicopter maintenance instructions 2, 2014)

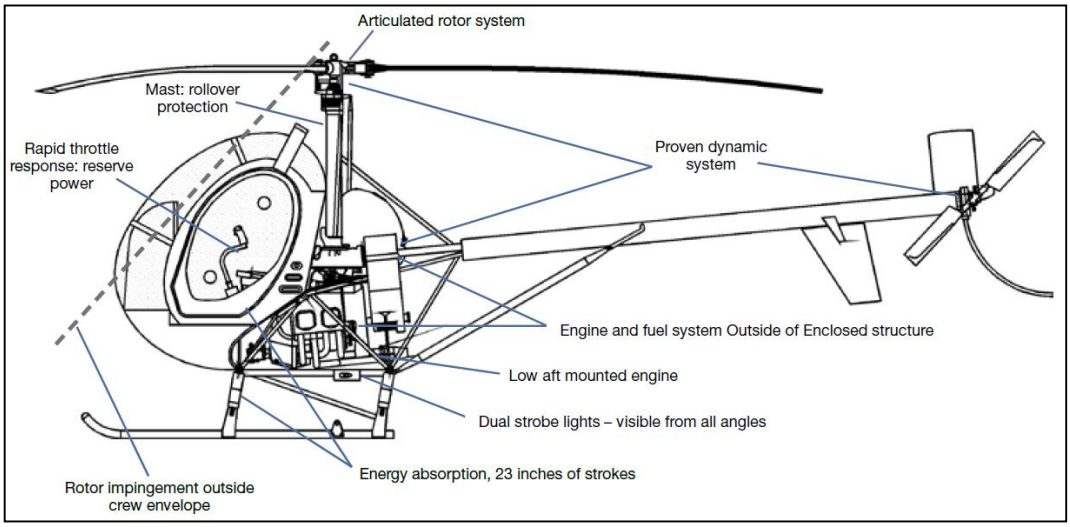

Figure A-2: Schweizer 300C Schweizer 300C crashworthiness features

(Schweizer 300C Helicopter Technical information/SZR-004, 2008)

Appendix-A3:

Generalization of Series Torsional Modeling (Whalley, Ebrahimi, & Jamil, The torsional response of rotor systems, 2005)

The procedure outlined in hybrid modeling section can be extended to accommodate system model for interconnected shaft-rotor-bearing systems with various shaft lengths, diameters, inertia loads, and bearing characteristics. If the system representation shown in figure (A-3) is considered then the first distributed-lumped section may be described by

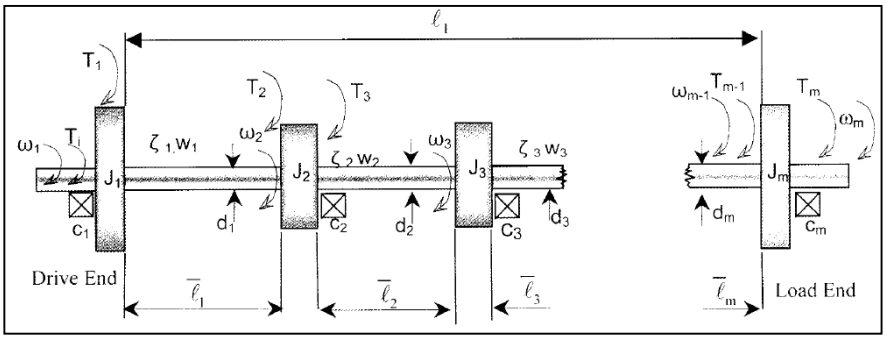

Figure A-3. Multiple rotor, series hybrid torsional modeling (Whalley, Ebrahimi, & Jamil, 2005)

$$\begin{bmatrix} T_1(s) \\ T_2(s) \end{bmatrix} = \begin{bmatrix} T_1(s) - J_1 s\omega_1 - c_1\omega_1(s) \\ T_3(s) + J_2\omega_2(s) + c_2\omega_2(s) \end{bmatrix}$$

$$= \begin{bmatrix} \xi_1 w_1(s) & -\xi_1 (w_1(s)^2 - 1)^{\frac{1}{2}} \\ \xi_1 (w_1(s)^2 - 1)^{\frac{1}{2}} & -\xi_1 w_1(s) \end{bmatrix} \begin{bmatrix} \omega_1(s) \\ \omega_2(s) \end{bmatrix} \quad \text{(A-1)}$$

From equation (A-1) the terminal relationship is

$$\begin{bmatrix} T_i(s) \\ T_3(s) \end{bmatrix} = \begin{bmatrix} \xi_1 w_1(s) + J_1 s + c_1 & -\xi_1 (w_1(s)^2 - 1)^{\frac{1}{2}} \\ \xi_1 (w_1(s)^2 - 1)^{\frac{1}{2}} & -\xi_1 w_1(s) - J_2 s - c_2 \end{bmatrix} \times \begin{bmatrix} \omega_2(s) \\ \omega_3(s) \end{bmatrix} \quad \text{(A-2)}$$

Thereafter the equation for the second section becomes

$$\begin{bmatrix} T_3(s) \\ T_4(s) \end{bmatrix} = \begin{bmatrix} \xi_2 w_2(s) & -\xi_2 (w_2(s)^2 - 1)^{\frac{1}{2}} \\ \xi_2 (w_2(s)^2 - 1)^{\frac{1}{2}} & -\xi_2 w_2(s) - J_3 s - c_3 \end{bmatrix} \times \begin{bmatrix} \omega_3(s) \\ \omega_4(s) \end{bmatrix} \quad \text{(A-3)}$$

And, for the $m-1$ shaft section

$$\begin{bmatrix} T_{m-1}(s) \\ T_m(s) \end{bmatrix} = \begin{bmatrix} \xi_{m-1} w_{m-1}(s) & -\xi_{m-1} (w_{m-1}(s)^2 - 1)^{\frac{1}{2}} \\ \xi_{m-1} (w_{m-1}(s)^2 - 1)^{\frac{1}{2}} & -\xi_{m-1} w_{m-1}(s) - J_m s - c_m \end{bmatrix} \times \begin{bmatrix} \omega_{m-1}(s) \\ \omega_m(s) \end{bmatrix} \quad \text{(A-4)}$$

To eliminate intermediate variables, equation (A-3) can be subtracted from equation (A-4), and so on, until all input torques other than $T_i(s)$ and $T_m(s)$ have been removed. Consequently, with $T_m(s) = 0$ and if the input torque is $T_i(s) = \sin(\omega t)$ then when $t \gg 0$ the output response is given by

$$[T_i(s), 0, 0, \dots 0]^T = \boldsymbol{A}(\boldsymbol{s})[\omega_1(s), \omega_2(s), \dots, \omega_m(s)]^T_{s=i\omega} \quad \text{(A-5)}$$

Where the matrix in equation (A-5) is

$$\boldsymbol{A}(s) = \begin{bmatrix} \xi_1 w_1(s) + \gamma_1(s) & -\xi_1 (w_1(s)^2 - 1)^{\frac{1}{2}} & 0 & 0 & \cdots & 0 \\ \xi_1 (w_1(s)^2 - 1)^{\frac{1}{2}} & -\xi_1 w_1(s) - -\xi_2 w_2(s) - \gamma_2(s) & \xi_2 (w_2(s)^2 - 1)^{\frac{1}{2}} & 0 & \cdots & 0 \\ 0 & & & & & \\ \vdots & & & & & \\ 0 & \dots & & 0 & -\xi_{m-1} (w_{m-1}(s)^2 - 1)^{\frac{1}{2}} & \xi_m w_{m-1}(s) + \gamma_m(s) \end{bmatrix}_{s=i\omega}$$

In the frequency domain where following the substitution of s = iω the parameters of A(iω) are

$$\xi_j = \sqrt{(L_j / C_j)}$$

$$w_j(s) = \frac{e^{2\Gamma_j(s)\bar{l}_j} + 1}{e^{2\Gamma_j(s)\bar{l}_j} + 1}$$

Where

$$\Gamma_j(s) = s\sqrt{(\mathrm{L_j C_j})}$$

And

$$w_j(i\omega) = \frac{(e^{i\varphi_j(\omega)} + 1)}{(e^{i\varphi_j(\omega)} - 1)} \qquad \text{(A-6)}$$

Where

$$\varphi_j(\omega) = 2\omega\bar{l}_j\sqrt{(\mathrm{L_j C_j})}$$

Evidently, from equation (A-6)

$$w_j(i\omega) = \frac{-i\sin\varphi_j(\omega)}{1-\cos\varphi_j(\omega)} \qquad 1 \le j \le m-1 \qquad \text{(A-7)}$$

Since

$$C_j = \frac{1}{G_j J_j}$$

And

$$L_j = \rho_j J_j$$

Then

$$\sqrt{(L_j C_j)} = \sqrt{(\rho_j / G_j)}$$

If for steel $\rho_j = 7980\ kg/m^3$

And $G_j = 80 \times 10^9\ \frac{N}{m^2}$

Then the propagation delay $\bar{l}_j\sqrt{(\mathrm{L_jC_j})}$ for metallic materials will be extremely small. Moreover, as in equation (A-7)

$$\omega_j(i\omega) = -if(\varphi_j(\omega)) \tag{A-8}$$

And

$$\xi_\mathrm{j}\left(\omega_\mathrm{j}(\mathrm{i}\omega)^2 - 1\right)^{\frac{1}{2}} = \mathrm{i}\xi_\mathrm{j}\mathrm{f}(\varphi_\mathrm{j}(\mathrm{i}\omega)^2 + 1)^{1/2} \tag{A-9}$$

$$j = 1,2,\dots,m-1$$

Where in equation (A-5)

$$\boldsymbol{A}(i\omega) = \Lambda + i\Gamma(\omega) \tag{A-10}$$

Where in equation (A-10) the m × m matrices are

$$\Lambda = daig(\mathrm{c}_1, \mathrm{c}_2, \dots, \mathrm{c}_\mathrm{m})$$

And

$\Gamma(i\omega)$

$$= \begin{bmatrix} -\xi_1 f(\varphi_1(\omega)) + J_1\omega & -\alpha_1(\omega) & 0 & \cdots & 0 \\ \alpha_1(\omega) & \xi_1 f(\varphi_1(\omega)) + \xi_2 f(\varphi_2(\omega)) - J_2\omega & \alpha_2(\omega) & \dots & 0 \\ 0 & -\alpha_2(\omega) & -\xi_2 f(\varphi_2(\omega)) + \xi_3 f(\varphi_3(\omega)) + J_3\omega & & \\ \vdots & & & & \alpha_{m-1}(\omega) \\ 0 & 0 & -\alpha_{m-1}(\omega) & & -\xi_{\mathrm{m}-1} f(\varphi_{m-1}(\omega)) + J_m\omega \end{bmatrix}$$

Where

$$\alpha_\mathrm{j}(\omega) = \mathrm{i}\xi_\mathrm{j}(f(\varphi_\mathrm{j}(\omega)^2 + 1)^{1/2}$$

$$\varphi_\mathrm{j} = 2\omega\bar{l}_j\sqrt{(L_j\xi_j)}. \qquad j = 1,2,\dots,m-1$$

Appendix-A4:

Matlab display for Lumped parameter model-LPM

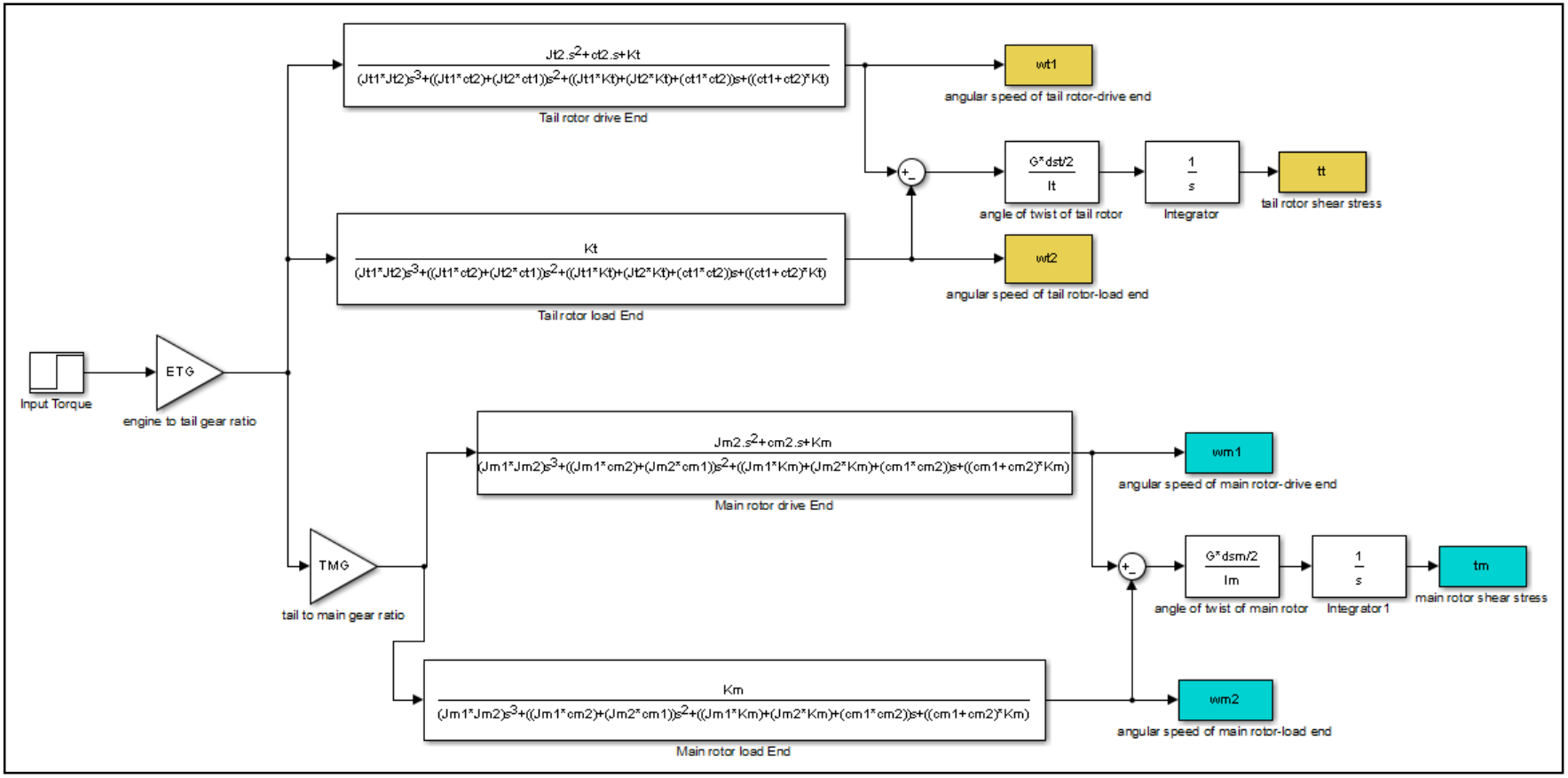

Figure A-4 Simulink block diagram for LPM

m. file of Lumped Parameter Model-LPM

```
% Lumped parameter model

%tail rotor model
lt=5.5                              % Length of tail shaft
in(m)
dst=0.09                            % Diameter of tail
shaft in (m)
Jst=((3.14*(dst^4))/32)             % Polar moment of
inertia of tail shaft      in(m^4)
dt1=0.31                            % Diameter of gearbox
at the drive end in tail shaft in (m)
Jt1=((3.14*(dt1^4))/32)             % Polar moment of
inertia of drive end gearbox of tail shaft in (m^4)
dt2=0.35                            % Diameter of gearbox
at the load end in tail shaft in (m)
Jt2=((3.14*(dt2^4))/32)             % Polar moment of
inertia of load end gearbox of tail shaft in (m^4)
Ct1=4                               % Viscous damping at
the drive end of tail shaft in (N.m.s/rad)
Ct2=20                              % Viscous damping at
the load end of tail shaft in (N.m.s/rad)
Kt=(G*Jst/lt)                       % Torsional stiffness
of the tail shaft in (N.m/rad)

%Main rotor model
lm=1.1                              % Length of main shaft
in(m)
dsm=0.07                            % Diameter of main
shaft in (m)
Jsm=((3.14*(dsm^4))/32)             % Polar moment of
inertia of main shaft in (m^4)
dm1=0.46                            % Diameter of gearbox
at the drive end in main shaft in (m)
Jm1=((3.14*(dm1^4))/32)             % Polar moment of
inertia of drive end gearbox of main shaft in (m^4)
dm2=0.35                            % Diameter of gearbox
at the load end in main shaft in (m)
Jm2=((3.14*(dm2^4))/32)             % Polar moment of
inertia of load end gearbox of main shaft in (m^4)
```

```
Cm1=4                                % Viscous damping at
the drive end of main shaft in (N.m.s/rad)
Cm2=20                               % Viscous damping at
the load end of main shaft in (N.m.s/rad)
Km=(G*Jsm/lm)                        % Torsional stiffness
of the main shaft in (N.m/rad)

% General Specifications
G=80*10^9                            % Shear modulus in
(N/m^2)
P=7980                               % Density in (kg/m^3)
MTG=20/60                            % Gear ratio in main
transmission gear
MRG=60/225                           % Gear ratio in tail-

main shaft transmission gear
```

Command window of Lumped Parameter Model-LPM

```
>> lumped

lt =

    5.5000

dst =

    0.0900

Jst =

   6.4380e-06

dt1 =

    0.3100

Jt1 =

   9.0620e-04

dt2 =

    0.3500

Jt2 =

    0.0015
```

Ct1 =

4

Ct2 =

20

Kt =

9.3643e+04

lm =

1.1000

dsm =

0.0700

Jsm =

2.3560e-06

dm1 =

0.4600

Jm1 =

0.0044

dm2 =

0.3500

Jm2 =

0.0015

Cm1 =

4

Cm2 =

20

Km =

1.7134e+05

```
G =

   8.0000e+10

P =

        7980

MTG =

    0.3333

MRG =

    0.2667

>>
```

Appendix-A5:

Matlab display for Finite Element model-FEM

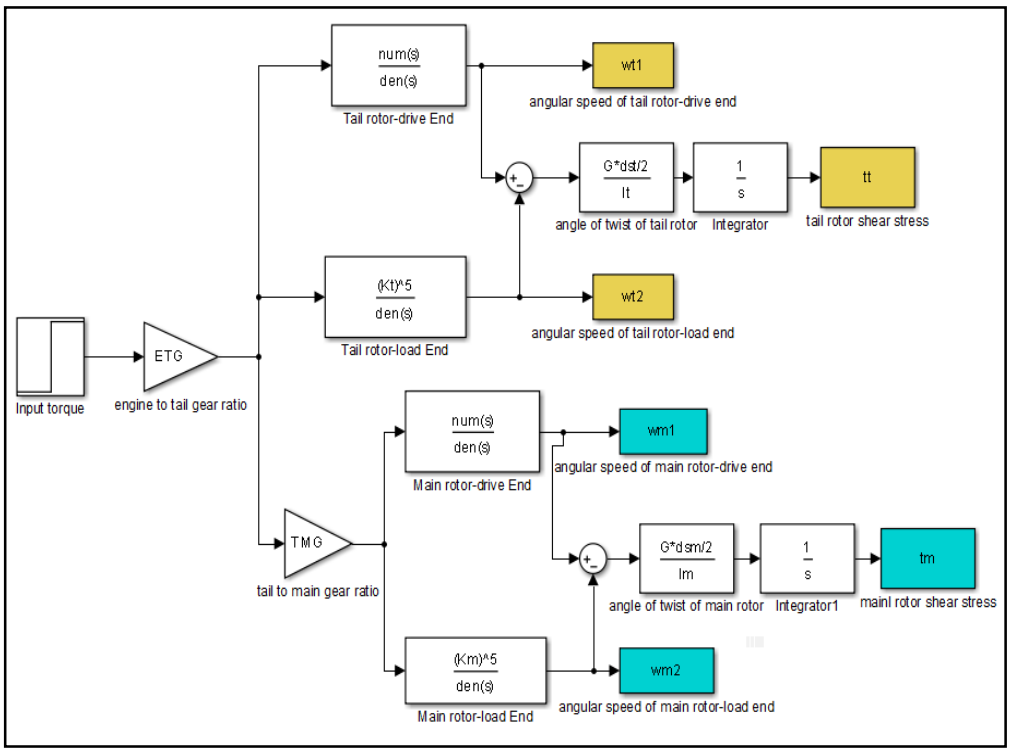

Figure A-5 Simulink Block Diagram-FEM

m. file of Finite Element Model-FEM

```
%Finite Element Model (five sections)

%tail rotor model
lt=5.5                          % Length of tail shaft
in(m)
dst=0.09                        % Diameter of tail shaft
in (m)
Jst=((3.14*(dst^4))/32)         % Polar moment of
inertia of tail shaft in(m^4)
dt1=0.31                        % Diameter of gearbox at
the drive end in tail shaft in (m)
Jt1=((3.14*(dt1^4))/32)         % Polar moment of
inertia of drive end gearbox of tail shaft in (m^4)
```

```
dt2=0.35                        % Diameter of gearbox at
the load end in tail shaft in (m)
Jt2=((3.14*(dt2^4))/32)         % Polar moment of
inertia of load end gearbox of tail shaft in (m^4)
Ct1=4                           % Viscous damping at the
drive end of tail shaft in (N.m.s/rad)
Ct2=20                          % Viscous damping at the
load end of tail shaft in (N.m.s/rad)
Kt=(G*Jst/lt)                   % Torsional stiffness of
the tail shaft in (N.m/rad)

%Main rotor model
lm=1.1                          % Length of main shaft
in(m)
dsm=0.07                        % Diameter of main shaft
in (m)
Jsm=((3.14*(dsm^4))/32)         % Polar moment of
inertia of main shaft in (m^4)
dm1=0.46                        % Diameter of gearbox at
the drive end in main shaft in (m)
Jm1=((3.14*(dm1^4))/32)         % Polar moment of
inertia of drive end gearbox of main shaft in (m^4)
dm2=0.35                        % Diameter of gearbox at
the load end in main shaft in (m)
Jm2=((3.14*(dm2^4))/32)         % Polar moment of
inertia of load end gearbox of main shaft in (m^4)
Cm1=4                           % Viscous damping at the
drive end of main shaft in (N.m.s/rad)
Cm2=20                          % Viscous damping at the
load end of main shaft in (N.m.s/rad)
Km=(G*Jsm/lm)                   % Torsional stiffness of
the main shaft in (N.m/rad)

% General Specifications
G=80*10^9                       % Shear modulus in
(N/m^2)
P=7980                          % Density in (kg/m^3)
MTG=20/60                       % Gear ratio in main
transmission gear
MRG=60/225                      % Gear ratio in tail-

main shaft transmission gear
```

Command window of Finite Element Model-FEM

```
>> Finite
lt =
    5.5000
dst =
    0.0900
Jst =
   6.4380e-06
dt1 =
    0.3100
Jt1 =
   9.0620e-04
dt2 =
    0.3500
Jt2 =
    0.0015
Ct1 =
     4
Ct2 =
    20
Kt =
   9.3643e+04
lm =
    1.1000
dsm =
```

```
    0.0700

Jsm =

   2.3560e-06

dm1 =

    0.4600

Jm1 =

   9.0620e-04

dm2 =

    0.3500

Jm2 =

    0.0020

Cm1 =

     4

Cm2 =

    20

Km =

   1.7134e+05

G =

   8.0000e+10

P =

        7980

MTG =

    0.3333

MRG =

    0.2667

>>
```

Appendix-A6:

Matlab display for Distributed-Lumped Parameter Model-DLPM

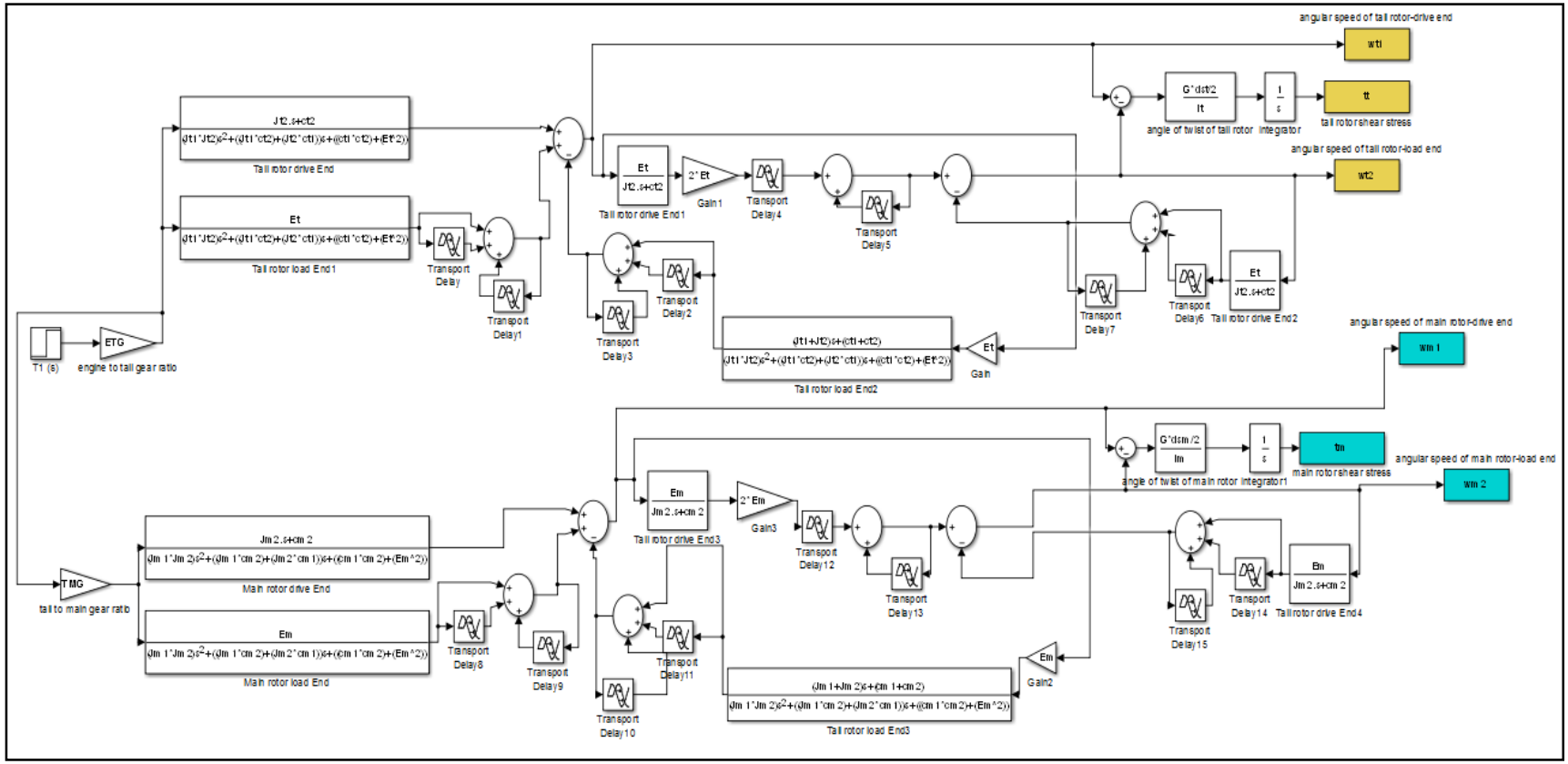

Figure A-6 Simulink block diagram of HM

m. file of Distributed-Lumped Parameter Model-DLPM

```
% Hybrid model

% tail rotor
lt=5.5                          % Length of tail shaft
in(m)
dst=0.09                        % Diameter of tail shaft
in (m)
Jst=((3.14*(dst^4))/32)         % Polar moment of inertia
of tail shaft in(m^4)
dt1=0.31                        % Diameter of gearbox at
the drive end in tail shaft in (m)
Jt1=((3.14*(dt1^4))/32)         % Polar moment of inertia
of drive end gearbox of tail shaft in (m^4)
dt2=0.35                        % Diameter of gearbox at
the load end in tail shaft in (m)
Jt2=((3.14*(dt2^4))/32)         % Polar moment of inertia
of load end gearbox of tail shaft in (m^4)
Ct1=4                           % Viscous damping at the
drive end of tail shaft in (N.m.s/rad)
Ct2=20                          % Viscous damping at the
load end of tail shaft in (N.m.s/rad)
Lt=(P*Jst)                      % Tail shaft polar moment
of inertia in(m^4)
Ct=1/(G*Jst)                    % Tail shaft compliance in
(N^-1 m^-2)
Et=Jst*sqrt(P*G)                % Characteristic impedance
of tail shaft in (kg.m^2/s^2)
Tt=2*lt*sqrt(Lt*Ct)             % Time delay of tail shaft
in (s)

% main rotor
lm=1.1                          % Length of tail shaft
in(m)
dsm=0.07                        % Diameter of tail shaft
in (m)
Jsm=((3.14*(dsm^4))/32)         % Polar moment of inertia
of tail shaft in(m^4)
```

```
dm1=0.46                        % Diameter of gearbox at
the drive end in tail shaft in (m)
Jm1=((3.14*(dm1^4))/32)         % Polar moment of inertia
of drive end gearbox of tail shaft in (m^4)
dm2=0.35                        % Diameter of gearbox at
the load end in tail shaft in (m)
Jm2=((3.14*(dm2^4))/32)         % Polar moment of inertia
of load end gearbox of tail shaft in (m^4)
Cm1=4                           % Viscous damping at the
drive end of tail shaft in (N.m.s/rad)
Cm2=20                          % Viscous damping at the
load end of tail shaft in (N.m.s/rad)
Lm= (P*Jsm)                     % Tail shaft polar moment
of inertia in(m^4)
Cm=1/(G*Jsm)                    % Tail shaft compliance in
(N^-1 m^-2)
Em=Jsm*sqrt(P*G)                % Characteristic impedance
of tail shaft in (kg.m^2/s^2)
Tm=2*lm*sqrt(Lm*Cm)             % Time delay of tail shaft
in (s)

% General Specifications
G=80*10^9                       % Shear modulus in (N/m^2)
P=7980                          % Density in (kg/m^3)
MTG=20/60                       % Gear ratio in main
transmission gear
MRG=60/225                      % Gear ratio in tail-main

shaft transmission gear
```

Command window of Distributed-Lumped Parameter Model-DLPM

```
>> Hybrid
lt =
    5.5000
dst =
```

0.0900

Jst =

6.4380e-06

dt1 =

0.3100

Jt1 =

9.0620e-04

dt2 =

0.3500

Jt2 =

0.0015

Ct1 =

4

Ct2 =

20

Lt =

0.0514

Ct =

1.9416e-06

Et =

162.6658

Tt =

0.0035

lm =

1.1000

dsm =

0.0700

Jsm =

2.3560e-06

dm1 =

0.4600

Jm1 =

0.0044

dm2 =

0.3500

Jm2 =

0.0015

Cm1 =

4

Cm2 =

20

Lm =

0.0188

Cm =

5.3056e-06

Em =

59.5276

Tm =

6.9483e-04

G =

8.0000e+10

P =

```
        7980

MTG =

    0.3333

MRG =

    0.2667

>>
```

Appendix-A7:

Matlab numerical calculation of lumped parameter model (tail rotor-drive end)

```
>> num=[Jt2 ct2 Kt]

num =

   1.0e+04 *

    0.0000    0.0020    9.3643

>> den=[(Jt1*Jt2) ((Jt1*ct2)+(Jt2*ct1)) ((Jt1*Kt)+(Jt2*Kt)+(ct1*ct2)) ((ct1+ct2)*Kt)]

den =

   1.0e+06 *

    0.0000    0.0000    0.0003    2.2474

>> G=tf(num,den)

G =

          0.001472 s^2 + 20 s + 9.364e04

  -----------------------------------------------

  1.334e-06 s^3 + 0.02401 s^2 + 302.7 s + 2.247e06

Continuous-time transfer function.

>>
```

Appendix-A8:

Matlab numerical calculation of lumped parameter model (tail rotor-load end)

```
>> num=[Kt]

num =

  9.3643e+04

>> den=[(Jt1*Jt2) ((Jt1*ct2)+(Jt2*ct1)) ((Jt1*Kt)+(Jt2*Kt)+(ct1*ct2))
((ct1+ct2)*Kt)]

den =

  1.0e+06 *

   0.0000    0.0000    0.0003    2.2474

>> G=tf(num,den)

G =

                9.364e04

  ------------------------------------------------

  1.334e-06 s^3 + 0.02401 s^2 + 302.7 s + 2.247e06

Continuous-time transfer function.

>>
```

Appendix-A9:

Matlab numerical calculation of lumped parameter model (main rotor-drive end)

```
>> num=[Jm2 cm2 Km]

num =

   1.0e+05 *

    0.0000    0.0002    1.7134

>> den=[(Jm1*Jm2) ((Jm1*cm2)+(Jm2*cm1))
((Jm1*Km)+(Jm2*Km)+(cm1*cm2)) ((cm1+cm2)*Km)]

den =

   1.0e+06 *

    0.0000    0.0000    0.0011    4.1123

>> G=tf(num,den)

G =

          0.001472 s^2 + 20 s + 1.713e05

  ---------------------------------------------

  6.469e-06 s^3 + 0.09376 s^2 + 1085 s + 4.112e06

Continuous-time transfer function.

>>
```

Appendix-A10:

Matlab numerical calculation of lumped parameter model (main rotor-load end)

```
>> num=[Km]

num =

   1.7134e+05

>> den=[(Jm1*Jm2) ((Jm1*cm2)+(Jm2*cm1))
((Jm1*Km)+(Jm2*Km)+(cm1*cm2)) ((cm1+cm2)*Km)]

den =

   1.0e+06 *

    0.0000    0.0000    0.0011    4.1123

>> G=tf(num,den)

G =

                 1.713e05

  ------------------------------------------------

  6.469e-06 s^3 + 0.09376 s^2 + 1085 s + 4.112e06

Continuous-time transfer function.

>>
```

Appendix-A11:

Matlab numerical calculation of finite element model (tail rotor-drive end)

```
>> num=[((Jst^4)*Jt2) ((Jst^4)*ct2) ((8*Kt*(Jst^3)*Jt2)+(Kt*(Jst^4)))
(8*Kt*(Jst^3)*ct2) ((7*(Jst^3)*(Kt^2))+(21*(Kt^2)*(Jst^2)*Jt2))
(21*(Kt^2)*(Jst^2)*ct2) ((15*(Kt^3)*(Jst^2))+(20*(Kt^3)*Jst*Jt2))
(20*(Kt^3)*Jst*ct2) ((5*(Kt^4)*Jt2)+(10*(Kt^4)*Jst)) (5*(Kt^4)*ct2)
(Kt^5)]

num =

  1.0e+24 *

 Columns 1 through 7

   0.0000    0.0000    0.0000    0.0000    0.0000    0.0000    0.0000

 Columns 8 through 11

   0.0000    0.0000    0.0077    7.2009

>> den=[(Jt1*(Jst^4)*Jt2) ((ct1*(Jst^4)*Jt2)+(Jt1*(Jst^4)*ct2))
((Kt*(Jst^4)*Jt2)+(8*Kt*Jt1*(Jst^3)*Jt2)+(Kt*Jt1*(Jst^4))+(ct1*(Jst^4)*ct2
))
((Kt*ct1*(Jst^4))+(8*Kt*ct1*(Jst^3)*Jt2)+(8*Kt*Jt1*(Jst^3)*ct2)+(Kt*(Jst
^4)*ct2))
((7*Jt1*(Jst^3)*(Kt^2))+(21*(Kt^2)*Jt1*(Jst^2)*Jt2)+((Kt^2)*(Jst^4))
+(8*Kt*ct1*(Jst^3)*ct2)+(7*(Kt^2)*(Jst^3)*Jt2))
((21*(Kt^2)*Jt1*(Jst^2)*ct2)+(7*ct1*(Jst^3)*(Kt^2))+(21*(Kt^2)*ct1*(Jst^
2)*Jt2)+(7*(Kt^2)*(Jst^3)*ct2))
((15*(Kt^3)*(Jst^2)*Jt2)+(20*(Kt^3)*Jt1*Jst*Jt2)+(6*(Jst^3)*(Kt^3))+(15*
(Kt^3)*Jt1*(Jst^2))+(21*(Kt^2)*ct1*(Jst^2)*ct2))
((15*(Kt^3)*ct1*(Jst^2))+(15*(Kt^3)*(Jst^2)*ct2)+(20*(Kt^3)*ct1*Jst*Jt2)
+(20*(Kt^3)*Jt1*Jst*ct2))
((5*(Kt^4)*Jt1*Jt2)+(20*(Kt^3)*ct1*Jst*ct2)+(10*(Kt^4)*Jt1*Jst)+(10*(Jst
^2)*(Kt^4))+(10*(Kt^4)*Jst*Jt2 ))
((5*(Kt^4)*ct1*Jt2)+(10*(Kt^4)*Jst*ct2)+(5*(Kt^4)*Jt1*ct2)+(10*(Kt^4)*
ct1*Jst )) (((Kt^5)*Jt2)+(4*(Kt^5)*Jst)+((Kt^5)*Jt1)+(5*(Kt^4)*ct1*ct2 ))
(((Kt^5)*ct1)+((Kt^5)*ct2 ))]

den =

  1.0e+26 *
```

```
  Columns 1 through 7

    0.0000    0.0000    0.0000    0.0000    0.0000    0.0000    0.0000

  Columns 8 through 12

    0.0000    0.0000    0.0000    0.0005    1.7282

>>

>> G=tf(num,den)

G =

  2.53e-24 s^10 + 3.436e-20 s^9 + 2.945e-13 s^8 + 3.998e-09 s^7

         + 0.01126 s^6 + 152.7 s^5 + 1.562e08 s^4 + 2.115e12 s^3

                  + 5.711e17 s^2 + 7.69e21 s + 7.201e24

  ---------------------------------------------------------------------

  2.292e-27 s^11 + 4.125e-23 s^10 + 2.673e-16 s^9 + 4.804e-12 s^8

         + 1.024e-05 s^7 + 0.1837 s^6 + 1.429e05 s^5 + 2.551e09 s^4

              + 5.333e14 s^3 + 9.352e18 s^2 + 4.807e22 s + 1.728e26

Continuous-time transfer function.

>>
```

Appendix-A12:

Matlab numerical calculation of finite element model (tail rotor-load end)

```
>> num=[(Kt)^5]

num =

   7.2009e+24

>> den=[(Jt1*(Jst^4)*Jt2) ((ct1*(Jst^4)*Jt2)+(Jt1*(Jst^4)*ct2))
((Kt*(Jst^4)*Jt2)+(8*Kt*Jt1*(Jst^3)*Jt2)+(Kt*Jt1*(Jst^4))+(ct1*(Jst^4)*ct2
))
((Kt*ct1*(Jst^4))+(8*Kt*ct1*(Jst^3)*Jt2)+(8*Kt*Jt1*(Jst^3)*ct2)+(Kt*(Jst
^4)*ct2))
((7*Jt1*(Jst^3)*(Kt^2))+(21*(Kt^2)*Jt1*(Jst^2)*Jt2)+((Kt^2)*(Jst^4))
+(8*Kt*ct1*(Jst^3)*ct2)+(7*(Kt^2)*(Jst^3)*Jt2))
((21*(Kt^2)*Jt1*(Jst^2)*ct2)+(7*ct1*(Jst^3)*(Kt^2))+(21*(Kt^2)*ct1*(Jst^
2)*Jt2)+(7*(Kt^2)*(Jst^3)*ct2))
((15*(Kt^3)*(Jst^2)*Jt2)+(20*(Kt^3)*Jt1*Jst*Jt2)+(6*(Jst^3)*(Kt^3))+(15*
(Kt^3)*Jt1*(Jst^2))+(21*(Kt^2)*ct1*(Jst^2)*ct2))
((15*(Kt^3)*ct1*(Jst^2))+(15*(Kt^3)*(Jst^2)*ct2)+(20*(Kt^3)*ct1*Jst*Jt2)
+(20*(Kt^3)*Jt1*Jst*ct2))
((5*(Kt^4)*Jt1*Jt2)+(20*(Kt^3)*ct1*Jst*ct2)+(10*(Kt^4)*Jt1*Jst)+(10*(Jst
^2)*(Kt^4))+(10*(Kt^4)*Jst*Jt2 ))
((5*(Kt^4)*ct1*Jt2)+(10*(Kt^4)*Jst*ct2)+(5*(Kt^4)*Jt1*ct2)+(10*(Kt^4)*
ct1*Jst )) (((Kt^5)*Jt2)+(4*(Kt^5)*Jst)+((Kt^5)*Jt1)+(5*(Kt^4)*ct1*ct2 ))
(((Kt^5)*ct1)+((Kt^5)*ct2 ))]

den =

  1.0e+26 *

 Columns 1 through 7

   0.0000    0.0000    0.0000    0.0000    0.0000    0.0000    0.0000

 Columns 8 through 12

   0.0000    0.0000    0.0000    0.0005    1.7282

>> G=tf(num,den)

G =
```

7.201e24

2.292e-27 s^11 + 4.125e-23 s^10 + 2.673e-16 s^9 + 4.804e-12 s^8

+ 1.024e-05 s^7 + 0.1837 s^6 + 1.429e05 s^5 + 2.551e09 s^4

+ 5.333e14 s^3 + 9.352e18 s^2 + 4.807e22 s + 1.728e26

Continuous-time transfer function.

>>

Appendix-A13:

Matlab numerical calculation of finite element model (main rotor-drive end)

```
>> num=[((Jsm^4)*Jm2) ((Jsm^4)*cm2)
((8*Km*(Jsm^3)*Jm2)+(Km*(Jsm^4))) (8*Km*(Jsm^3)*cm2)
((7*(Jsm^3)*(Km^2))+(21*(Km^2)*(Jsm^2)*Jm2))
(21*(Km^2)*(Jsm^2)*cm2)
((15*(Km^3)*(Jsm^2))+(20*(Km^3)*Jsm*Jm2)) (20*(Km^3)*Jsm*cm2)
((5*(Km^4)*Jm2)+(10*(Km^4)*Jsm)) (5*(Km^4)*cm2) (Km^5) ]

num =

  1.0e+26 *

 Columns 1 through 7

   0.0000    0.0000    0.0000    0.0000    0.0000    0.0000    0.0000

 Columns 8 through 11

   0.0000    0.0000    0.0009    1.4769

>> den=[(Jm1*(Jsm^4)*Jm2) ((cm1*(Jsm^4)*Jm2)+(Jm1*(Jsm^4)*cm2))
((Km*(Jsm^4)*Jm2)+(8*Km*Jm1*(Jsm^3)*Jm2)+(Km*Jm1*(Jsm^4))+(c
m1*(Jsm^4)*cm2))
((Km*cm1*(Jsm^4))+(8*Km*cm1*(Jsm^3)*Jm2)+(8*Km*Jm1*(Jsm^3)*c
m2)+(Km*(Jsm^4)*cm2))
((7*Jm1*(Jsm^3)*(Km^2))+(21*(Km^2)*Jm1*(Jsm^2)*Jm2)+((Km^2)*(Js
m^4)) +(8*Km*cm1*(Jsm^3)*cm2)+(7*(Km^2)*(Jsm^3)*Jm2))
((21*(Km^2)*Jm1*(Jsm^2)*cm2)+(7*cm1*(Jsm^3)*(Km^2))+(21*(Km^2)
*cm1*(Jsm^2)*Jm2)+(7*(Km^2)*(Jsm^3)*cm2))
((15*(Km^3)*(Jsm^2)*Jm2)+(20*(Km^3)*Jm1*Jsm*Jm2)+(6*(Jsm^3)*(K
m^3))+(15*(Km^3)*Jm1*(Jsm^2))+(21*(Km^2)*cm1*(Jsm^2)*cm2))
((15*(Km^3)*cm1*(Jsm^2))+(15*(Km^3)*(Jsm^2)*cm2)+(20*(Km^3)*cm
1*Jsm*Jm2)+(20*(Km^3)*Jm1*Jsm*cm2))
((5*(Km^4)*Jm1*Jm2)+(20*(Km^3)*cm1*Jsm*cm2)+(10*(Km^4)*Jm1*J
sm)+(10*(Jsm^2)*(Km^4))+(10*(Km^4)*Jsm*Jm2 ))
((5*(Km^4)*cm1*Jm2)+(10*(Km^4)*Jsm*cm2)+(5*(Km^4)*Jm1*cm2)+(
10*(Km^4)*cm1*Jsm ))
(((Km^5)*Jm2)+(4*(Km^5)*Jsm)+((Km^5)*Jm1)+(5*(Km^4)*cm1*cm2 ))
(((Km^5)*cm1)+((Km^5)*cm2 ))]

den =
```

```
   1.0e+27 *

  Columns 1 through 7

    0.0000    0.0000    0.0000    0.0000    0.0000    0.0000    0.0000

  Columns 8 through 12

    0.0000    0.0000    0.0000    0.0008    3.5445

>> G=tf(num,den)

G =

  6.304e-26 s^10 + 6.162e-22 s^9 + 3.668e-14 s^8 + 3.585e-10 s^7

         + 0.007005 s^6 + 68.44 s^5 + 4.854e08 s^4 + 4.741e12 s^3

                  + 8.838e18 s^2 + 8.619e22 s + 1.477e26

  ----------------------------------------------------------------

  5.713e-29 s^11 + 8.105e-25 s^10 + 3.325e-17 s^9 + 4.717e-13 s^8

         + 6.355e-06 s^7 + 0.0901 s^6 + 4.41e05 s^5 + 6.246e09 s^4

            + 8.07e15 s^3 + 1.139e20 s^2 + 7.822e23 s + 3.545e27

Continuous-time transfer function.

>>
```

Appendix-A14:

Matlab numerical calculation of finite element model (main rotor-load end)

```
>> num=[(Km)^5]

num =

   1.4769e+26

>> den=[(Jm1*(Jsm^4)*Jm2) ((cm1*(Jsm^4)*Jm2)+(Jm1*(Jsm^4)*cm2))
((Km*(Jsm^4)*Jm2)+(8*Km*Jm1*(Jsm^3)*Jm2)+(Km*Jm1*(Jsm^4))+(c
m1*(Jsm^4)*cm2))
((Km*cm1*(Jsm^4))+(8*Km*cm1*(Jsm^3)*Jm2)+(8*Km*Jm1*(Jsm^3)*c
m2)+(Km*(Jsm^4)*cm2))
((7*Jm1*(Jsm^3)*(Km^2))+(21*(Km^2)*Jm1*(Jsm^2)*Jm2)+((Km^2)*(Js
m^4)) +(8*Km*cm1*(Jsm^3)*cm2)+(7*(Km^2)*(Jsm^3)*Jm2))
((21*(Km^2)*Jm1*(Jsm^2)*cm2)+(7*cm1*(Jsm^3)*(Km^2))+(21*(Km^2)
*cm1*(Jsm^2)*Jm2)+(7*(Km^2)*(Jsm^3)*cm2))
((15*(Km^3)*(Jsm^2)*Jm2)+(20*(Km^3)*Jm1*Jsm*Jm2)+(6*(Jsm^3)*(K
m^3))+(15*(Km^3)*Jm1*(Jsm^2))+(21*(Km^2)*cm1*(Jsm^2)*cm2))
((15*(Km^3)*cm1*(Jsm^2))+(15*(Km^3)*(Jsm^2)*cm2)+(20*(Km^3)*cm
1*Jsm*Jm2)+(20*(Km^3)*Jm1*Jsm*cm2))
((5*(Km^4)*Jm1*Jm2)+(20*(Km^3)*cm1*Jsm*cm2)+(10*(Km^4)*Jm1*J
sm)+(10*(Jsm^2)*(Km^4))+(10*(Km^4)*Jsm*Jm2 ))
((5*(Km^4)*cm1*Jm2)+(10*(Km^4)*Jsm*cm2)+(5*(Km^4)*Jm1*cm2)+(
10*(Km^4)*cm1*Jsm ))
(((Km^5)*Jm2)+(4*(Km^5)*Jsm)+((Km^5)*Jm1)+(5*(Km^4)*cm1*cm2 ))
(((Km^5)*cm1)+((Km^5)*cm2 ))]

den =

  1.0e+27 *

 Columns 1 through 7

   0.0000    0.0000    0.0000    0.0000    0.0000    0.0000    0.0000

 Columns 8 through 12

   0.0000    0.0000    0.0000    0.0008    3.5445

>> G=tf(num,den)

G =
```

1.477e26

5.713e-29 s^11 + 8.105e-25 s^10 + 3.325e-17 s^9 + 4.717e-13 s^8

+ 6.355e-06 s^7 + 0.0901 s^6 + 4.41e05 s^5 + 6.246e09 s^4

+ 8.07e15 s^3 + 1.139e20 s^2 + 7.822e23 s + 3.545e27

Continuous-time transfer function.

>>